Optimal Energy Management of Electrified Propulsion Systems with Data-driven Li-ion Battery and PEM Fuel Cell Performance and Degradation Predictions

by

Bo Pang
M.Sc, Northeastern University, 2016
B.Eng, Liaoning Normal University, 2014

A Dissertation Submitted in Partial Fulfillment
of the Requirements for the Degree of

DOCTOR OF PHILOSOPHY

in the Department of Mechanical Engineering

Supervisory Committee

Optimal Energy Management of Electrified Propulsion Systems with Data-driven Li-ion Battery and PEM Fuel Cell Performance and Degradation Predictions

by

Bo Pang
M.Sc, Northeastern University, 2016
B.Eng, Liaoning Normal University, 2014

Supervisory Committee

Dr. Zuomin Dong, Department of Mechanical Engineering

Supervisor

Dr. Yang Shi, Department of Mechanical Engineering

Departmental Member

Dr. Daniela Constantinescu, Department of Mechanical Engineering

Departmental Member

Dr. Aaron Gulliver, Department of Electrical and Computer Engineering

Outside Member

Abstract

Electrified propulsion systems for vehicles and marine vessels, including engine-battery hybrid, fuel cell-battery hybrid, and battery electric propulsion systems, present clean propulsion solutions for improving performance, energy efficiency, emissions and lifecycle costs (LCC). Battery energy storage systems (BESSs) are essential in these systems, storing and delivering electrical energy to complement or replace the onboard energy converter.

With the rapid development of Lithium-ion (Li-ion) battery technology, battery electric vehicles (BEVs) are becoming increasingly popular for personal transportation. Fuel cell electric vehicles (FCEVs), powered by a proton exchange membrane fuel cell (PEMFC) system and a BESS supplement, offer a zero-emission propulsion solution for heavy-duty applications, overcoming some of the limitations of BEVs. Liquefied natural gas (LNG), a low-cost cleaner fuel, is a viable replacement for diesel in compression ignition (CI) engines for heavy-duty engine-battery hybrid electric propulsions to reduce fuel consumption, air pollutants and GHG emissions.

However, BESSs and PEMFC systems suffer relatively short service lives and high replacement costs. A better understanding and modelling of their degradation patterns and corresponding optimal system design and energy management are vital to extending their service lives to reduce the vehicles' LCCs. Ultracapacitors (UCs), known for their high-power density and insensitivity to operating temperatures, if properly designed and controlled, can be combined with the BESS to form hybrid energy storage systems (HESS) to extend battery life, system performance and energy efficiency.

The performance of BESSs and PEMFCs depends on their degradation levels. Usage patterns and temperature conditions influence their degradation rate. This study collected performance and degradation data for Li-ion batteries and PEMFCs under various usage conditions to develop advanced battery and PEMFC performance, degradation, and thermal models. These models aid in optimizing the hybrid electric propulsion and HESS design and energy management across different operating scenarios. The research also introduced new methods for dynamically updating the BESS and PEMFC degradation models using real-time operational data to improve the optimal energy management of electrified vehicles and marine vessels.

This work developed new methods for generating integrated optimal system design and energy management strategy using nested global optimizations to satisfy system design requirements and achieve maximum energy efficiency and minimum life cycle costs. Dynamic programming (DP) was used to search for the optimal energy management solutions for each system design, and a simulation-based, top-level global optimization was formulated to identify the best system design solution and solved using a very efficient metamodel global optimization algorithm.

Methods for generating real-time optimal energy management and control for the hybrid electric propulsion system and HESS, segment by segment, based on an extended model prediction control (MPC), were introduced. New methods for using real-time operation data to dynamically update the Li-ion battery degradation model using identified equivalent total charge/discharge cycle number and the PEMFC degradation model using identified actual active area were introduced. Jointly considering the measured vehicle speed and benchmark test cycle, as well as the BESS and PEMFC operating data and updated degradation models using the Extended Kalman filter (EKF), these approaches provided improved real-time optimal control for the hybrid propulsion system and HESS.

Case study 1 involves a fuel cell electric ferry ship powered by a PEMFC system and BESS. The approach minimizes LCC by balancing system performance, fuel economy, and degradations of the PEMFC and BESS. An optimal EMS is developed for the ship based on real-time operational data by introducing accurate performance and degradation models. This approach significantly reduces LCC, promoting clean ship propulsion technologies.

Case study 2 focuses on a global optimal propulsion system design for an LNG-fueled hybrid electric ferry ship. The system addresses the increased CO2 equivalent emissions due to methane leakage from LNG engines and the high costs associated with BESS replacements. The optimal integration of the LNG engine, BESS, and EMS is achieved using DP, while an EKF models real-time changes in ship propulsion power. MPC is used to develop an optimal control strategy that optimizes fuel consumption, BESS degradation, and emissions. This case highlights the advantages of global optimization and real-time control.

Case study 3 introduces a new approach to optimizing the design and EMS of a battery-UC HESS. The approach improves Li-ion battery operation under high current charge/discharge, mitigates low-temperature impact, and significantly extends battery life. The combination of battery and UC improves overall performance, while adding an active UC-based battery thermal management strategy (TMS) in the optimal EMS reduces the LCC of the BEVs. Updating the battery performance and degradation models in real time continuously enabled more precise optimal control through MPC.

These case studies demonstrate the feasibility, advantages and benefits of the newly introduced integrated modelling, design and control optimization methods.

Contents

Chapter 1. Introduction 1
1.1. General Background 1
1.2. Research Problem and Objective 2
1.3. Dissertation Organization 3
Chapter 2. Related Work 4
2.1. Performance and Degradation Modelling of Li-ion Batteries 4
2.2. Performance and Degradation Modelling of PEMFCs 7
2.3. Optimal Design, Control and EMS for Electrified Vehicles and Vessels 10
2.4. Real-time Optimal Control for Electrified Vehicles and Vessels 14
Chapter 3. Li-ion Batteries Performance and Degradation Modelling 17
3.1. Battery Performance Model 17
3.2. Battery Degradation Prediction 18
3.2.1. Battery Performance Data under Different Use Patterns 18
3.2.2. Battery Performance Data under Different Temperatures 20
3.2.3. Battery Capacity Degradation Modelling 22
3.2.4. Battery Performance Degradation Modelling 25
3.3. Real-time Battery SOH Estimation and Prediction 27
3.4. Battery Thermal Model 28
3.5. New Data-driven Model Parameter Determining Method 28
Chapter 4. PEMFC Performance and Degradation Model 35
4.1. PEMFC Performance Model 35
4.2. PEMFC SOH Estimation and Prediction 36
4.2.1. PEMFC Experimental Data 36
4.2.2. PEMFC Degradation Model 37
4.3. Data-driven Modelling of PEMFC Performance and Degradation 38
Chapter 5. Integrated Design and Control Optimizations and Real-time Optimal Control 40
5.1. Design Problem 40
5.2. Integrated Global Design Optimization for Minimum Lifecycle Costs 42
5.2.1. Optimal Sizing of Key Propulsion System Components 42
5.2.2. Baseline Optimal Energy Management Strategies by Dynamic Programming 45
5.2.3. Solution of the Nested Global Optimization Problem 46
5.3. Applying Extended Kalman Filter to Blended Data 47

5.4. Real-time Optimal Control Strategy 48
5.5. A new MPC real-time optimal control method 49
5.5.1. Purpose of the New MPC Method 49
5.5.2. Components of the New MPC Method 50
5.5.3. Algorithm Implementation 50
5.5.4. Adjustment Methods for Computing Time/Capacity 51
5.6. Testing and Applications of the Introduced New Methods 52
Chapter 6. Case Study on Fuel Cell and Battery Hybrid Electric Marine Propulsion System 53
6.1. Literature and Motivation 53
6.2. Hybrid Electric Fuel Cell Vessel 56
6.2.1. Vessel Operation Profile 56
6.2.2. Vessel Technical Specification 57
6.3. Optimal Vessel EMS Considering Life Cycle Costs 58
6.3.1. Battery and PEMFC Degradation and Life Cycle Cost 58
6.3.2. Fuel Efficiency 60
6.3.3. Globally Optimal System Design and Operation 60
Chapter 7. Case Study on NG-Engine Hybrid Electric Marine Propulsion System Design 65
7.1. Literature and Motivation 65
7.2. NG-diesel Engine Hybrid Electric Marine Propulsion System 67
7.2.1. Example Marine Vessel and Hybrid Electric Propulsion System Design 68
7.2.2. Stochastic Vessel Operation Profile 68
7.2.3. NG-diesel Dual-fuel CI Engine Fuel Efficiency and Emission Models 69
7.2.4. Integrated Hybrid System Design Optimization and Baseline Optimal EMS 70
7.3. Optimal Control Schemes for Hybrid Electric Propulsion 73
7.3.1. CO_2 Emissions for Pure NG-Fueled Electric Propulsion System 73
7.3.2. Minimum Fuel Consumption and Associated CO_2 Emissions 73
7.3.3. Minimum NG Fuel Consumption and CO2e Emissions 74
7.3.4. Minimum NG Fuel Consumption, CO_{2e} Emissions and LCC 74
7.4. Real-time Propulsion Power and ESS SOH Predictions 75
7.4.1. Dynamic Change of Battery SOH and Degradation Model Updates 76
7.4.2. Accurate Propulsion Power Prediction Using Real-time Operation Data 76
7.5. Real-time Globally Optimal Control of the Propulsion System 77
7.5.1. Varying Vessel Operating Profile 77

7.5.2. A Dedicated Adaptive MPC Method 77
7.6. Results and Discussions 78
Chapter 8. Case Study on BEV Battery-UC HESS for Low-Temperature Operations 82
8.1. Literature and Motivation 82
8.2. ESS System Design and Energy Management for EVs 85
8.3. Modelling of HESS and Its Other Components 87
8.3.1. Li-ion Battery-UC HESS 87
8.3.2. UC Model 87
8.3.3. DC/DC Converter Model 88
8.4. Battery-UC HESS Design and Baseline Optimal EMS 89
8.5. Optimal Sizing of Battery and UC for Minimum LCC 92
8.5.1. Optimal Sizing of Battery and UC for Minimum LCC 92
8.5.2. Optimal HESS Power Control and Baseline EMS Using DP 93
8.5.3. Advantages of HESS and Comparison 95
8.5.4. Solution of the Nested Global Optimization Problem 97
8.6. Real-time Optimal Control of HESS 98
8.7. Result Discussions 99
8.8. Real-time implementation 102
Chapter 9. Conclusions 103
9.1. Summary 103
9.2. Original Research Contributions 106
Chapter 10. Future Work 108
References 109

List of Tables

Table 1. Advantages and disadvantages of different methods. 5
Table 2. Technical data sheet of Li-ion battery 19
Table 3. Battery performance and degradation rate under different temperatures 24
Table 4. Parameters in different cycles 27
Table 5. Comparison of different algorithms for battery capacity 31
Table 6. Technical Specifications of Skeena Queen Ferry 57
Table 7. Crossing cost comparison in different SOH (US$) 63
Table 8. General information about the ferry ship Skeen 68
Table 9. Minimum Overall LCC Measure Results under Different Vessel Operations ($*) 81
Table 10. Vehicle Design Parameters of Electric Medium-Duty Truck (MDT) 89
Table 11. Comparison of BESS, HESS (No Temp) and HESS (With Temp) 97
Table 12. Comparison of two algorithms 97
Table 13. Parameters of energy storage components 98
Table 14. Minimum Overall LCC Measure Results under Different Vehicle Operations 101
Table 15. Implementation options of the new MPC method 102

List of Figures

Figure 1. A diagram of a hydrogen fuel cell. 8
Figure 2. Dual Polarization model. 18
Figure 3. Product appearance and schematic diagram of battery size [101]. 19
Figure 4. Battery capacity changes in test cycles. 20
Figure 5. Voltage variation during different capacity test cycles. 20
Figure 6. Discharge voltage change curve: (a) 0.1C discharge rate; (b) 0.25C discharge rate; (c) 0.5C discharge rate; (d) 0.75C discharge rate; (e) 1C discharge rate [102]. 21
Figure 7. Effect of temperature on Li-ion battery capacity. 22
Figure 8. Battery SOH variation under different temperatures. 24
Figure 9. ΔVoc changes in different temperatures and C_{rate}. 25
Figure 10. Voltage surfaces in different temperatures. 25
Figure 11. Resistance obtained using PSO-based fitting. 26
Figure 12. Real capacity and predicted capacity in different cycles. 28
Figure 13. Signal flow diagram of BP algorithm. 29
Figure 14. Voltage variation during different test cycles. 30
Figure 15. Estimation of battery capacity based on cycling train cycles and test cycles. 32
Figure 16. Estimation for resistance based on cycling training cycles and test cycles. 32
Figure 17. Battery voltage in different SOC and C-rate. 33
Figure 18. Voltage surfaces in different cycles. 33
Figure 19. SOH evaluation in different cycles. 34
Figure 20. Voltage (left) and current (right) data of the stack. 37
Figure 21. Modelled active area changes of PEMFC. 38
Figure 22. Estimation of the active area. 38
Figure 23. Real-time optimal control unit for a hybrid propulsion system. 40
Figure 24. Optimization flowchart. 43
Figure 25. Real-time optimal control method of HESS. 48
Figure 26. Skeena Queen Ferry of BC Ferry Services. 56
Figure 27. Power demand from Salt Spring Island and Victoria. 57
Figure 28. PEMFC propulsion system. 57
Figure 29. PEMFC power in different degradation models. 59
Figure 30. ESS power in different degradation models. 59
Figure 31. Illustration of optimal EMS for an electrified propulsion system 61
Figure 32. ESS power in different SOH. 62
Figure 33. PEMFC power in different SOH. 62
Figure 34. ESS power in different cases. 64
Figure 35. PEMFC power in different cases. 64
Figure 36. Proposed hybrid electric ferry propulsion system. 68
Figure 37. Power demand of Skeena Queen Ferry during a trip. 69
Figure 38. Engine fuel efficiency and HC/CO/NOx emissions maps. 70
Figure 39. Engine operating points for pure NG-fueled electric propulsion systems. 73

Figure 40. Engine operating points on fuel efficiency map. 74
Figure 41. Engine operating points based on CDE map..... 74
Figure 42. Engine power and SOC in different cases. 75
Figure 43. Power demand prediction. 76
Figure 44. Power demand under different wind speeds. 77
Figure 45. Architecture of the novel adaptive MPC method. 77
Figure 46. Engine power and SOC based on DP for different wind speeds. 79
Figure 47. Engine power and SOC based on MPC for different wind speeds. 79
Figure 48. Engine power and SOC in different battery SOH for Wind 1. 80
Figure 49. Engine power and SOC in different battery SOHs for the Wind3 Case. 80
Figure 50. Energy power diagram for (a) HEV, (b) BEV and (c) HESS-EV. 86
Figure 51. Composite electric energy system structure of Li-ion battery-UC. 87
Figure 52. UC equivalent circuit model. 87
Figure 53. DC/DC converter efficiency map model [174]. 88
Figure 54. A typical electric MDT. 90
Figure 55. Vehicle simulation model. 91
Figure 56. Vehicle speed of WLTC cycle. 91
Figure 57. Vehicle propulsion power demand based on the WLTC cycle. 92
Figure 58. DP algorithm. 95
Figure 59. Battery SOC, UC SOC, temperature and delta SOC of both HESS and BESS. 96
Figure 60. Power demand under different conditions. 98
Figure 61. The novel adaptive MPC method. 99
Figure 62. Battery SOC, Temperature and Delta SOC, and UC SOC and SOH (Standard Cycle) ... 100
Figure 63. Battery SOC, Temperature and delta SOC, and UC SOC and SOH (Actual Driving). 101

List of Abbreviations

BESS	battery energy storage system
BEV	battery electric vehicle
BMS	battery management system
BP	backpropagation
CI	compression ignition
CO	carbon monoxide
CO_2	carbon dioxide
CO_{2e}	carbon dioxide equivalent
DOD	depth of discharge
DP	dynamic programming
ECMS	equivalent consumption minimization strategy
EIS	Electrical impedance spectroscopy
EKF	extended Kalman filter
EMS	energy management strategy
ESS	energy storage system
EV	electrified vehicle
FCEV	fuel cell electric vehicle
FCHEV	fuel cell hybrid electric vehicle
FCV	fuel cell vessel
GA	genetic algorithms
GHG	greenhouse gas
GPR	Gaussian process regression
GSSEM	generalized steady-state electrochemical model
GWP	global warming potential
HC	hydrocarbons
HESS	hybrid energy storage system
HEV	hybrid electric vehicle
ICE	internal combustion engine
IMO	international maritime organization
IPS	integrated power system
KF	Kalman filter
LFP	LiFePO4
Li-ion	Li-ion
LLC	lifecycle cost
LNG	liquefied natural gas
MPC	model predictive control
MSSR	multi-start space reduction
NG	natural gas
NOx	nitrogen oxides
OCV	open-circuit voltage
PEM	proton exchange membrane
PEMFC	proton exchange membrane fuel cell

PHEVs	plug-in hybrid electric vehicle
PMP	Pontryagin's minimum principle
PSO	particle swarm optimization
RMSE	root mean square error
RUL	remaining useful life
SOC	state of charge
SOH	state of health
SVM	support vector machine
TMS	thermal management strategy
UC	ultracapacitor
WLTP	worldwide harmonized light vehicle test cycles

Nomenclature

V_{oc}	battery open circuit voltage
V_t	battery terminal voltage (or output voltage)
V_i^m	battery measured voltage
V_i^s	battery simulated output voltage
$R_i,$	battery inner resistance
V_i, V_1, V_2	the voltage of inner resistance and two RC circuits
R_1, R_2	resistance in battery RC circuits
C_1, C_2	capacitance in battery RC circuits
I	current
t	time
Q_{max}	the maximum capacity of the battery
Q_{cap}	battery energy storage capacity
Q_i^{pre}	predicted battery capacity
Q_i^{act}	actual battery capacity
Q_i^{ave}	average battery capacity
$\mathrm{E_{RMSE}}$	root mean square error
$\mathrm{E_{MAE}}$	mean absolute error
V_{cell}	fuel cell voltage
E_{nernst}	fuel cell Nernst voltage
η_{act}	fuel cell activation overvoltage
η_{ohmic}	fuel cell ohmic overvoltage
η_{conc}	fuel cell concentration overvoltage
$C_{O_2}^{Interface}$	concentration of oxygen around the catalyst
i	current density
r_M	membrane-specific resistivity for the flow of hydrated protons
l	membrane thickness
R_u	universal gas constant
F	Faraday's constant
i_L	limiting current density
C_{Batt}	degradation-induced costs for the BESS
C_{FC}	degradation-induced costs for the PEMFC system
C_{H_2}	hydrogen fuel cost
$\omega_1, \omega_2, \omega_3$	weighting factors
t_0	start time
t_1	finish time
FC_{op}	hydrogen fuel consumption cost
FC_{deg}	degradation model of the PEMFC system
ESS_{deg}	degradation model of the BESS
n_s	the number of battery cells in series
n_p	the number of battery cells in parallel
P_{dmd}	total power demand

P_{eng}	engine power
P_{ESS}	ESS power
η_{eng}	generator's efficiency of the engine
η_{ESS}	generator's efficiency of the ESS
ω_{opt}	optimal engine speed
T_{opt}	optimal engine torque
SOC_{ini}	initial SOC
SOC_{end}	end SOC
C_{inv}	investment cost
C_{NG}	NG fuel consumption costs
C_{deg}	degradation-induced costs
C_{CO2e}	tailpipe CO_{2e} emissions of the NG engine
P_{heat}	heat power
h_{bat}	heat transfer coefficient
η_{heat}	heating efficiency
T_{env}	ambient temperature
n_s^{uc}	the number of UCs in series
n_p^{uc}	the number of UCs in parallel
C_{uc}	capacity of the UC pack
C_M	capacity of UC cells
V_{uc}^{ocv}	open circuit voltage of the UC module
V_{uc}	OCV of the UC pack

Acknowledgments

I would like to express my heartfelt gratitude to my supervisor, Professor Zuomin Dong, for his invaluable guidance and unwavering support throughout my doctoral studies. His insightful perspectives have profoundly inspired me to tackle complex engineering challenges in the realms of clean automotive and marine transportation research.

I am also deeply thankful to my friends in the research group for their invaluable suggestions and stimulating discussions. In particular, I owe a special debt of gratitude to Haijia Zhu for his guidance in fundamental principles and simulations of vehicle propulsion systems, which significantly enriched my research.

My sincere thanks also go to the committee members for their dedicated time and effort in reviewing this work. Their constructive feedback and critical insights have greatly enhanced the quality of this thesis.

Finally, I am profoundly grateful to my family for their steadfast support and encouragement. Your unwavering belief in me has been a constant source of motivation. Thank you for everything you have done for me.

Chapter 1. Introduction

1.1. General Background

In the present context, the transportation sector constitutes a significant contributor, accounting for approximately 30% of greenhouse gas (GHG) emissions and a notable volume of harmful air pollutants [1]. Electrified vehicles (EVs) and marine vessels emerge as promising solutions for cleaner transportation to reduce or eliminate petroleum fuel consumption, GHG emissions, and airborne contaminants. The electrification and hybridization of EVs depending on the electric energy storage system (ESS), serving either as the sole propulsion energy source for a battery electric vehicle (BEV) or as an energy reservoir for a hybrid electric vehicle (HEV), increasing the operational efficiency and energy utilization of internal combustion engines (ICEs) or hydrogen fuel cell systems.

Today, the prevailing electric ESS of choice revolves around Lithium-ion (Li-ion) batteries. Conversely, hydrogen fuel cells offer a tailpipe emissions-free energy conversion solution with considerably superior efficiency to traditional ICEs. These fuel cells use electrochemical reactions between hydrogen gas and oxidant air, effectively replacing the combustion of conventional petroleum fuels. The proton exchange membrane fuel cell (PEMFC) system, noted for its lower operational temperature and rapid start-up, has emerged as the preferred solution for various eco-friendly transportation applications. Li-ion batteries and PEMFCs are vital in cleansing and decarbonizing transportation.

Despite their fundamental differences, both Li-ion batteries and PEMFCs operate via electrochemical reactions between their anodes and cathodes. They constitute the costliest components of electrified/hybridized powertrain systems, contributing to approximately one-third to one-half of the total cost of BEVs and fuel cell electric vehicles (FCEVs) [2][3]. A critical method for reducing these components' lifecycle costs (LCC) lies in extending their operational lifespans, thereby avoiding performance degradation.

Achieving accurate modelling and prediction of the performance degradation of Li-ion batteries and PEMFCs under varying use scenarios establishes a fundamental underpinning. It aids in optimizing powertrain component sizing and facilitates the optimal power control/energy management of electrified powertrain systems, ultimately striving for minimized LCC. However, the accurate modelling and prediction of battery and fuel cell performance degradation, alongside their remaining operational life, remain complicated tasks. By addressing these factors through innovative modelling approaches and robust data analytics, significant progress can be made in accurately predicting the performance degradation and remaining operational life of batteries and fuel cells.

In HEVs and fuel cell hybrid electric vehicles (FCHEVs), combining a battery energy storage system (BESS) and/or a PEMFC system is critical to ensuring robust performance and prolonged fuel cell operational life. To validate the recently introduced performance

degradation models for Li-ion batteries and PEMFCs, these models can be analyzed through practical application examples. This study aims to affirm their applicability and value to the domain.

By considering the complex interaction between battery decay, life-shortening, and fuel consumption costs, a two-pronged approach is developed. An offline global optimal energy management strategy (EMS) and a real-time updated EMS are devised. The overall objective is to make a balance between fuel efficiency and battery longevity while fulfilling the demands of driving. The real-time EMS uses the comprehensive global control strategy derived across typical road conditions to extract optimal values in instantaneous states.

When steering the course of a PEMFC hybrid electric ferry, an expanded range of cost-influencing factors demands attention to achieve minimal lifecycle expenditures. Enhancing energy efficiency to restrain hydrogen fuel consumption costs must balance with factoring in replacement costs triggered by fuel cell and battery performance degradation. The key lies in optimizing lifecycle expenditures while upholding functional excellence and zero tailpipe emissions of electrical propulsion and fuel cell technology.

Ultimately, battery and fuel cell lifetime prediction models are used to develop globally optimized HEV and FCEV design blueprints and optimal energy control strategies. This innovative approach paves the way for cutting-edge technologies, ensuring sustained performance, economic feasibility, and environmental consciousness.

1.2. Research Problem and Objective

This thesis aims to tackle the intricate challenges associated with designing and operating hybrid propulsion systems optimally for vehicles and ships. Using advanced data-driven models, it attempts to bridge critical gaps in Li-ion battery and fuel cell modelling within the marine and automotive sectors, focusing on slowing down performance degradation. Additionally, this thesis draws upon extensive design knowledge from the automotive industry, complemented by optimization methodologies derived from broader optimization domains, to effectively deal with the complexities of design and control.

This comprehensive study includes hybrid propulsion system design, component sizing, and the development of optimal control strategies. At the key of the control strategy lies the optimal allocation of power demand across various power sources, with the overall goal of minimizing fuel consumption and emissions while lighting battery and fuel cell degradation rates.

Utilizing advanced optimization methods is important to accomplish this objective, ensuring that hybrid systems are tuned to yield the maximum economic and environmental benefits. This thesis confronts multifaceted challenges by combining hybrid electric propulsion system design optimization with real-time optimal control.

Traditionally, the marine and automotive sectors have heavily relied on engineering expertise yet have been hindered by the absence of robust model-based propulsion system design and optimization tools. This difficult situation is further aggravated by the complex nature of Li-ion batteries and the degradation of fuel cell performance, which complicates the integration of BESSs. As a remedy, this study introduces an integrated platform specifically for designing hybrid marine and automotive propulsion systems. Including precise battery performance degradation and lifetime prediction models facilitates informed design and control decisions, considering both initial costs and broader life cycle considerations.

Moreover, this thesis explains the necessity of real-time adjustment of optimal control strategies during ship and vehicle operations. This dynamic approach factors in evolving climate conditions, ambient temperatures, and the inevitable aging of batteries and fuel cells, ensuring sustained optimal performance throughout the operational life cycle. Through these efforts, this thesis sets forth a new hybrid propulsion system optimization method to enhance economic efficiency and environmental sustainability.

1.3. Dissertation Organization

This dissertation is organized into nine chapters. Chapter 2 reviews the related work, comprehensively surveying existing research on batteries, PEMFCs, optimal design, and real-time optimal control strategies. Chapter 3 focuses on performance and degradation modelling for Li-ion batteries, incorporating real-time updates based on operational data to improve control accuracy. Chapter 4 examines PEMFC performance and degradation, exploring strategies to optimize lifecycle performance under varying conditions. Chapter 5 introduces an integrated global design optimization framework for minimizing lifecycle costs, combining design and real-time control strategies to enhance system performance and longevity. The effectiveness of these methods is demonstrated through three case studies: Chapter 6 details the design of a fuel cell and battery hybrid electric marine propulsion system; Chapter 7 investigates a natural gas engine hybrid electric propulsion system, emphasizing trade-offs in performance and emissions; and Chapter 8 explores a battery-ultracapacitor HESS for BEVs operating under harsh loads and in low-temperature conditions, highlighting active thermal management and real-time optimal control. Finally, Chapter 9 summarizes the dissertation's findings, contributions, and implications, concluding with recommendations for future research to address emerging challenges in clean propulsion system optimization.

Chapter 2. Related Work

2.1. Performance and Degradation Modelling of Li-ion Batteries

The Li-ion battery is the most mature battery technology, has stable performance and is the most widely used battery. Electric vehicles have been commercialized and are developing rapidly. The quality of the battery will affect the driving experience of the vehicles. Compared with other commonly used batteries, Li-ion batteries have the characteristics of high energy density, high power density, long life, and environmental protection, serving as one of the most commonly used power sources in clean transportation. However, the safety, durability and cost problems limit the broad application of Li-ion batteries in automobiles [4]. Furthermore, the battery life can hardly meet users' needs, which restricts the further development of electric vehicles [5].

Optimizing battery design and management should consider the impact of aging mechanisms and battery degradation. To design a better battery and improve its life span, the energy density, power density, size, shape and other vital parameters should be considered for multi-objective optimization [6]. The battery system usually comprises hundreds or thousands of single cells, and the battery management system (BMS) is essential. The BMS should be capable of estimating the battery's state of health (SOH) and applying adaptive control strategies accordingly. The performance of the battery will decrease as the battery ages. To ensure the normal use and safety of the battery, the estimation of the battery's SOH is critical. Since different working conditions have distinct effects on the future life of the battery, BMS can use optimization methods to coordinate the charging, discharging and temperature of the battery according to the aging mechanism and degradation model under different working conditions. The remaining useful life (RUL) prediction is useful for online battery management and used car evaluation. The attenuation characteristics of batteries are nonlinear, and reliable predictions are needed. A reasonable design and management system can protect the cells and battery packs from damage; make the battery work within the appropriate voltage and temperature range, ensure safety as much as possible, and extend its service life; keep the battery running at a level where the battery can meet the requirements of the vehicle state. Inaccurate SOH estimation and prediction can easily lead to misjudgment of battery operating status and increase the risk of potential safety hazards in the battery system [7][8][9].

As the SOH of Li-ion batteries is difficult to measure and susceptible to interference, a high-precision SOH estimation and prediction is a core technical challenge that needs to be solved urgently. Accurately estimating the SOH of Li-ion batteries is very important for energy management, and it has become a research hotspot for many scholars in recent years.

The latest Li-ion battery prediction and health monitoring research was reviewed in [10] and focused on summarizing technologies, algorithms, and RUL predictions for SOC estimation, current/voltage estimation, capacity estimation, and remaining power. The monitoring methods of battery charge status, capacity, impedance parameters, available power, health status, and remaining service life were reviewed in [11], and their advantages and disadvantages were compared when used online. The advantages and disadvantages of online BMS applications and their accuracy and precision were examined in [12]. It also introduced a new and promising method to estimate SOH in practical applications. In the context of embedded applications, models and estimation techniques were classified, and the working principles of each classification method were introduced in [13]. From the implementation and operating efficiency perspective in embedded systems, a comprehensive set of indicators was introduced to evaluate SOH/RUL estimation technology. The influence of external factors on battery degradation was introduced in [14], laying the foundation for SOH estimation. It also discussed the goals of SOH monitoring and summarized its application from a short-term and long-term perspective accordingly. The estimation methods were classified in [15] according to the underlying models/algorithms of big data analysis and related statistical/computing tools, and their advantages and limitations were discussed. SOH estimation methods were classified [16] according to the signals used to extract health indicators, and basic theories, advantages and disadvantages were introduced and discussed. We will study different types of typical methods and analyze their applications.

Table 1. Advantages and disadvantages of different methods.

SOH estimation and prediction method	Advantages	Disadvantages
Electrochemical model	Direct link to the theoretical foundation, able to determine the reaction process and intensity	Difficult to obtain model parameters and to conduct online prediction, low prediction accuracy, narrow applications
Empirical Model	Easy to use	Only suitable for specific types of battery
Semi-empirical model	Practical and easy to use, fewer parameters, strong timeliness	Moderate prediction accuracy
Data-driven method	No need for a physics model; it is accurate for similar cases	Poor timeliness, intensive computation

The electrochemical model can determine the internal electrochemical reaction process and reaction intensity during the battery's aging process and accurately characterize the movement law of Li-ion and the changing trend of the positive and negative active materials, which has strong theoretical support. However, the electrochemical system of Li-ion batteries is relatively complicated and has poor versatility for different conditions and strengths. Therefore, it has disadvantages such as low prediction accuracy, narrow application range, and difficulty with online prediction. The impedance from 10 MHz to 1

kHz was analyzed, and a model with good simulation accuracy was established [17]. The contribution of each component to the total impedance characteristic of each frequency band was analyzed and described. A capacity degradation model based on battery capacity test data and an empirical internal resistance growth model based on electrochemical impedance spectroscopy test data were developed in [18]. The above two models were merged to obtain a new RUL estimation degradation model, greatly improving the prediction accuracy. Incremental capacity, differential voltage, and electrochemical impedance spectroscopy on the same data set were compared, and whether these technologies provide similar information on the causes of battery degradation was analyzed [19]. The excitation current generated by the motor controller was used in [20] to amplify and filter the voltage and current to demonstrate the accurate impedance measurement obtained by using multiple sinusoidal and noisy excitation signals and comparing it with a high-precision laboratory impedance analyzer.

Empirical modelling was the first mathematical model developed for battery life estimation. The loss of discharge capacity occurs whether the battery is inactive or exercised. The inactive state, known as calendar aging, refers to storing unused batteries with no current flow. The exercised state, known as cycle aging, refers to the charging or discharging of the battery and usually has higher capacity loss and power loss than the calendar aging process [21]. Using extended cycling and calendar life tests of Li-ion batteries, the effect of aluminum concentration in the cathode on the area-specific impedance versus time behaviour of the battery was investigated in [21]. The cycle-induced capacity fading of LiFePO4 batteries was studied in [22], and a cycle life model was established. Empirical models are easy to use, but only for certain types of batteries. Existing models struggle to predict longevity accurately. Completing a calendar life model takes years, which is unrealistic in rapidly updated material. The cycle life calculation model is difficult to obtain. The proposed model does not consider the aging charging rate and is hardly used [23].

As a commonly used semi-empirical model, the equivalent circuit model constructs a mathematical model to represent a Li-ion battery and is used to describe the characteristics of the decrease in the capacity of the Li-ion battery. The equivalent circuit model does not need an in-depth analysis of the electrochemical reaction inside the battery. It uses the circuit to describe the open-circuit voltage (OCV), DC internal resistance, and polarization internal resistance of the battery to characterize the battery's external characteristics. Common equivalent circuit models include the Rint, RC, and Thevenin models. The equivalent circuit model has strong engineering practicability. Compared with the electrochemical model, it has fewer parameters and strong timeliness. However, the approximate calculation in the model will limit the prediction accuracy and cannot meet the higher accuracy requirements. Various impedance-based equivalent circuit models used for vehicle state-of-available-power prediction were compared in [24]. The dependence of voltage estimation and state-of-available-power prediction accuracy

on state-of-charge, temperature and applied current rate was analyzed in different prediction time ranges. A simplified model was proposed in [25] to ensure the model's accuracy while greatly reducing the computational complexity. The extended Kalman filter (EKF) was used to estimate the SOC of the battery under different SOH. Gray neural network was used in [26] training health indicators as the input of the gray neural network model and battery capacity degradation as its output. The proposed indicators can effectively represent the battery health status, and the model has high accuracy. The temperature compensation fractional-order model for Li-ion batteries and supercapacitors was introduced, and a global optimization was proposed based on particle swarm optimization (PSO) for online parameter identification with strict constraints in [27], which was proved by dynamic cycling conditions at different temperatures accuracy of the proposed model.

The data-driven method does not need to consider the complex electrochemical changes and related mathematical models inside Li-ion batteries. The relationship between feature parameters and health status is established by extracting the feature values of directly or indirectly measured parameters combined with data mining algorithms. As the number of samples increases, the accuracy of SOH prediction continues to improve. However, the cost of collecting data is very high, and a large number of samples also greatly increase the complexity of the algorithm and the amount of calculation, resulting in poor timeliness. The equivalent circuit and electrochemical models were combined to establish an improved battery model [28]. An enhanced battery SOH estimation method based on the unscented Kalman filter (KF) algorithm was proposed, which considered the different values of battery internal resistance under other working conditions. A new hybrid adaptive observer and EKF method was proposed in [29] to jointly estimate Li-ion batteries' SOC, internal resistance and SOH. This method provided robust performance against model uncertainty and good parameter convergence characteristics. The method of estimating the battery cell SOH from the collision deformation characteristics was studied in [30]. The artificial neural network classified the cells as safe, potentially dangerous, and unsafe according to the deformation characteristics. The finite element method was proposed to simulate the impact of the battery module. The battery SOH prediction was solved in [31] based on the deep learning technology of the cyclic neural network with memory. The estimation results were accurate for different temperatures.

2.2. Performance and Degradation Modelling of PEMFCs

As an energy conversion device, a hydrogen fuel cell system generates electrical energy through an electrochemical reaction of hydrogen fuel and oxidant air (Figure 1). Hydrogen enters from the anode and releases electrons under the action of the catalyst to form positively charged hydrogen ions. The hydrogen ions run from the anode through the electrolyte membrane to the negative electrode and combine with oxygen to produce water. At the same time, electrons continuously flow into the circuit to form an electric

current. When hydrogen fuel and oxidant air are supplied continuously, the fuel cell system continuously generates electricity.

The most suitable fuel cell technology for passenger cars is the proton exchange membrane (PEM) fuel cell, which is superior to other fuels in terms of energy density, operating temperature, fuel adaptability and material cost [32][33]. Compared with other fuels, the advantage of hydrogen is its ultra-high mass-energy density and acceptable volume energy density [34], and a fuel cell system has zero tailpipe or pump-to-wheel/wake (PTW) emissions. When green hydrogen is produced through renewable sources, the fuel cell system has zero well-to-wheel/wake (WTW) emissions.

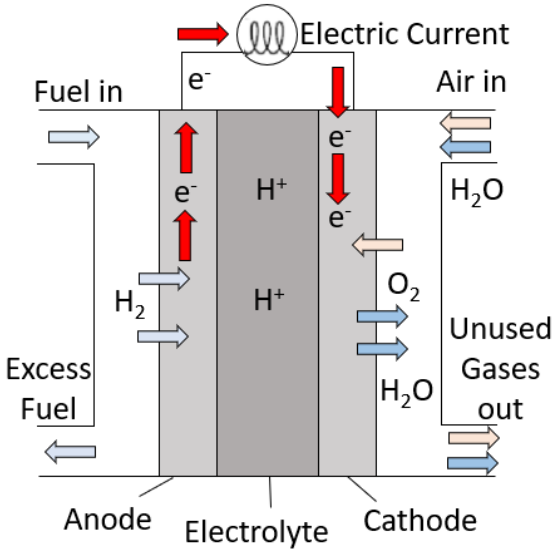

Figure 1. A diagram of a hydrogen fuel cell.

To extend the service life and reduce the cost, it is necessary to know the exact aging state of the PEMFCs, which one or more degradation indicators can characterize. The existing PEMFC prognostic methods can be roughly divided into four categories: mass transfer, empirical, semi-empirical, and data-driven. Therefore, developing more efficient and general methods is crucial for studying PEMFCs.

Mass transfer modelling involves capturing the transport of reactants, reaction products, and inerts in a fuel cell. In a PEMFC, the reactants are hydrogen on the anode and oxygen on the cathode, and the reaction product is water. Based on the dynamic cycle of fuel cells and the resulting water and gas shortage problems, the reasons for the decline of fuel cell life have been analyzed in [35], and some solutions have been proposed. Since the start-stop condition significantly influences the life of the fuel cell, the gas distribution process of the fuel cell during the start-stop process was analyzed in [36], and the main mechanisms and factors leading to the deterioration were summarized. The mechanism under start-off conditions was investigated in [37]. The cathode suffers severe and non-uniform structural damage due to carbon corrosion through a reverse current mechanism.

The significant effect of long-term enhanced road vibration conditions on the durability of fuel cell stacks has been studied in [38], with mass transfer losses increasing mainly in the high current density range.

As a standard empirical model, polarization curves are among the most common methods for testing fuel cells. The polarization curves show the voltage output of the fuel cell at a given current density load. The polarization curve is generated using a potentiostat to draw a fixed current from the fuel cell and measure the fuel cell output voltage. Slowly increasing the load on the potentiostat can determine the voltage response of the fuel cell. Polarization curves, used as an accelerated stress test for electrocatalyst degradation, were used to analyze the degradation of PEM fuel cells exposed to voltage cycling [39]. Through the experimental study on the characteristic change of the polarization curve, the steady-state performance of the fuel was analyzed in [40], and it was concluded that the enhanced road vibration has a significant effect on the steady-state performance of the fuel cell stack. Based on the cell polarization curves, the degradation mechanism of fuel cells has been studied in [41]. The early stage of the decline in fuel cell performance is mainly attributed to catalyst decay, while the subsequent sharp decline is likely caused by membrane failure. From the polarization curves, the oxygen diffusion polarization of the catalyst layer and the gas diffusion layer was evaluated in [42]. The polarization curves before and after long-term operation were analyzed, and the effects of catalyst layer degradation and gas diffusion layer were evaluated.

The semi-empirical degradation model is established as a compromise between the mechanism and empirical degradation models. The main framework of the model is based on the degradation mechanism of PEMFCs, and some parameters in the model are determined according to experimental data or expert experience [43]. Based on the observer of the extended Kalman filter, a method robust to model errors was proposed in [44]. The dynamics of the SOH and degradation are estimated; thus, the remaining life was estimated. The quality of the decay model was improved in [45] by addressing the effects of the PEMFC stack recovery behaviour. Polarization resistance parameters estimated from EIS help improve RUL prediction accuracy, and integrating SOH estimates into RUL predictions leads to a better understanding of PEMFC behaviour. A prediction method based on two sets of degradation indicators has been proposed in [46], combining directly observable stack voltage-related signals and periodic measurements of stack physical properties, resulting in methods with better accuracy than a single model.

Data-driven models have been widely used in recent years. Still, they may have difficulty adapting to the degenerate behaviour of the stack due to poor algorithm consistency or because lack of data requires more complex models to adapt to changing observations, resulting in large uncertainties and higher computational costs. A data-driven prediction method has been proposed in [47], with less learning data fitting. The prediction of stack aging was more clearly reflected, making the application easier. Based on the analysis of

the variance method, the influence of different parameters of a novel neural network paradigm was analyzed in [48], and the three sets of parameters used correspond to the parameters with greater influence in the case of fuel cell voltage aging prediction. A method based on an adaptive neuro-fuzzy inference system has been proposed in [49] to construct a prediction of the output voltage.

2.3. Optimal Design, Control and EMS for Electrified Vehicles and Vessels

In recent years, a profound transition towards electrification has permeated the automotive and maritime sectors, accelerated by a collective drive towards sustainability and urgency to restrain carbon emissions [50]. Within this period of transformation, hybrid-electric propulsion systems represent a significant step forward in the realm of transportation innovation. By integrating multiple power sources like diesel generators, batteries, and fuel cells, these configurations offer enhanced efficiency, reduced emissions, and increased flexibility compared to traditional propulsion systems. The growing interest in hybrid-electric propulsion systems signals a significant departure from conventional diesel-mechanical propulsion methods. The appeal of hybrid-electric propulsion systems extends far beyond just their ability to propel vehicles. They offer many advantages that contribute to a more sustainable and efficient transportation landscape. The most significant benefit of hybrid-electric units is their potential to reduce emissions substantially. Integrating electric power sources alongside traditional combustion engines can significantly mitigate greenhouse gas emissions and air pollutants, thus contributing to improved air quality and reduced environmental impact [51].

However, harnessing the full potential of hybrid-electric propulsion systems requires more than just assembling the right components. It involves a comprehensive process of optimization that spans both the design and control aspects, ensuring integration into the broader vehicle or ship powertrain. This optimization journey is a multifaceted endeavour characterized by a nuanced interplay of various elements such as objective functions, design variables, algorithms, and constraints. The goal is to achieve the optimal balance between performance, efficiency, and cost while meeting the specific requirements of the vehicle or vessel.

The optimal design of vehicles and ships is paramount, as it directly impacts their efficiency, fuel consumption, operational costs, and environmental footprint. A well-designed vehicle or ship can maximize fuel economy, reducing both operational expenses and emissions, thus contributing to sustainability efforts and ecological preservation.

[52] introduced an improved class of real-coded genetic algorithms for solving complex optimization problems, featuring three novel algorithms (GA–DEx, GA–DExSPS, and GA–aDExSPS) that enhance search ability through innovative crossover and selection strategies, validated on a challenging benchmark suite, demonstrating superior performance compared to existing methods. [53] presented a coordinated optimization

approach for the parameters and control strategy of plug-in hybrid electric vehicles (PHEVs), utilizing real-time optimal control based on efficiency and applying standard genetic algorithm (SGA) and quantum genetic algorithm (QGA) to enhance fuel economy and emission performance, with QGA showing superior results by suppressing premature convergence. [54] introduced the application of accelerated PSO for optimizing SoC in PHEVs, comparing its performance with standard PSO regarding charging time and battery capacity, demonstrating improvements in fitness and computation time. [55] presented a novel approach for sizing HEV powertrains using chaos-enhanced accelerated PSO, investigating various chaotic mapping strategies to achieve global optimization and demonstrating its superiority over standard accelerated PSO through Monte Carlo analysis and reputation evaluation, with logistic mapping strategy identified as the most effective algorithm for intelligent sizing. [56] presented a convex modelling approach for optimizing battery size and energy management in plug-in hybrid powertrains, demonstrating its efficiency compared to dynamic programming (DP) and highlighting its potential for optimizing problems with multiple state variables and sizing considerations due to its low computation time.

[57] presented a comprehensive design approach for coastal hybrid ships, employing constrained multi-objective optimization to size power sources and deterministic DP to devise EMSs. Through coastal ferry application examples, the method demonstrated the potential for hybrid PEMFC and battery propulsion systems to achieve substantial life-cycle GHG emission reductions, with case studies indicating at least a 65% decrease. [58] seek to optimize the ship's electrical system configuration, considering fuel cells and batteries, to minimize CO2 emissions while accommodating battery cycles and ship modifications for platform supply vessels, achieving a notable 10.69% reduction in CO_2 emissions with a specific hybrid setup. [59] proposed a multi-objective optimization approach that utilized the NSGA-II algorithm to balance fuel consumption, GHG emissions, and life cycle costs for a hybrid diesel/battery/shore power system on an anchored tug supply vessel, demonstrating significant reductions in emissions and costs compared to single-objective optimization while showcasing advantages over traditional propulsion systems. [60] introduced bi-objective optimization, integrating fuel consumption and GHG emissions, utilizing the NSGA-II algorithm and real-time experiments to validate optimal designs, demonstrating closer approximation to the ideal point compared to single-objective optimization while highlighting key variables impacting the trade-off between fuel consumption and emissions through sensitivity analysis. [61] presented a method to optimize the sizing of photovoltaic, diesel generator, and ESSs in ship power setups, aiming to minimize investment, fuel, and CO2 emissions, incorporating corrections for photovoltaic output based on seasonal and geographical variations along specific navigation routes, with detailed case studies showcasing algorithm applicability. [62] introduced a bi-objective optimization method for an uncrewed sail-assisted patrol boat's hybrid photovoltaic/battery/shore power system, leveraging NSGA-II to explore Pareto

optimal solutions and demonstrating effective reduction of GHG emissions alongside relatively low life cycle costs compared to systems without PV arrays.

We present a comprehensive review of the studies investigating optimal control strategies aboard vehicles and vessels, specifically focusing on the critical role of control and EMS. Control strategies aboard vehicles and vessels encompass various approaches, from rule-based to optimization-based methodologies. Rule-based EMS relies on predefined algorithms and heuristics to regulate system behaviour, offering simplicity and reliability in operation. Conversely, optimization-based EMS uses advanced mathematical models and algorithms to dynamically optimize system performance in real-time, accounting for diverse operational conditions and objectives. These EMS play a crucial role in coordinating the operation of onboard systems by intelligently allocating power and resources based on operational profiles and input parameters.

[63] proposed a double fuzzy control strategy for parallel HEVs, enhanced by genetic algorithm optimization validated through DP optimization, demonstrating improved engine efficiency and fuel economy performance. [64] introduced the slope-weighted energy-based rapid control analysis technique for managing energy flows in power split HEVs, demonstrating its capability to achieve near-optimal fuel economy with reduced computational costs, indicating its potential for rapid component sizing of HEV powertrains. [65] presented a DP approach to optimize the instantaneous electrical generation/electrical storage power split in series HEVs, incorporating realistic cost calculations and penalty functions for efficient computation and obtaining results for the FUDS drive cycle. [66] presented a procedure for designing a near-optimal power management strategy for hybrid vehicles using DP, aiming to minimize fuel consumption and selected emissions over a driving cycle, with implementable control rules extracted from the analysis of DP control actions, demonstrating significant emission reduction potential with a minor increase in fuel consumption. [67] introduced a predictive EMS for PHEVs, utilizing an extreme learning machine for short-term speed prediction considering travel route information and incorporating battery temperature into the cost function, demonstrating improved prediction accuracy and effectiveness compared to existing methods like PMP, model predictive control (MPC), and CD-CS. [68] presented a predictive adaptation strategy for the equivalent consumption minimization strategy (ECMS) in hybrid vehicles, utilizing future driving information to adjust the equivalence factor systematically, demonstrating less than 1.5% loss of fuel optimality under real-world driving conditions, with potential extension to other vehicle configurations. [69] introduced a novel driving-behaviour-aware modified stochastic MPC method for plug-in hybrid electric buses, incorporating driver behaviour classification and ECMS modification to achieve improved fuel economy in real-world city bus routines compared to traditional strategies. [70] proposed an energy management method for power-split PHEVs, utilizing quadratic equations to approximate fuel-rate based on battery current, applying Pontryagin's minimum principle (PMP) to determine battery current commands,

simulated annealing algorithm for engine-on power and maximum current coefficient calculation, and introducing battery SOH for improved efficiency, demonstrated through simulation to reduce fuel consumption compared to charge-depleting and charge-sustaining modes. [71] proposed a predictive EMS for multi-mode PHEVs, utilizing multi-neural networks trained on offline optimal results derived from DP and PMP, enabling real-time optimal control with reduced computation duration and improved fuel economy compared to conventional methods. [72] presented the development and experimental implementation of an energy management controller for HEVs using game theory, specifically a feedback Stackelberg equilibrium, demonstrating improved fuel consumption and NOx emissions performance over various driving cycles compared to a deterministic DP solution.

[73] proposed an optimal EMS for fuel cell hybrid electric ships that minimizes fuel consumption and power source aging costs by transforming non-convex constraints and objective terms into convex terms and integer linear forms. This work demonstrates the effectiveness of the strategy through simulation and comparative analysis. [74] developed an intelligent EMS for naval vessels with hybrid propulsion, optimizing multiple conflicting goals such as fuel savings, maintenance costs, noise, and infrared signature. It demonstrated its effectiveness through simulations on a Holland class Patrol Vessel model. [75] proposed a sizing method and real-time optimization control strategy for the HESS of a fuel cell hybrid electric excursion ferry, aiming to prolong fuel cell lifetime and improve fuel economy, system durability, and dynamic performance, demonstrated more effectively than wavelet-based and rule-based control strategies. [76] introduced a multi-scheme EMS for hybrid fuel cell/battery passenger ships, designed to optimize power distribution and improve energy efficiency, achieving significant reductions in energy and hydrogen consumption compared to traditional strategies, as demonstrated on the FUEL CELLS Alsterwasser ship model. [77] presented a method for optimizing voyage planning and multi-objective energy management in all-electric ship power systems with HESS, aiming to minimize operation cost, emissions, and ESS degradation by addressing sea state conditions and load forecasting uncertainties. [78] introduced a multi-objective optimization approach for all-electric ships that prioritizes operational cost reduction and GHG emission mitigation by integrating ESS dispatch with generation and voyage scheduling, utilizing optimal control and the non-dominated sorting genetic algorithm II. [79] introduced an enhanced energy management system for plug-in hybrid fuel cell and battery propulsion systems using a double deep Q-network, achieving a 5.5% cost reduction and a 93.8% decrease in training time compared to traditional Double Q-learning, and proposes an adaptive deep reinforcement learning scheme for dynamic environments. [80] introduced a double Q reinforcement learning-based energy management system for hybrid fuel cell and battery propulsion systems in coastal ships, achieving near-optimal average voyage costs (96.9%) compared to DP, without prior knowledge of future power demands. [81] proposed an optimal power management

method for ship electric power systems with fully electric propulsion and energy storage, aiming to minimize operation costs and GHG emissions while adhering to technical and operational constraints.

The combinatorial optimal design and control of energy systems is developed for both vehicles and ships. The design studies concentrate on selecting optimal component sizes for various propulsion system configurations, ensuring that each combination is tailored for maximum performance, energy efficiency and emission reduction. Regarding the operation control for a given propulsion system design, the EMS is optimized to achieve an efficient power share among the primary energy sources, such as batteries, fuel cells, and engines. This approach is crucial as it addresses the interplay between design and control, thereby preventing premature component performance degradation and extending the overall lifespan and reliability of the power systems.

The main contribution of [82] was the development and application of a robust multidisciplinary dynamic system design optimization method to identify the optimal component designs, state trajectories, and control strategies for a power-split HEV powertrain, accounting for system uncertainties to improve overall vehicle performance and cost efficiency. [83] developed an integrated design strategy that simultaneously optimizes both the controller and plant design of a motor driving system using a nested optimization approach and guaranteed cost control, ensuring robust performance and improved reliability under parametric uncertainties. [84] developed an operation optimization model for a PEMFC/LIB ferry propulsion system, combined with Monte-Carlo analysis, to assess the long-term effects of cost uncertainties, especially hydrogen cost, on optimal ferry operation considering performance degradation. [85] developed a multi-objective optimization method using Mixed-Integer Linear Programming and a hierarchical approach to design and operate hybrid PEM fuel cell/Li-ion battery powertrains for small passenger ferries, significantly reducing fuel cell degradation while balancing capital and operating expenditures. [86] developed a multiobjective bi-level optimization method for hybrid electric propulsion systems that simultaneously optimizes component sizing and energy management, demonstrating significant performance improvements over independent single-level optimizations through real-time hardware-in-the-loop experiments.

2.4. Real-time Optimal Control for Electrified Vehicles and Vessels

HEVs and hybrid vessels provide numerous benefits compared to traditional vehicles and vessels solely relying on ICEs. These advantages stem from their dual power sources: an ICE and an electric motor. This dual powertrain system can deliver significant benefits, including improved fuel efficiency and reduced emissions. Achieving the advantages of hybrid systems relies heavily on complex real-time control strategies that manage the interplay between the ICE and the electric motor. These strategies are crucial for optimizing fuel economy and minimizing emissions.

The control system dynamically allocates power between the ICE and the electric motor based on real-time driving conditions, battery state of charge (SOC), and driver demand. This approach ensures that each power source operates in its most efficient range. Algorithms can predict the optimal moments to switch between the ICE and the electric motor or to use both simultaneously, maximizing fuel economy. Real-time strategies can minimize emissions by ensuring the ICE operates within its cleanest operating range as much as possible and using the electric motor in situations where the ICE would be less efficient or produce higher emissions.

[87] presented an optimization problem and real-time EMS for electric and plug-in hybrid vehicles that combine UCs with Li-ion batteries to minimize fuel consumption, extend battery cycle life, and improve fuel economy by dynamically regulating power-sharing based on vehicle load estimation and driver commands. [88] presented a benchmark study for real-time optimal control of connected HEVs, utilizing a two-layer hierarchical predictive control framework to integrate eco-velocity planning and power management, significantly reducing fuel consumption while ensuring compliance with traffic rules and demonstrating feasibility through simulations and experimental assessments. [89] introduced the real-time energy-optimal deceleration planning system for connected and autonomous vehicles, utilizing real-time data and a polynomial-based deceleration model to optimize speed planning and enhance energy-recuperation efficiency by over 40% compared to drivers through DP and MPC strategies. [90] presented a reinforcement learning-based energy management system for electrified powertrains, using a real-time implementable Q-learning algorithm to develop an updated optimal control policy that dynamically determines the power-split between electric machines and the ICE in real-world driving scenarios. [91] introduced a model-based control approach for PHEVs to minimize overall CO_2 emissions through a supervisory EMS, addressing challenges such as battery depletion and vehicle-to-grid interaction, and validated through simulation studies and experimental data to optimize PHEV performance under various usage conditions and environmental factors in real-time. [92] introduced a hierarchical multilayer MPC approach for connected HEVs, utilizing approximate DP to optimize speed and power profiles in real-time, resulting in over 20% energy savings demonstrated through virtual and in-vehicle testing. [93] compared offline and online EMSs for improving the efficiency of a 48V hybrid system in an SUV, demonstrating the effectiveness of predictive online strategies like online ECMS in achieving additional fuel savings compared to non-predictive implementations, with detailed investigations into battery requirements and interactions with the energy management system through simulation-based vehicle development. [94] proposed an adaptive real-time optimal EMS for Plug-in hybrid electric buses, optimizing segment characteristics of driving cycles through offline optimization of equivalent factors and real-time adjustments based on a 2-dimensional look-up table, leading to significant improvements in fuel economy of up to 16.02% compared to baseline strategies, as validated through simulation and hardware in the loop

tests, highlighting the theoretical support for PHEV control optimization. [95] proposed a real-time cost-minimization EMS for fuel cell/battery-based HEVs, utilizing MPC to incorporate hydrogen consumption and energy source degradations in the multi-objective cost function, demonstrating significant reductions in operating costs and prolonging fuel cell lifetime by 14.17% and 8.48% on average compared to a rule-based benchmark, with online computation time per step averaging 266.26 ms, ensuring real-time practicality. [96] introduced a computationally efficient method to optimize the EMS of Formula 1 hybrid electric powertrains for achieving the best lap time, separating velocity profile optimization from energy management and formulating the problem as a convex optimal control problem, providing a benchmark for real-time strategies in race scenarios.

[97] proposed a real-time MPC-based EMS for mitigating load fluctuations in electrified ships, utilizing a battery-ultra-capacitor HESS to compensate for fluctuations, with experimental results demonstrating superior performance in system reliability, HESS efficiency, self-sustained time, and battery life compared to a baseline filter-based strategy, highlighting advantages such as reduced bus voltage variation and energy storage losses by up to 38% and 65%, respectively. [75] proposed a methodology leveraging time scale separation in IPS dynamics to achieve real-time optimization for power management in all-electric ships, developing a dynamic model capturing relevant dynamics of IPS with gas turbine and fuel cell power plants to ensure computational efficiency and optimization accuracy, with results demonstrating the real-time feasibility of the proposed strategy on a simulator. [98] introduced a novel multi-agent system cooperative controller for medium voltage AC systems in all-electric ship power systems, aiming to balance load and generation in real-time while satisfying operational constraints and prioritizing loads, effectively reducing the impact of pulse load changes on power quality, as demonstrated through dynamic behaviour evaluations in PSCAD software. [99] presented an IPS for an all-electric ship, incorporating fuel cell, battery, photovoltaic panels, and diesel generators, utilizing a dual active bridge converter and decentralized MPC strategy for efficient power management and voltage regulation, demonstrating its suitability for longer voyages and system-level studies through simulation in MATLAB/SIMULINK environment with good long-term response. [100] introduced an optimized power management strategy for all-electric ships with a DC-grid configuration, utilizing MPC and reinforcement learning methods to reduce total ownership costs by considering fuel cost, emission penalty, power device degradation, and equipment replacement cost, demonstrated through simulations of a typical tugboat load profile and comparison with traditional rule-based control.

In essence, the success of HEVs and hybrid vessels depends on the efficiency and effectiveness of these control strategies, which play a crucial role in maximizing the benefits of hybrid technology.

Chapter 3. Li-ion Batteries Performance and Degradation Modelling

The primary aim of this chapter is to develop a novel Li-ion battery degradation model capable of estimating and predicting the energy attenuation that occurs over the battery's operational lifespan. This model is segmented into two core components: a performance model and a degradation model. The performance model represents the immediate operational behaviour of the battery. The degradation model, in contrast, is designed to capture the longer-term decline in battery performance and is further subdivided into two distinct types of attenuation: permanent degradation and reversible degradation. Permanent degradation models the irreversible loss of capacity resulting from factors such as material fatigue, electrode wear, and chemical side reactions that occur over extended use. Conversely, reversible degradation addresses the capacity loss that can be recovered under certain conditions, such as temperature changes, and primarily affects short-term battery performance.

By analyzing and synthesizing extensive experimental data, we have developed a methodology for assessing the real-time health status of the battery. This approach leverages real-time measurement data, including parameters like temperature, load, current, and voltage, captured during actual battery use to update the degradation model dynamically. Through this iterative process, the model parameters are continuously refined to accurately reflect the battery's current health, enabling more precise predictions of energy attenuation and providing valuable insight into operational adjustments that can extend battery life.

3.1. Battery Performance Model

The widely used dual-polarization equivalent circuit modelling approach is adopted to represent the LFP battery performance due to its better accuracy, impedance-test attainable model parameters and ease of use in electric propulsion system design and control. The dual-polarization resistance-capacitance circuit simulates the battery's concentration and electrochemical polarization processes. As shown in Figure 2, the model has a battery open circuit voltage, V_{oc}, an internal resistor, R_i, and two resistance-capacitance circuits with R_1, C_1 and R_2, C_2. These model parameters need to be determined.

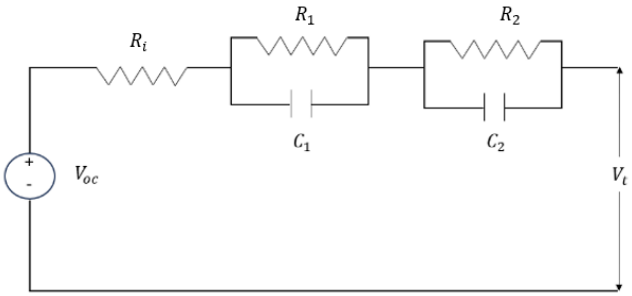

Figure 2. Dual Polarization model.

The dynamics of the dual-polarization model are described as follows:

$$\begin{aligned} \dot{V}_1(t) &= -\frac{1}{R_1 C_1} V_1(t) + \frac{1}{C_1} I(t) \\ \dot{V}_2(t) &= -\frac{1}{R_2 C_2} V_2(t) + \frac{1}{C_2} I(t) \\ S\dot{O}C(t) &= \frac{1}{Q_{cap}} I(t) \end{aligned} \tag{1}$$

where $V_1(t)$ and $V_2(t)$ are the voltage across C_1 and C_2 respectively, $I(t)$ is current, $SOC(t)$ is the SOC, and Q_{cap} is the battery's energy storage capacity.

Open circuit voltage is a function of the $SOC(t)$ that can be expressed in a polynomial form. The coefficients of this function need to be fitted by experimental data.

$$V_{oc}(SOC) = \sum_{i=1}^{m} \alpha_i SOC^i \ \ \alpha_i \in \mathbb{R} \tag{2}$$

The terminal voltage is derived from the Kirchhoff laws.

$$V_t = V_{oc} - V_i - V_1 - V_2 \tag{3}$$

3.2. Battery Degradation Prediction

3.2.1. Battery Performance Data under Different Use Patterns

The LiFePO4 (LFP) battery performance degradation data used in this work was provided by the State Electric Vehicle Power Battery Testing Center in Beijing, China. The tested battery is an LFP/C-type battery, which has an LFP cathode, graphite anode, and electrolyte comprised of an organic solvent with Li salt (ethylene carbonate (EC), dimethyl carbonate (DMC), and LIPF6) and various additives. The technical parameters of the battery are shown in Figure 3 and Table 2.

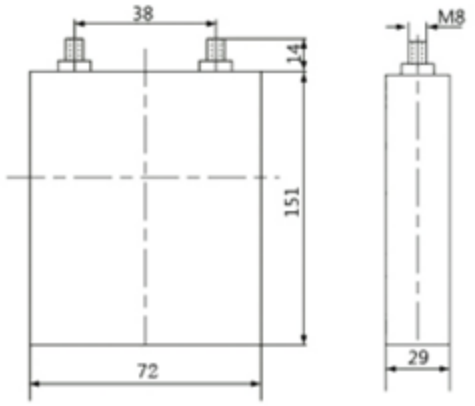

Figure 3. Product appearance and schematic diagram of battery size [101].

Table 2. Technical data sheet of Li-ion battery

Cell Technical Data Sheet	
Model	HP-NE-3R2-180A
Shell Material	AL3003
Rated Voltage	3.2V
Rated Capacity	18Ah
Weight	620±30g
Internal Resistance	~3.0 mΩ
Weight Energy Density	~120 Wh/kg
Volume Energy Density	~225 Wh/L
Power Density	≥1500 W/kg
Charge Cut-off Voltage	3.6 V
Discharge Cut-off Voltage	2.5 V

The battery is subjected to repeated charge-discharge cycles in an environmental chamber at a controlled temperature of 25^{o}C to measure the battery's capacity degradation through cycling curves. The battery was first charged at a constant current, and when the voltage reached 3.6V, it was charged at a constant voltage until the current reached 0. After a 20-minute rest, the battery was discharged at a constant current until it reached the cut-off voltage of 2.5V and rested for 20 minutes, which constituted a cycle.

Cycling tests are performed at 1C charge and 2C discharge current rates, with a capacity test of 1/3C charge and 1/3C discharge approximately every 26 cycles, where 1C means the battery is fully discharged in 1 hour. The battery capacity shows a decreasing trend over about 2,000 full charge-discharge cycles, as shown in Figure 4.

Several typical capacity cycle test data under capacity test cycles are shown in Figure 5. With the increase in the number of cycles, the charging and discharging time tends to shorten, so it can be concluded that the capacity of the battery to store energy is gradually decreasing, and the maximum capacity is decreasing.

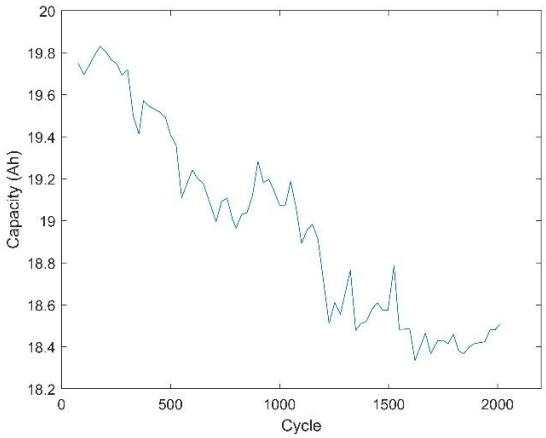

Figure 4. Battery capacity changes in test cycles.

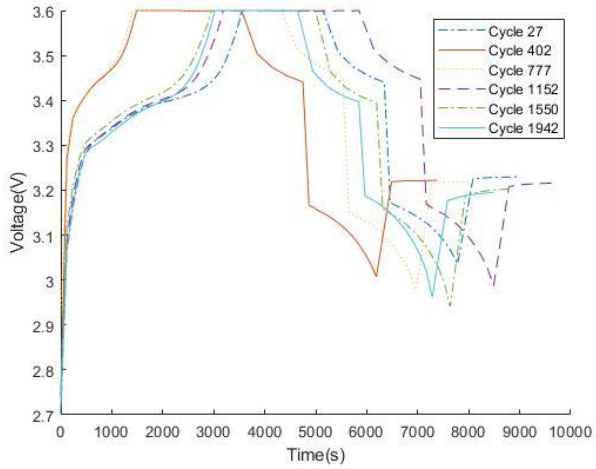

Figure 5. Voltage variation during different capacity test cycles.

The purpose of battery performance and degradation modelling is to capture the characteristics of battery performance and degradation. These models can be categorized into electrochemical, empirical and semi-empirical models. The generic electrochemical model is based on the battery's internal reactions during operations and aging. However, accurately modelling the battery's complex electrochemical reactions under different operation conditions is extremely difficult. On the other hand, the empirical models built using test data directly reflect the behaviour of a specific battery under a particular operation and time, with limited value for broader electric propulsion applications. As a result, the semi-empirical models that use theoretical model formulas and experimentally determined model parameters combine both advantages and become the most commonly used modelling platform.

3.2.2. Battery Performance Data under Different Temperatures

The battery OCV changes under different temperatures. The cold temperature slows down the chemical reactions within the battery, reducing the availability of electrons and ions,

which results in a lower OCV. [102] shows the changes in battery voltage under different C-rates from 40 to -25 °C. The battery voltage changes with time during discharge at various ambient temperatures of −20°C, −5°C, 10°C, 25°C, and 40°C at the different discharge rates are shown in Figure 6.

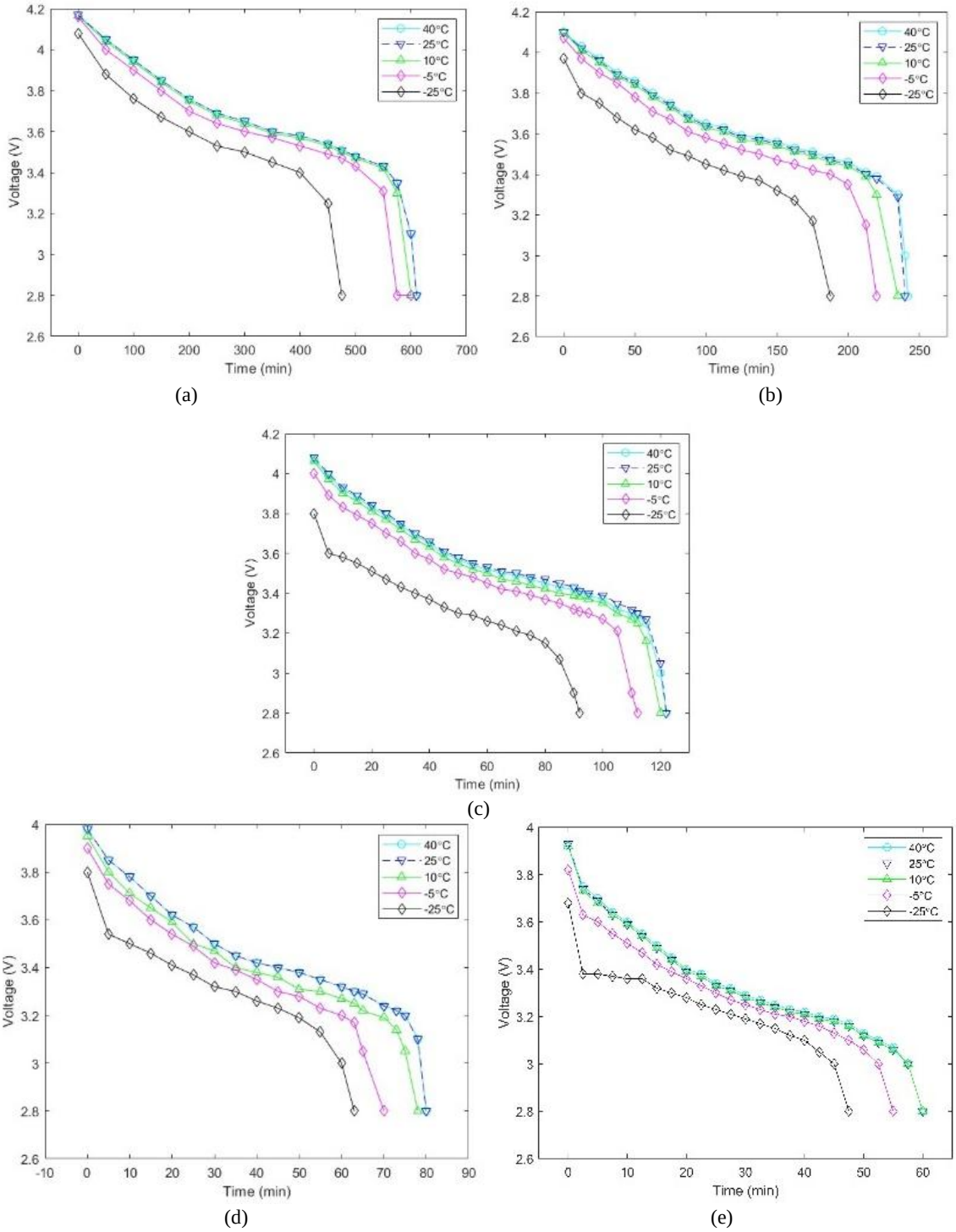

Figure 6. Discharge voltage change curve: (a) 0.1C discharge rate; (b) 0.25C discharge rate; (c) 0.5C discharge rate; (d) 0.75C discharge rate; (e) 1C discharge rate [102].

Studies [103][104][105] illustrate the temperature-induced variations in battery capacity. The red solid line is the fitting result.

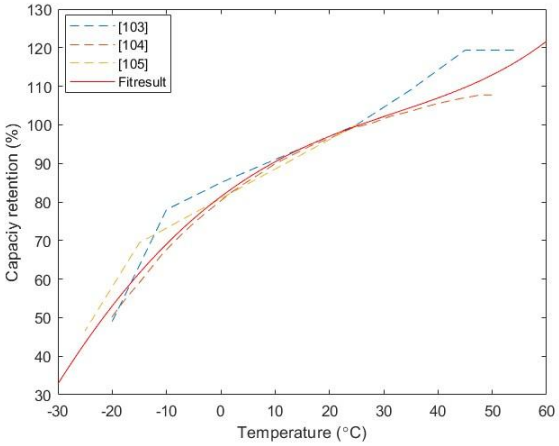

Figure 7. Effect of temperature on Li-ion battery capacity.

3.2.3. Battery Capacity Degradation Modelling

The degradation of Li-ion batteries consists of energy capacity loss and power performance loss. The energy capacity loss of the batteries over their operational cycles is commonly observed over time at different operating temperatures. The capacity loss has a power-law relationship with time or charge throughput. The battery's charge/discharge capacity degrades over its operational life of around 2,000 full charge and discharge cycles. The speed of degradation depends upon many factors, including the use pattern (charge/discharge current (*C), the depth of charge, the frequency of use, the use of the battery at almost full and almost empty), operating temperature, etc. The power performance of the battery is also slowly deteriorating over time but is less captured. In principle, the battery performance model for each charge/discharge cycle differs due to the SOH decay. These would lead to different equivalent-circuit battery performance models over the battery's operation life. These changes can be captured using varying parameters of the dual-polarization model.

The decreasing capacity of the battery is represented using the same equivalent-circuit battery performance model of the fresh batteries with a capacity correction term. The full charge/discharge cycle number, battery use pattern, and operating temperature determine this capacity correction term. The generic correction term can be described as

$$Q_{cap} = Q_{max}(1 - A \cdot e^{\frac{B+C \cdot C_{rate}}{RT}}(Ah)^D) \quad (4)$$

where C_{rate} is the discharge rate; R is the gas constant (J/(mol·K)); T the absolute temperature (K); Ah is the amount of charge delivered by the battery during cycling, expressed as $Ah = Q_{max} \cdot DOD \cdot N$, Q_{max} is the maximum capacity of the battery, N is the cycling number, and A, B, C and D are the data-fitted model parameters.

This work uses this existing semi-empirical battery capacity degradation model to guide the machining process. The state-space equations can be written as follows:

$$\begin{aligned} x_k &= [A_k; B_k; C_k; D_k] \\ A_k &= A_{k-1} + u_a \;\; u_a \sim N(0, \sigma_a) \\ B_k &= B_{k-1} + u_b \;\; u_b \sim N(0, \sigma_b) \\ C_k &= C_{k-1} + u_c \;\; u_c \sim N(0, \sigma_c) \\ D_k &= D_{k-1} + u_d \;\; u_d \sim N(0, \sigma_d) \\ y_k &= Q_{cap}(x_k) + v_k \;\; v_k \sim N(0, \sigma) \end{aligned} \tag{5}$$

By adding this battery capacity correction term, the battery's gradually degrading energy holding capacity, or capacity degradation, is captured. For a fresh battery, the five parameters of the equivalent circuit model, R_i, R_1, C_1, R_2, C_2, were determined by fitting the battery test data with minimum root mean square error (RMSE) between the measured and model output voltage. Since each specific BESS in an electrified propulsion system will undergo unique operation cycles, these laboratory cycle-life-test-determined baseline degradation model parameters should be adjusted. As different HEVs go through variant operation conditions, the same batch of batteries will present the same degradation trend with some differences in deterioration characteristics. Therefore, the parameters of the battery degradation model will change accordingly with battery aging. With fixed and predetermined degradation model parameters, a specific BESS's true performance and capacity capabilities will depart from the predicted values. A way to dynamically update these parameters using online acquired battery voltage and current data is introduced in this work to support the propulsion system's real-time optimal power control and energy management better.

Alterations in battery performance induced by temperature fluctuations are, in many cases, reversible. These changes often correspond to temporary shifts in the electrochemical processes and internal reactions within the battery. Many of these effects can be mitigated or reversed when the temperature returns to the battery's optimal operating range. Additionally, extreme temperature conditions can cause permanent damage to a battery in certain cases, leading to irreversible performance loss.

Changes in battery performance caused by specific usage patterns are generally irreversible. These usage-related changes typically result from the wear and tear that batteries experience over time because of charging, discharging, and cycling. While temperature-related effects can often be reversible when the battery returns to its ideal operating conditions, performance changes tied to usage patterns tend to be cumulative and permanent.

Low temperatures hinder the battery's chemical reactions and lead to reduced battery performance, including lower energy storage capacity, as shown in Figure 8, lower voltage output, and diminished charge and discharge efficiency. The capacity loss may be

reversible to some extent as the temperature increases, but repeated exposure to low temperatures can contribute to permanent capacity loss over time.

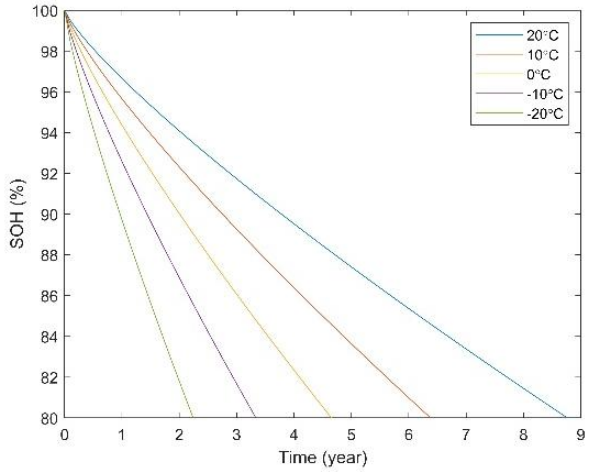

Figure 8. Battery SOH variation under different temperatures.

The temperature influence on battery performance is shown in Table 3, with an evident downward trend as temperatures decrease. At -20°C degrees, the battery's performance is significantly halved compared to its original state. Extended exposure to low temperatures exacerbates the issue, contributing to irreversible decay. This decay is evident in a decline in capacity, compromised charge retention, and an overall shorter lifespan. As temperatures drop, the battery's attenuation rate accelerates, reaching three times the original rate at -20°C.

Table 3. Battery performance and degradation rate under different temperatures

Temperature	20℃	10℃	0℃	-10℃	-20℃
Performance	100%	93%	83%	68%	50%
Degradation rate	100%	130%	169%	222%	308%

Warming up the batteries before use can help to improve their performance and mitigate these issues. Electric vehicles often incorporate BMS to monitor and optimize battery performance, including temperature control, to reduce the impact of extreme temperatures on the battery's permanent decay. Using energy in the UCs for the initial heating makes it more effective, reducing BEV performance drop and battery decay.

The figure shows the obvious voltage drop trend of the battery at low temperatures. However, the battery's voltage remains relatively stable at 25°C. The parameters correct the OCV at different temperatures to:

$$V_{oc}^{tem}(SOC) = V_{oc}(SOC) + \Delta V_{oc}(Temperature, C_{rate}) \quad (6)$$

Using the PSO algorithm to process the data, the regular changes in ΔV_{oc} can be fitted, as shown in Figure 9.

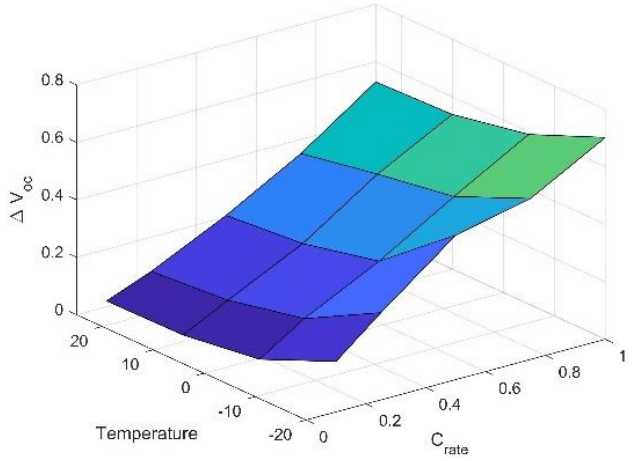

Figure 9. ΔV_{oc} changes in different temperatures and C_{rate}.

Hence, the battery voltage exhibits varying surfaces at different temperatures, notably demonstrating a conspicuous decline as temperature decreases.

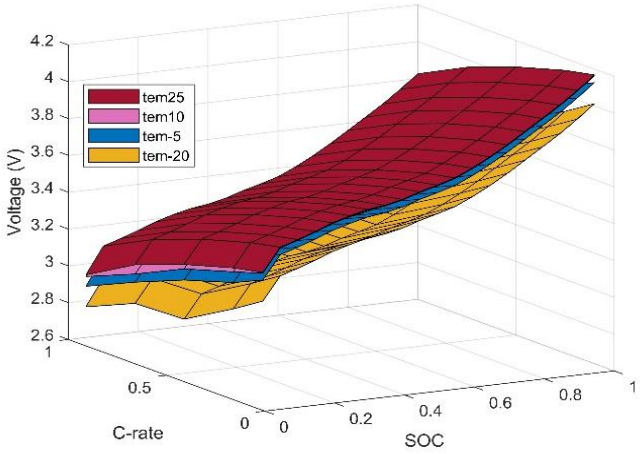

Figure 10. Voltage surfaces in different temperatures.

These valuable data were obtained and reformatted through an extensive search of numerous related literature to support this work. The values illustrated in this work provide guiding directions and scope for battery laboratory testing.

3.2.4. Battery Performance Degradation Modelling

On the other hand, the material deterioration of the battery also causes its internal resistance to increase, reducing the battery's current output capability. This power performance degradation is not captured if the same dual-polarization equivalent-circuit model is used. Therefore, adjustments to the parameters of the equivalent-circuit model are also needed. To address this source of modelling error, in this work, we identify a way

to capture the change of the internal resistance, R_i, in the equivalent circuit model, include the power performance degradation of the battery. Based on previous literature [101][106] and our modelling tests using the battery test data, we found that changes in the short-term and long-term effects of battery dynamic responses, V_1 and V_2 of the model are minimal, thus assuming capacitances C_1 and C_2 and resistances R_1 and R_2, remain unchanged during the battery's operation life. The obvious upward trend of R_i as the battery ages is captured using continuously obtained battery operation data.

Model parameters can be determined using four approaches [107]: analytical equations, least-square-based methods, heuristic optimization algorithms and Kalman filter-based methods. In this work, we use the least-square-based methods and heuristic optimization algorithms to calculate the parameters in the battery model. Then, we use Kalman filter-based methods to update the parameters of the battery degradation model in real-time using battery operation data. The battery's resistance, R_i, will change as the battery decays and its values are determined by:

$$\begin{aligned} &\min_{x} \sqrt{\frac{1}{n}\sum_{i=1}^{n}\left(V_i^m(x) - V_i^s(x)\right)^2} \\ &s.t.\ g(x) \le 0 \end{aligned} \tag{7}$$

where V_i^m is the measured voltage, V_i^s is the simulated output voltage, $x = R_i$ is the unknown parameters, and $g(x)$ is the parameter constraint.

The PSO global optimization search method is a widely-recognized optimization search scheme that provides accurate results. The variation trend of R_i, obtained using PSO, is shown in Figure 11.

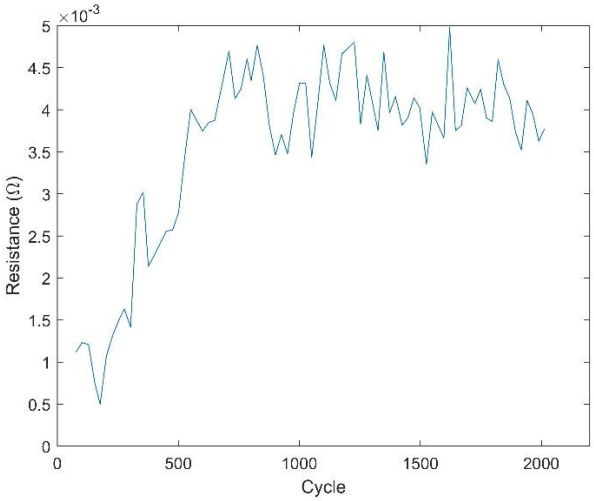

Figure 11. Resistance obtained using PSO-based fitting.

3.3. Real-time Battery SOH Estimation and Prediction

Kalman filtering algorithm uses linear system state equations to optimally estimate system states through system input and output observation data. Since the observation data includes noise and interference in the system, the optimal estimation can also be considered a filtering process. KF is an optimal recursive data processing algorithm, the most efficient and valuable method. It is widely used in various fields, including robotics, navigation, control, etc. KF estimates the state of a linear random system. However, in practice, many systems are nonlinear. When dealing with these systems, there are two common methods. EKF applies Taylor series expansion to linearize a nonlinear system, while UFK uses probability distribution to approximate nonlinearity.

The state equation and observation equation of EKF are

$$\begin{aligned} x_k &= f(x_{k-1}) + s_k,\ s_k \sim N(0, Q) \\ y_k &= h(x_k) + v_k,\ v_k \sim N(0, R) \end{aligned} \tag{8}$$

Expand (10) with Taylor's expansion at the last estimate $\hat{x}_{k-1}$ and state prediction x'_k, respectively.

$$\begin{aligned} x_k &= f(x_{k-1}) + s_k = f(\hat{x}_{k-1}) + F_{k-1}(x_{k-1} - \hat{x}_{k-1}) + s_k \\ y_k &= h(x_k) + v_k = h(x'_k) + H_k(x_k - x'_k) + v_k \end{aligned} \tag{9}$$

where F_{k-1} and H_k denote the Jacobian matrices of functions f and h at $\hat{x}_{k-1}$ and x'_k, respectively.

The EKF algorithm optimally estimates nonlinear system state through system input and output observation data. When the battery capacity is updated, EKF can correct the parameters of the degradation model in real-time, as shown in Figure 12. As a result, the updated model describes the attenuation speed of the battery more accurately, as shown in

Table 4.

Table 4. Parameters in different cycles

Number of Charge/ Discharge Cycles	A	B	C	D
Number of Charge/ Discharge Cycles	A	B	C	D
30	0.30	-15162	1516	0.77
50 1000	0.30 0.35	-15162 -15162	1516 1516	0.77 0.80
1000 2000	0.35 0.38	-15162 -15162	1516 1516	0.80 0.83
2000	0.38	-15162	1516	0.83

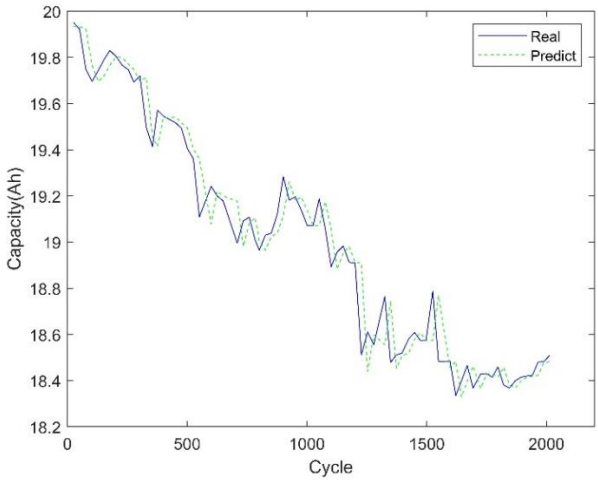

Figure 12. Real capacity and predicted capacity in different cycles.

3.4. Battery Thermal Model

Operating temperature plays a pivotal role in determining battery degradation rate, and gaining a thorough comprehension of the temperature fluctuations induced by heat generation during battery charge and discharge is essential for precise capacity loss prediction. For this purpose, [108] proposed and validated the thermal-electrochemical model, which simplifies the internal heat generation during standard charge/discharge operations as follows:

$$\dot{Q}_{cell} = I_{cell}\left(V_{oc} - U_{cell}^{avg}\right) + I_{cell}T_{cell}\frac{\partial U_{cell}^{avg}}{\partial T_{cell}} \tag{10}$$

Considering the heating device, the complete battery thermal model is described as [109]:

$$n_s n_p C_{cell}\frac{dT_{cell}}{dt} = P_{heat}\eta_{heat} - h_{cell}(T_{cell} - T_{env}) + n_s n_p \dot{Q}_{cell} \tag{11}$$

where C_{cell} is the thermal capacity of the battery cell, P_{heat} is the heat power, h_{bat} is the heat transfer coefficient, η_{heat} is the heating efficiency and T_{env} is the ambient temperature.

Heating of the batteries at low temperatures is done through active heating using the energy from the UCs in the HESS and by the self-generated heat from the battery use, as described in the following sections.

3.5. New Data-driven Model Parameter Determining Method

Predicting the impact on the remaining useful life of the battery under various working conditions, including the current, depth of discharge (DOD), and frequency of charges and discharges, is critical to the optimal sizing of the battery ESS and the optimal power control/energy management of the battery ESS for EVs, marine vessels and all

mechatronic systems using a battery ESS. These impacts are application-specific, and custom optimal design and EMSs are needed to reduce the system's life cycle cost.

The data-driven modelling and prediction method uses historical data to predict the battery's aging trend without understanding the complex and less predictable aging mechanism and expansion law. Furthermore, this method does not build a specific physical model but a statistical or machine-learning model using experimental data. Because the data-driven method avoids the complex form identification and parameter fitting processes in theoretical and semi-empirical modelling, the approach is more flexible and easier to use. As a result, it has attracted widespread attention from researchers worldwide.

GPR is a valuable tool in machine learning. Regression aims to find a function that describes a given set of data points as closely as possible. A Gaussian process assigns each such role a probability value for this purpose. The mean of this probability distribution represents the most likely representation of the data. The basic idea of GPR is that n points (x, y) are known, and the original n ys are regarded as obeying Gaussian distribution. For the new $n+1$, the $n+1$ ys still follow a joint normal distribution.

ANN is a nonlinear, adaptive information processing system composed of many interconnected processing units. It consists of a large number of interconnected nodes. Each node represents an activation function. Each connection between two nodes represents a weighted value for the signal passing through that connection. The network's output varies according to the network's connection method, weight value, and excitation function.

BP neural network is a multi-layer feedforward network trained by an error BP algorithm, and it is one of the most widely used neural network models. The BP network can learn and store a large number of input-output pattern mapping relationships without revealing the mathematical equations describing this mapping relationship in advance. Its learning rule is to use the steepest descent method to continuously adjust the weights and thresholds of the network through BP to minimize the sum of squared errors of the network.

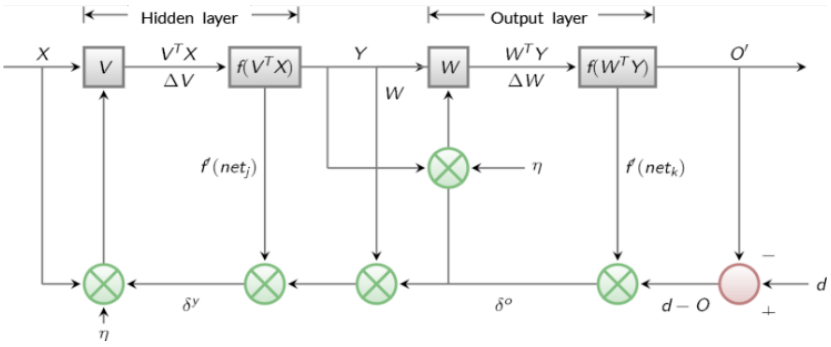

Figure 13. Signal flow diagram of BP algorithm.

In this chapter, since the voltage shows regular changes in different cycles, the voltage values at various time points are used to estimate and predict the battery's capacity.

To evaluate the prediction performance of the proposed ensemble method, we use the RMSE $\mathrm{E_{RMSE}}$, the mean absolute error $\mathrm{E_{MAE}}$ and the $\mathrm{R^2}$ coefficient as the evaluation indicator.

$$\begin{aligned} E_{RMSE} &= \sqrt{\frac{1}{T}\sum_{i=1}^{T}\left(Q_i^{pre} - Q_i^{act}\right)^2} \\ E_{MAE} &= \frac{1}{T}\sum_{i=1}^{T}\left|\frac{Q_i^{pre} - Q_i^{act}}{Q_i^{act}}\right| \\ R^2 &= 1 - \frac{\sum_{i=1}^{T}\left(Q_i^{pre} - Q_i^{act}\right)^2}{\sum_{i=1}^{T}\left(Q_i^{ave} - Q_i^{act}\right)^2} \end{aligned} \tag{12}$$

where Q_i^{pre}, Q_i^{act} and Q_i^{ave} represent the predicted, actual and average battery capacity. For the indicators E_{RMSE} and E_{MAE}, when their value is close to 0, the estimation accuracy is higher. The estimation accuracy is higher for the indicator, R^2, when its value is close to 1.

Several specific capacity cycle test data under capacity test cycles are shown in Figure 14. With increased cycle numbers, the charging and discharging time declines, indicating a gradual decrease in the battery's maximum energy storage capacity.

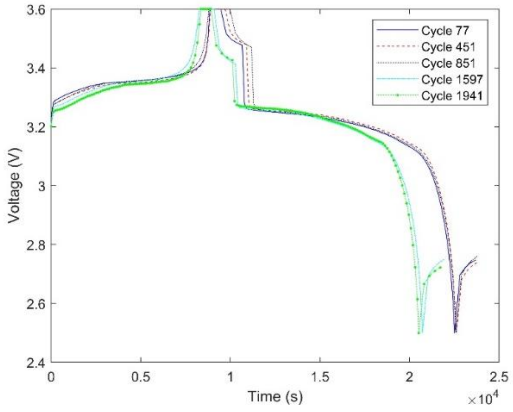

Figure 14. Voltage variation during different test cycles.

Since the offline global optimization requires extensive computation and time, it is not conducive to the real-time estimation of the battery's SOH. The battery voltage exhibits a continuous change in operation, and voltage values at various times are used in this work as features to estimate and predict the capacity and resistance of the battery.

The model testing set is uniformly sampled using ¼ of the total battery experimental data. The remaining ¾ of the experimental data is used as the model training data set, considering the characteristics of the voltage curve sampled at different time points as input. In GPR, the distribution of possible functions is updated by probabilistic inference

and data points, while in ANN, a function is approximated by updating parameters. After the training set is trained based on different algorithms, the battery's capacity in the test set is estimated. Then, based on the generalized model of the battery, KF is used to predict the SOH in the future cycles of the battery. Finally, the results of different combinations of algorithms are compared in terms of accuracy and needed computation time.

The data-driven modelling and prediction method uses historical data to predict the aging trend of the battery without fully understanding the aging mechanism and expansion law. Furthermore, this method does not build a specific physical model but a statistical or machine-learning model using data. Since the data-driven method avoids the complex form identification and parameter fitting processes in theoretical and semi-empirical modelling, the approach is more flexible and easier to use, thus attracting widespread attention from researchers worldwide. The tested data-driven modelling and prediction methods include GPR, BP neural network and Support vector machines (SVM). The accuracy of the three data-driven methods is relatively high. Comparing the conclusions in **Error! Reference source not found.**, GPR has the highest accuracy in the training set a nd takes 0.5s, which is much shorter than BP and SVM. The BP accuracy is relatively low, taking 0.7s, and it is a comparatively efficient method. SVM has the highest accuracy in the test set, but it takes 2.7 seconds, which is longer than the other two algorithms.

Compared with directly using the optimization algorithm that takes more than 2,000 seconds, the data-driven method is more conducive to real-time updating of battery parameters during use, slowing down battery decay and prolonging battery life.

Table 5. Comparison of different algorithms for battery capacity

Testing Object	$\boldsymbol{RMSE}$	$\boldsymbol{MAE}$	$\boldsymbol{R^2}$
Train_GPR_Cap	0.058710	0.002234	0.984227
Train_BP_Cap	0.073021	0.002247	0.975131
Train_SVM_Cap	0.053577	0.002267	0.986612
Test_GPR_Cap	0.081044	0.003346	0.973332
Test_BP_Cap	0.098060	0.004325	0.963013
Test_SVM_Cap	0.060300	0.002677	0.985237
Train_GPR_R	0.000076	0.019895	0.994817
Train_BP_R	0.000331	0.073684	0.900441
Train_SVM_R	0.000174	0.055141	0.972568
Test_GPR_R	0.000394	0.087962	0.893481
Test_BP_R	0.000477	0.162650	0.852312
Test_SVM_R	0.000341	0.116310	0.920083

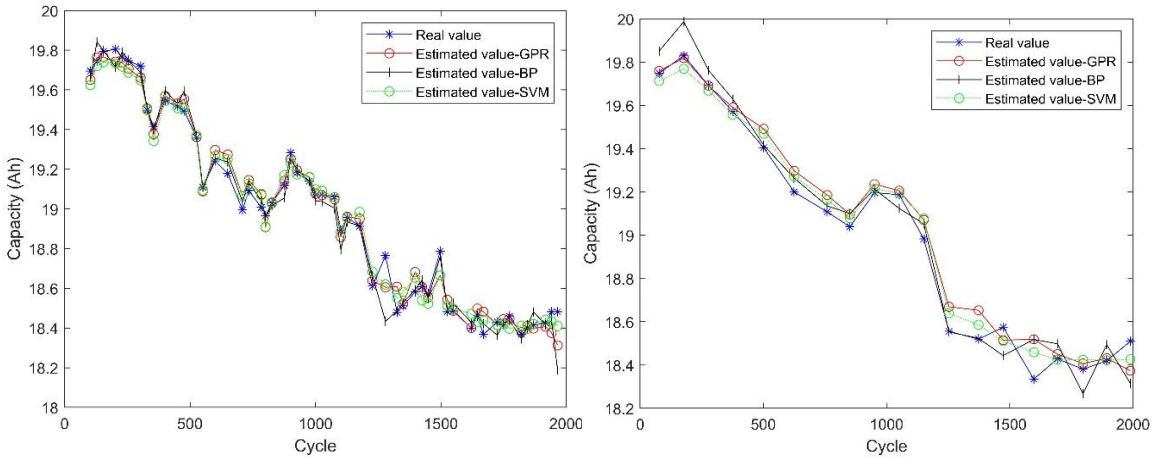

Figure 15. Estimation of battery capacity based on cycling train cycles and test cycles.

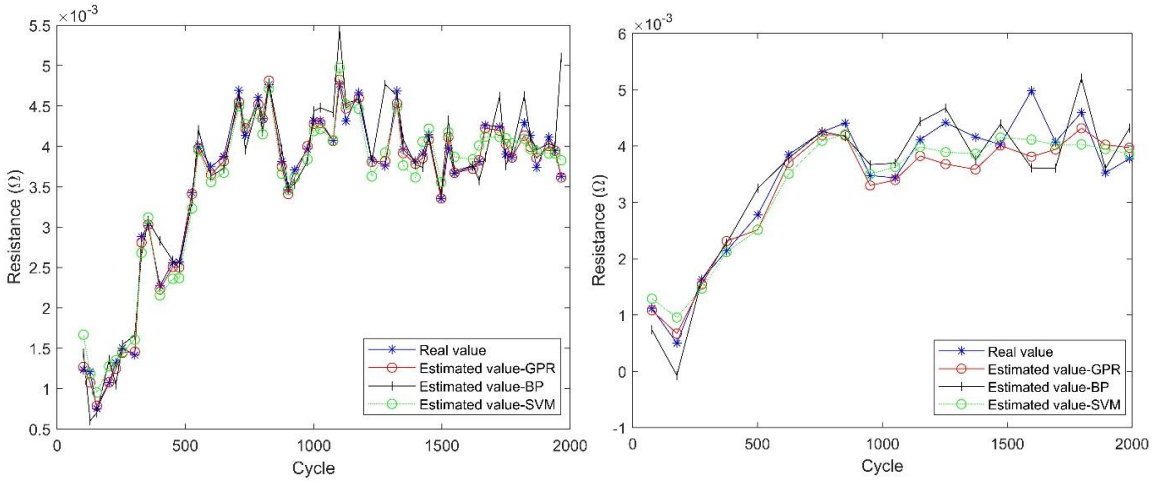

Figure 16. Estimation for resistance based on cycling training cycles and test cycles.

The BESS is a key component of the hybrid electric propulsion system that decouples the direct link between the vessel's propulsion power demands and the propulsion power supply from the gensets. The NG engine's higher fuel efficiency and lower emissions at preferred operating torque and speed region are obtained using the BESS to absorb excessive energy at low power demand and release stored energy at high power demand. The capability of the BESS is measured by its electric power output and energy storage capacities using its performance model. These capacities, however, will decay differently depending on the actual battery use patterns, measured by its performance and capacity degradation models. Since the vessel performance affecting batteries' internal resistance and energy-holding capacity cannot be measured in real-time, the electric current and voltage declines are used to gauge the degradation and estimate the batteries' SOH.

The attenuation process may accelerate under undesirable use of the battery. Certain usage patterns can stress the battery more and contribute to faster capacity decay.

Monitoring the battery's health status in real-time and adjusting the hybrid propulsion system's EMS accordingly can reduce battery decay and optimize its performance. The enhanced EMS optimizes the hybrid electric propulsion system's operation and minimizes the rate of battery capacity decay, thereby improving the overall performance and longevity of the battery. This approach allows for timely adjustments to the control strategy based on the actual SOH of the battery, optimizing its operation and mitigating degradation.

Under the same SOH, different discharge rates and SOC will produce different battery output voltages. The general trend is that the higher the battery SOC, the higher the voltage, and the higher the discharge rate, the lower the voltage. The experimental data of the battery is shown in Figure 17. Two curves of 1/3C and 2C were obtained.

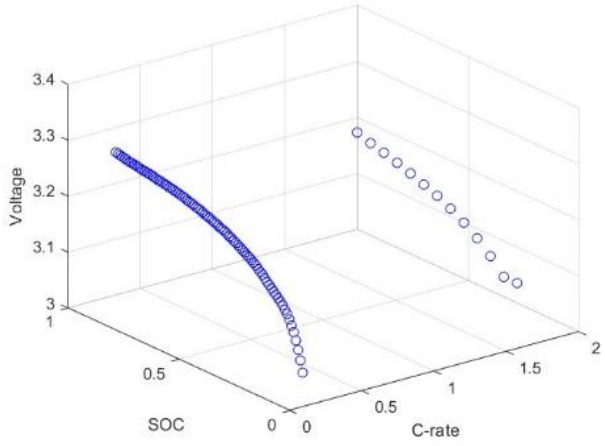

Figure 17. Battery voltage in different SOC and C-rate.

These two curves can produce a surface model through polynomial fitting. Various surface models can be generated using different cycle data. As batteries age, their output voltage shows a clear downward trend. Analyzing over the 2,000 cycle data led to 16 surfaces, denoting various SOH. Figure 18 illustrates six of these representative surface models.

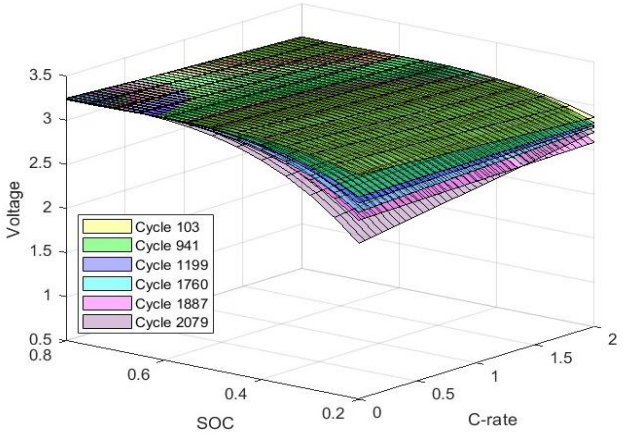

Figure 18. Voltage surfaces in different cycles.

By measuring the distance between the battery's present status point and the voltage surface, an understanding of the battery's health status and its proximity to different stages of degradation can be obtained. In Figure 19, the evaluation of the battery's health state among the 16 levels is depicted over each cycle. With cycle progression, the battery transitions progressively from surface 1 to surface 16, aligning with the principle of decay.

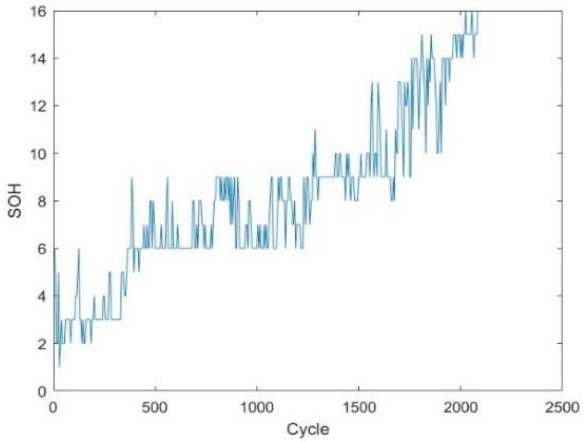

Figure 19. SOH evaluation in different cycles.

The LFP/C battery's performance and degradation data obtained from extensive laboratory tests and acquired during the ferry operation should present closely resembled behaviours due to their shared chemistry, production process and packaging. The output voltage surface is used as a reference to categorize the battery's different health stages or levels. The battery status point refers to the voltage observed during laboratory testing and vessel operation. This information is used to monitor BESS' SOH, predict the remaining useful life, and adjust the EMS of the hybrid propulsion system.

Chapter 4. PEMFC Performance and Degradation Model

Over the past years, significant efforts have been dedicated to modelling PEMFC performance and degradation. One of the primary factors contributing to PEMFC degradation is the frequently changing load conditions, which lead to dynamically shifting operating environments. These fluctuations cause voltage variations at the PEMFC outputs, adversely affecting the materials and components of the fuel cell. As a result, the active area of the PEMFC gradually diminishes over time, leading to a decrease in overall performance and efficiency. This degradation process underscores the importance of developing robust EMSs to mitigate the impact of such fluctuations and extend the lifespan of PEMFC systems.

4.1. PEMFC Performance Model

The polarization curves of the PEMFC at different periods over two years are generated to observe and compare the SOH of the PEMFCs [110][111]. The PEMFC system model is based on the semi-empirical Generalized Steady-State Electrochemical Model (GSSEM) that can reliably predict the performance of a PEMFC system [112][113][114]. The polarization curves at different SOHs were fitted to determine the parameters of the GSSEM models.

The voltage of the PEMFC is described as [114]:

$$V_{cell} = E_{nernst} + \eta_{act} + \eta_{ohmic} + \eta_{conc}, \tag{13}$$

where E_{nernst} is the Nernst voltage, an expression for the electromotive force for a given product and reactant activity; η_{act} is the activation overvoltage, the amount of voltage used to drive the reaction; η_{ohmic} is the ohmic overvoltage, the amount of voltage lost by the electron flow resistance in the electrode and ion flow resistance in the electrolyte, and η_{conc} is the concentration overvoltage, covering the voltage lost when the concentration of the reactant at the electrode decreases.

The loss of activation overvoltage can be reduced if the temperature or pressure in the PEMFC increases, thereby increasing the reaction rate. However, activation overvoltage irreversibility is significant for PEMFCs operating in the temperature range around 65–85℃. Its semi-empirical equation is described as follows [114][115]:

$$\eta_{act} = \xi_1 + \xi_2(A)T + \xi_3 T ln\left(C_{O_2}^{Interface}\right) + \xi_4 l\, n(i), \tag{14}$$

where $C_{O_2}^{Interface}$ is the concentration of oxygen around the catalyst, T is the stack temperature, i is the current density, ξ coefficients are determined empirically for each PEMFC, and $\xi_2(A)$, as a function of effective active cell area, which includes the degradation term proposed to account for the linear degradation model of the reduction in catalytic activity.

The ohmic voltage produced by the reaction is lost due to the resistance to the flow of electrons in the electrodes and graphite collector plates and the resistance to the flow of ions in the electrolyte and can be expressed according to Ohm's law as [113]:

$$\eta_{ohmic} = -i\left(R_{electronic} + R_{protonic}\right), \quad (15)$$

where $R_{electronic}$ is assumed to be a constant over the operating temperature of the PEMFC, but it is insignificant compared to $R_{protronic}$, thus ignored. $R_{protronic}$ is a function of the moisture content and distribution in the membrane. The general expression is given by [116][117]:

$$R_{protonic} = \frac{r_M(i,T)l}{A}, \quad (16)$$

where r_M is the membrane-specific resistivity for the flow of hydrated protons, l is the membrane thickness.

Concentration loss is caused by mass transfer; when hydrogen and oxygen are extracted, the concentration of the reaction will decrease, leading to a voltage loss due to the pressure drop of the reacting gas. The concentration overvoltage depends on the drawn current and the physical characteristics of the gas supply system [22].

$$\eta_{conc} = \frac{R_u T}{2F} \ln\left(1 - \frac{i}{i_L}\right) \quad (17)$$

where R_u is the universal gas constant, F is Faraday's constant, i_L is the limiting current density.

4.2. PEMFC SOH Estimation and Prediction

4.2.1. PEMFC Experimental Data

The FCEV operation data used in this study were recorded from operating a PEMFC and LFP BESS hybrid city bus. During the one-year (361 days) operation, the PEMFC system worked 1,908 hours, and the FCEV travelled 50,935 km. The data sampling interval is 10 seconds. The voltage and current data of the PEMFC stack at different times are shown in Figure 20.

The output power of the PEMFC system showed an obvious downward trend, and the corrosion of the electrocatalyst layer is an important factor affecting the durability and life of the PEMFC [110]. Catalyst degradation is due to platinum agglomeration and oxidation. Sustained degradation reduces the available catalyst surface in the anode and cathode, leading to power loss [110][111].

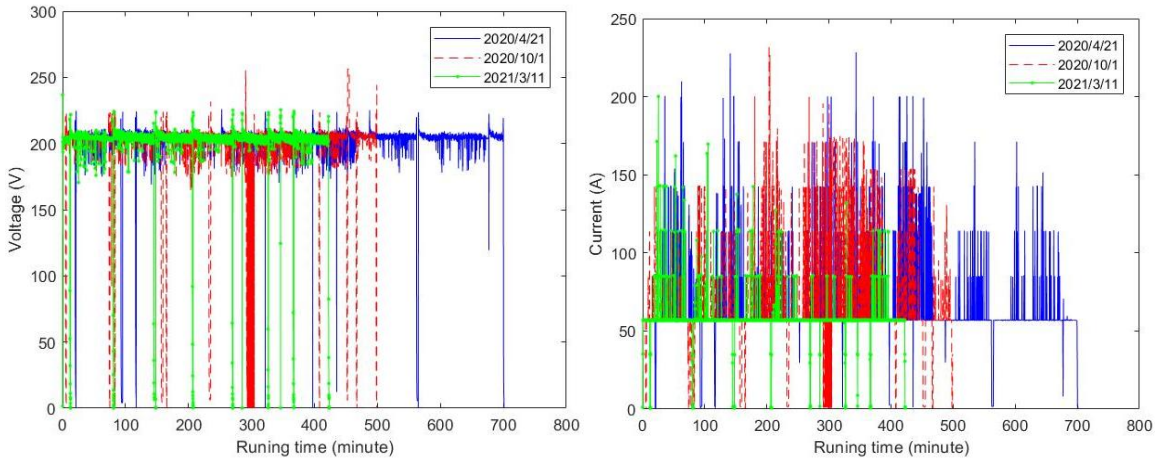

Figure 20. Voltage (left) and current (right) data of the stack.

4.2.2. PEMFC Degradation Model

Considering the activation, ohmic and concentration losses, the PEMFC voltage degradation can be represented as [116]:

$$v_{cell} = E_{Nernst} + a_0 + \delta_a t + b_0 ln(i) + (R_0 + \delta_R t)i + \frac{R_u T}{2F} ln\left(1 - \frac{i}{i_{L0} + \delta_L t}\right) \quad (18)$$

where a_0, R_0 and i_{L0} are the initial value of $\xi_1 + \xi_2(A)T + \xi_3 T ln\left(C_{O_2}^{Interface}\right)$, $R_{electronic} + R_{protonic}$ and i_L respectively; δ_a, δ_R and δ_{L0} are the increasing rates.

The active area of the PEMFC will gradually decrease with the degrading catalyst and deteriorating health. Unfortunately, the active area, *A*, cannot be measured experimentally or obtained in real-time. Instead, these active areas at different times are determined by fitting the measured voltages using an optimization algorithm, such as the genetic algorithm.

$$\begin{aligned} &\min_A \sqrt{\frac{1}{n}\sum_{i=1}^{n}\left(V_i^m(A) - V_i^s(A)\right)^2} \\ &s.t.\ g(A) \le 0 \end{aligned} \quad (19)$$

where V_i^m is the measured voltage, V_i^s is the simulated output voltage, and $g(A)$ is the constraint on the model parameters. The active area at different times is shown in Figure 21, showing a clear downward trend.

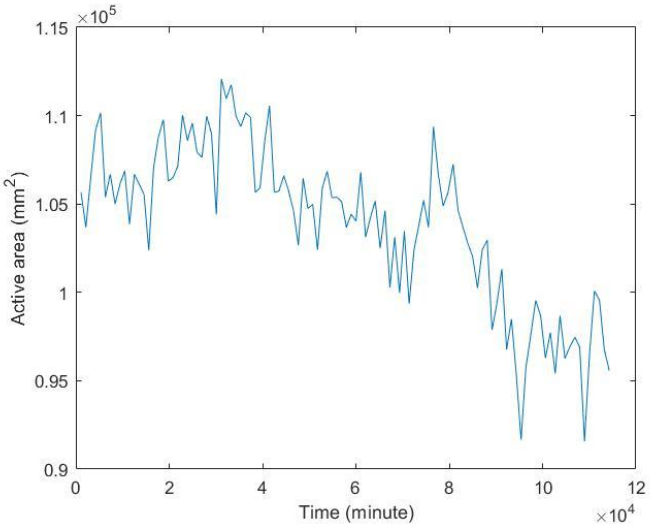

Figure 21. Modelled active area changes of PEMFC.

Compared to the previous work that used observed voltage drop and nonlinear methods for predicting PEMFC lifetime [116][117], the GSSEM method improved modelling accuracy by 54%. Furthermore, if only the voltage drop trend is observed, hydrogen consumption and PEMFC decay cannot be accurately calculated under different power outputs. Estimating the active area loss using GSSEM is more accurate and useful.

4.3. Data-driven Modelling of PEMFC Performance and Degradation

The current and voltage of the PEMFC are recorded in its operation. Current and corresponding voltage values and operation time data are used as training data sets to form the models for predicting PEMFC's active area. One-third of the collected data were used to verify the capabilities of these trained models. The results are shown in Figure 22.

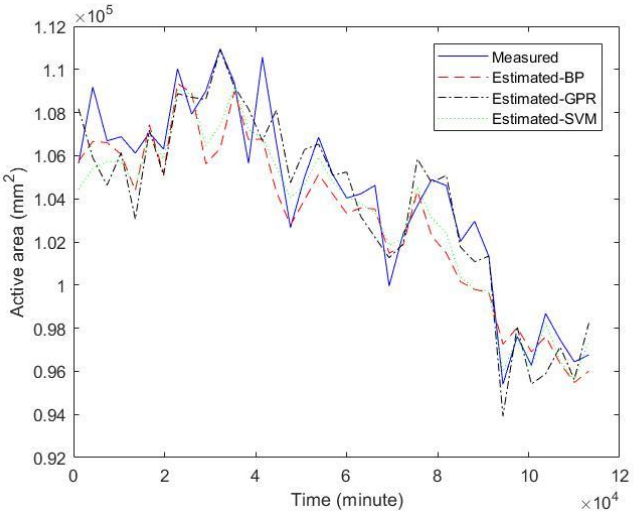

Figure 22. Estimation of the active area.

The predicted active area is an important parameter of the PEMFC performance and degradation models. It indicates the PEMFC's performance and level of degradation. This parameter is updated in real time during PEMFC operation to support more accurate, optimal power control and EMS.

Chapter 5. Integrated Design and Control Optimizations and Real-time Optimal Control

5.1. Design Problem

The EV market is expanding rapidly, driven by increasing environmental awareness and fluctuating gasoline prices. CEs have served as the dominating power plants for ground and marine propulsions for over a century. Still, they are major contributors to air pollution and greenhouse gas emissions. These engines rely on fossil fuels like gasoline and diesel, which release significant amounts of CO_2, NO_x, and particulate matter (PM). Additionally, ICEs are inefficient, converting only about 25-30% of the fuel's energy into mechanical power, with the remainder lost as heat. This inefficiency and environmental concerns have accelerated the push for alternative propulsion systems, such as BEVs and FCEVs.

Hydrogen fuel cells offer even greater environmental benefits by producing only water as a byproduct and can be sourced from renewable energy, enabling zero-emission transportation. However, they face challenges, including limited infrastructure for hydrogen production, storage, and distribution and degradation over time, which reduces their efficiency. LNG presents another cleaner option, emitting fewer pollutants than gasoline and leveraging existing infrastructure, particularly for large-scale applications like shipping. However, LNG still produces carbon emissions and requires cryogenic storage due to its low boiling point, complicating its handling and distribution. Replacing gasoline with batteries can achieve zero tailpipe emissions and significantly reduce greenhouse gas emissions, especially if the electricity comes from renewable sources. Batteries are more efficient than ICEs and require less maintenance due to having fewer moving parts. However, battery capacity degrades over time, reducing performance and range.

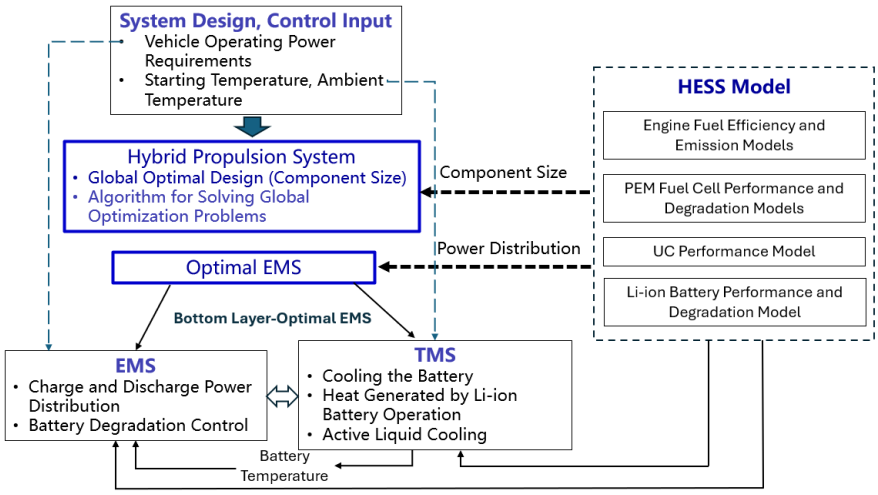

Figure 23. Real-time optimal control unit for a hybrid propulsion system.

Hybrid propulsion systems are emerging as a promising solution to address these challenges. They combine multiple power sources, typically integrating an ICE or hydrogen fuel cell with an electric motor powered by a battery or supercapacitor. This hybrid approach allows for the complementary use of energy sources, where the ICE or fuel cell provides high energy density and range. At the same time, the electric motor enhances efficiency and reduces emissions, particularly at low speeds or during start-stop operations. Hybrid systems also benefit from regenerative braking, which recaptures energy to recharge the battery or supercapacitor. Although more complex and costly to design and maintain, hybrid systems strike a practical balance between conventional and renewable energy technologies.

Optimizing hybrid systems requires advanced control strategies to manage power distribution between the ICE, fuel cell, battery, and supercapacitor. Real-time control algorithms are crucial for dynamically adjusting power flows based on driving conditions, thereby improving system efficiency and extending the lifespan of energy storage components. These systems can allocate power from supercapacitors during high-demand situations, reducing stress on the battery and enhancing overall performance.

In addition to energy management, thermal management is a critical aspect of HESS, especially given the susceptibility of Li-ion batteries to temperature fluctuations. Extremely high or low temperatures can significantly impact battery performance and lifespan. High temperatures can accelerate battery degradation and increase the risk of thermal runaway, while low temperatures can reduce the battery's capacity and power output. Therefore, an effective TMS is crucial to maintain the batteries within an optimal temperature range. The TMS must be designed to handle the specific thermal characteristics of each component in the HESS. For instance, Li-ion batteries may require active cooling systems, such as liquid cooling, to dissipate excess heat to the environment or a heat-pump system during high-power operations or under high environmental temperatures. At the same time, UCs might be able to power the active TMS. The TMS should also be integrated with the vehicle’s overall control system to adjust cooling or heating efforts dynamically based on real-time operating conditions. Advanced TMS control strategies can optimize the energy consumption of the cooling/heating system, thereby minimizing its impact on the overall energy efficiency of the vehicle.

Real-time TMSs continuously monitor the temperature of each component and dynamically adjust the cooling or heating to maintain the optimal operating temperature of the batteries. For example, during a cold start, the TMS can heat the battery using stored energy to ensure it operates within its optimal temperature range. By integrating thermal management with real-time control of the energy storage components, the overall efficiency and reliability of the HESS can be significantly improved. By continuously monitoring the temperature and state of charge of the battery, the control system can

take preemptive actions, such as reducing the load on the battery or activating additional cooling, to mitigate the risk of thermal runaway.

The transition from ICEs to more sustainable propulsion technologies like hydrogen fuel cells and battery-electric vehicles presents both opportunities and challenges. While hydrogen fuel cells offer a clean alternative to ICEs, they face challenges related to durability, cost, and infrastructure. Similarly, while efficient, Li-ion batteries are prone to degradation and require careful energy and thermal management to ensure longevity. HESS, which combines these technologies, offer a promising solution, but its success depends on advanced real-time control strategies. These control systems are crucial for optimizing energy management, extending components' lifespan, and ensuring electric vehicle safety and reliability. As the EV market continues to grow, developing and refining real-time control systems will be key to unlocking the full potential of sustainable transportation.

5.2. Integrated Global Design Optimization for Minimum Lifecycle Costs

The design and controls of a HEPS are interrelated. HEPS design covers mechanical, electrical and embedded control systems. Producing suitable power control and energy management strategies is important to system design. On the other hand, an inadequate system design will hinder optimal power control and energy management. Integrating a HEPS's design and control optimizations can effectively improve system efficiency and reduce the costs associated with these complex systems over their entire lifecycles. This approach involves a comprehensive optimization process that integrates various design elements and operational considerations to achieve cost efficiency from initial design to end-of-life. This approach ensures that design decisions lead to the most cost-effective solutions across the entire lifecycle of ships and vehicles, enhancing their economic and environmental performance.

A hybrid propulsion system and a hybrid energy storage system consist of multiple components, working coordinately to complement each other. To fully realize their potential, these components must be appropriately connected, properly sized, and well-coordinated, corresponding to the optimal system architecture design, sizing and control/energy management. The variation of system architecture is normally limited and, thus, can be easily compared. The optimal component sizing and system control involve infinite variations of different combinations; therefore, they need to be studied closely and conducted jointly, as just stated, as discussed in the following sections.

5.2.1. Optimal Sizing of Key Propulsion System Components

Optimal sizing of key propulsion system components such as ICE, PEMFC system, BESS, and propulsion motors and optimal sizing of key HESS components, including battery and ultracapacitor modules and DC/DC converter, requires a detailed analysis of system requirements, energy demands, and operational profiles.

The onboard energy converter, including the ICE and PEMFC systems, should be sized to meet the overall propulsion power and energy demand for different operating scenarios and to be able to operate at peak efficiency in the hybrid system most of the time. BESS must be sized to supplement the ICE/PEMFC system power under peak power demand, effectively absorb braking and surplus power to maintain maximum system efficiency and avoid quick degradation to minimize the propulsion system's lifecycle costs (LCC). Similarly, the ultracapacitors in the HESS, which are used to provide high power and thermal management power at extreme temperatures, should be sized to be able to handle large and shallow discharges/charges to reduce the load from the battery module under short-term peak power demands and absorb regenerative braking energy, extending the operation life of the battery module in the HESS. The optimal sizing must meet power demands, satisfy design constraints, and balance trade-offs between system efficiency, emissions, and LCC. This optimization is conducted by accurately modelling system performance, energy efficiency, and LCC, including investment, energy consumption, and component degradation costs, especially for high-cost and short-life PEMFCs and BESS. Simulations using the introduced system model support the performance and cost evaluations and form the design's and control optimizations' objective and constraint functions. Alternative designs can be quantitively evaluated, and the best combination of design parameters, such as component sizes and power allowance among different components, can be identified to ensure all components work together efficiently and cost-effectively over the system's lifecycle.

In the optimal design and EMS of the hybrid propulsion system, a nested global optimal model provides a comprehensive framework for balancing real-time operational efficiency with strategic design considerations, as illustrated in Figure 24.

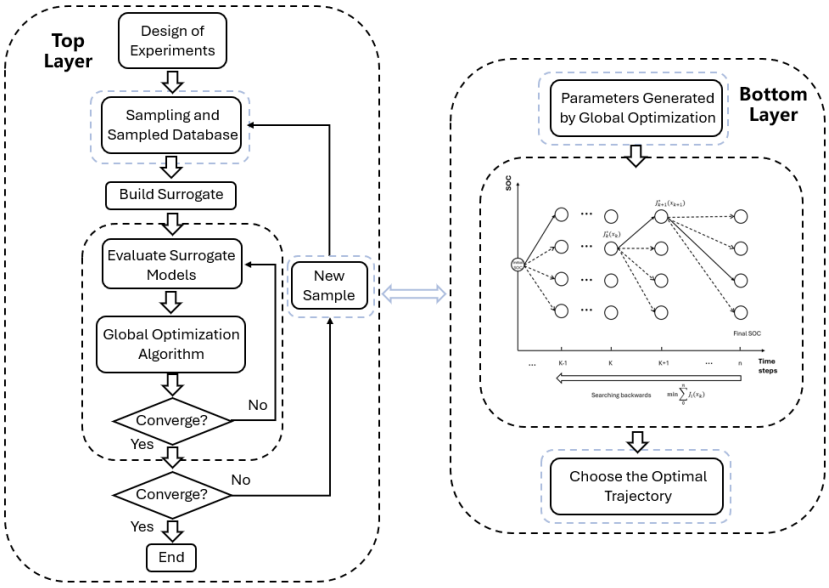

Figure 24. Optimization flowchart.

At the bottom layer, Dynamic programming (DP) search optimizes the energy allocation and flow among various energy conversion and storage components—such as ICE, PEMFC, batteries, and UCs based on current and predicted system power demands and operation conditions. This layer addresses energy needs and adjusts the system's operation at each time instance. For example, DP can optimize when to draw power from different sources, how to absorb regenerative braking energy, and how to handle power load fluctuations, ensuring that the system meets performance requirements and operates efficiently.

At the top layer, global design optimization determines the optimal sizes and configurations of the hybrid propulsion system components. This top-level design task evaluates how the system meets the overall design objectives and identifies each key system component's best size and capacity. The goal is to balance trade-offs between performance, system efficiency, emissions, costs, weight, space, and LCC. For instance, in a HESS design optimization, the lower-level DP decides how the system energy demand should be distributed between the battery and UC modules of given sizes, and the top-level global optimization might determine the optimal battery and UC module sizes to provide sufficient energy storage while considering design constraints and LCCs. This work considers the battery performance degradation costs induced by the loss of battery operation life. Adding a load-cycle and temperature-insensitive UC module to the HESS ultracapacitor capacity or best balancing system energy efficiency and battery degradation under aggressive use is the best overall system design.

The optimal design of a hybrid propulsion system can be formulated as a minimization problem with the following objective components:

- Fuel Efficiency: This objective seeks to minimize fuel/energy consumption by optimizing the energy flow between system components, such as internal combustion engines, electric motors, and energy storage devices. It often involves engine operating points, regenerative braking efficiency, and power-split strategies.
- Emissions: This objective minimizes the environmental impact by reducing the emission of harmful pollutants (e.g., CO_2, NO_x, particulate matter).
- LCC: This includes both the initial investment cost and operational costs over the system's lifetime, such as fuel, maintenance, and replacement costs. It also considers the degradation and lifespan of critical components like batteries and PEMFCs.

The minimization problem can be expressed as:

$$\min_x J = \omega_1 J_{fuel}(x) + \omega_2 J_{emission}(x) + \omega_3 J_{LLC}(x) \quad (20)$$

where $J_{fuel}(x)$, $J_{emission}(x)$ and $J_{LLC}(x)$ are fuel consumption cost, emission cost and LLC functions, respectively, x is the number of propulsion system components, ω_1, ω_2 and ω_3 are the weighting factors reflecting the relative importance of each objective.

5.2.2. Baseline Optimal Energy Management Strategies by Dynamic Programming

Optimal energy management must first meet system power demands. For electrified vehicles and marine vessels, the needed propulsion power depends on the operation velocity of the vehicle or vessel and its payloads. Accurate prediction of propulsion power can be obtained using vehicle dynamics or vessel hydrodynamic models. Based on statistical data, the standard vehicle/vessel operation speed or driving cycles are proven representative operation speed patterns. Many formed international standards, and others were derived from specific applications.

Optimal energy management aims to find the best power control and energy flow solution among system components simultaneously to meet the stated system power demands. Among different solution methods, DP optimization search provides the most accurate solution. DP involves solving a complex decision-making problem by breaking the problem into simpler, manageable subproblems over the complete duration of the operation cycle. This approach is particularly effective for systems where decisions are made sequentially over time and future states depend on current actions. The optimal EMS produced by DP using standard driving cycles is thus called Baseline Optimal EMS.

To apply DP for optimal energy management, you first define the system's state space, which includes variables such as energy levels in storage components (like batteries and ultracapacitors), power demand, and operational conditions. Next, you formulate an objective function that represents the goals of the energy management system, such as minimizing operational costs or maximizing energy efficiency, while also considering constraints like maximum power limits and storage capacities.

The core of DP involves creating a transition model that describes how the system evolves from one state to another based on different actions or decisions. Then, solve the problem by iteratively evaluating the value of each state-action pair, ultimately determining the optimal policy. This policy specifies the best action to take in each state to achieve the desired objectives.

As DP seeks the optimal global solution over the entire cycle or trip time, the power demand over the whole period must be known. The approach is ideal for supporting the generic system design optimization, which covers optimal system architecture, component sizing and optimal energy management strategies (EMS) for the given statistical driving cycle. However, it cannot be directly used in real-time optimal propulsion system control since the travelling speed, and thus the propulsion power demand, for the rest of the trip is unknown. The actual vehicle/vessel speed always departs from the statistical driving cycle during operation. In addition, DP requires extensive optimization search over a long computation time, precluding its real-time application. However, suppose there is a way to accurately predict the vehicle and vessel's travelling speed and the speed-determined propulsion demands over a very short period in the future. In that

case, DP can be applied to identify the best energy management solutions for this brief period. Section by section, a solution close to a globally optimal solution can be sought. This study introduced this approach, as discussed in the following section.

5.2.3. Solution of the Nested Global Optimization Problem

Global optimization is the ideal approach to identify the absolute best solution to complex problems by thoroughly exploring the entire search space and avoiding the pitfalls of local optima. Unlike local optimization, which only finds the best solution within a limited area, global optimization aims to uncover the true global optimum across all possible configurations. This process employs advanced techniques such as evolutionary algorithms, which simulate natural selection to evolve solutions over time, swarm intelligence methods like particle swarm optimization that mimics collective behaviour, and simulated annealing, inspired by metal cooling processes, to probabilistically explore solutions. Despite its intensive computational demands, global optimization is crucial in fields ranging from engineering design to finance, as it provides a comprehensive strategy for finding optimal solutions in complex and nonlinear scenarios, ensuring that the most effective and efficient solutions are discovered.

A surrogate model is a simplified approximation of a complex system or process that expedites optimization and analysis in the objective/constraint functions by using a simpler and quicker-to-evaluate metamodel to reduce the intensive computations needed to run the original complex optimization objective/constraint functions, thus reducing computational costs and time. Instead of relying on the computationally intensive true model, the surrogate metamodel provides a less resource-demanding way to approximate the system's behaviour based on training data. It captures the essential characteristics of the true model, allowing for faster evaluations and iterations in optimization tasks. Surrogate models are particularly valuable when evaluating the true model, which is expensive or time-consuming, such as in complex engineering designs. Using surrogate models can perform extensive optimization more efficiently, ultimately facilitating more effective decision-making and system design.

Global optimization methods based on surrogate models offer significant advantages by making the optimization process more efficient and manageable. These methods utilize surrogate models—computationally inexpensive approximations of the true objective function—to quickly evaluate potential solutions, thus dramatically reducing the computational cost associated with complex or time-consuming evaluations. This efficiency enables more effective search space exploration, allowing the optimization algorithm to focus on the most promising areas and accelerating the discovery of optimal solutions. Surrogate models can handle large-scale and high-dimensional problems by providing scalable solutions, while their ability to adapt and improve over time enhances convergence towards the global optimum. Additionally, the flexibility of surrogate models makes them suitable for a wide range of functions and constraints, accommodating

various problem complexities. By integrating surrogate models, global optimization methods manage computational resources more effectively and provide deeper insights, leading to better-informed decision-making and improved overall performance in solving complex optimization problems.

5.3. Applying Extended Kalman Filter to Blended Data

The propulsion power demand of a ship or vehicle is subject to continuous fluctuations due to various dynamic factors such as weather conditions, terrain, speed, and load variations. For ships, wind speed and direction, wave height, sea currents, and ambient temperature can significantly alter the hydrodynamic resistance, demanding more or less power to maintain speed and stability. Similarly, for vehicles, the terrain's topography—such as inclines and declines—and surface conditions like wet or icy roads directly impact the power required to propel the vehicle forward. Variations in speed due to traffic or navigational requirements, as well as changes in load (such as the number of passengers or the weight of cargo), further complicate the power demand.

Instantaneous operating data is indispensable to manage these fluctuations effectively. Real-time data acquisition from an array of sensors monitoring parameters like speed, acceleration, engine output, environmental conditions, and load status enables the development of accurate predictive models. These models anticipate future power demands based on historical trends and current conditions, allowing propulsion systems to adjust power settings preemptively. In HESS, this real-time data is crucial for optimizing the power flow between different energy sources. For example, ultracapacitors in HESS can be deployed to handle sudden bursts of high power demand, while batteries manage more sustained energy requirements, improving overall system efficiency and responsiveness.

The extended Kalman filter (EKF) is particularly well-suited for this application due to its ability to process noisy and uncertain measurements and accurately estimate the system's state, which in this context refers to the propulsion power demand.

With Taylor's expansion at the last estimate $\hat{x}_{k-1}$ and state prediction x'_k, the state equation and observation equation are.

$$x_k = f(x_{k-1}) + s_k = f(\hat{x}_{k-1}) + F_{k-1}(x_{k-1} - \hat{x}_{k-1}) + s_k, s_k \sim N(0, Q) \quad (21)$$

$$y_k = h(x_k) + v_k = h(x'_k) + H_k(x_k - x'_k) + v_k, v_k \sim N(0, R) \quad (22)$$

where F_{k-1} and H_k denotes the Jacobian matrices of functions f and h at $\hat{x}_{k-1}$ and x'_k, respectively.

The EKF prediction and updating steps are given as

Prediction:

$$x'_k = f(\hat{x}_{k-1})$$
$$\Sigma'_k = F_{k-1}\Sigma_{k-1}F_{k-1}^T + Q$$

Updating:

$$S'_k = \left(H_k\Sigma'_k H_k^T + R\right)^{-1}$$
$$K'_k = \Sigma'_k H_k^T S'_k$$
$$\hat{x}_k = x'_k + K'_k\left(y_k - h(x'_k)\right)$$
$$\Sigma_k = (I - K'_k H_k)\Sigma'_k$$

In the prediction step, the EKF uses a mathematical model of the system's dynamics, the current state estimate, and control inputs to predict the next state. In the update step, the Kalman Filter receives new measurements, such as real-time sensor data from the propulsion system or environmental sensors. It then compares these measurements to the predicted state, calculates the discrepancy (or residual), and uses this information to update the state estimate. The filter balances the new measurement against the predicted state, weighting them by their respective uncertainties. This process allows the EKF to refine its prediction of the propulsion power demand, making it more accurate over time as it continuously integrates new data.

5.4. Real-time Optimal Control Strategy

In advanced ESSs for ships or vehicles, real-time control is achieved through performance and degradation models with live operational data, as shown in Figure 25. The process begins with collecting real-time data from the system, including operational parameters such as speed, load, and power, as well as the actual output voltage of the battery pack.

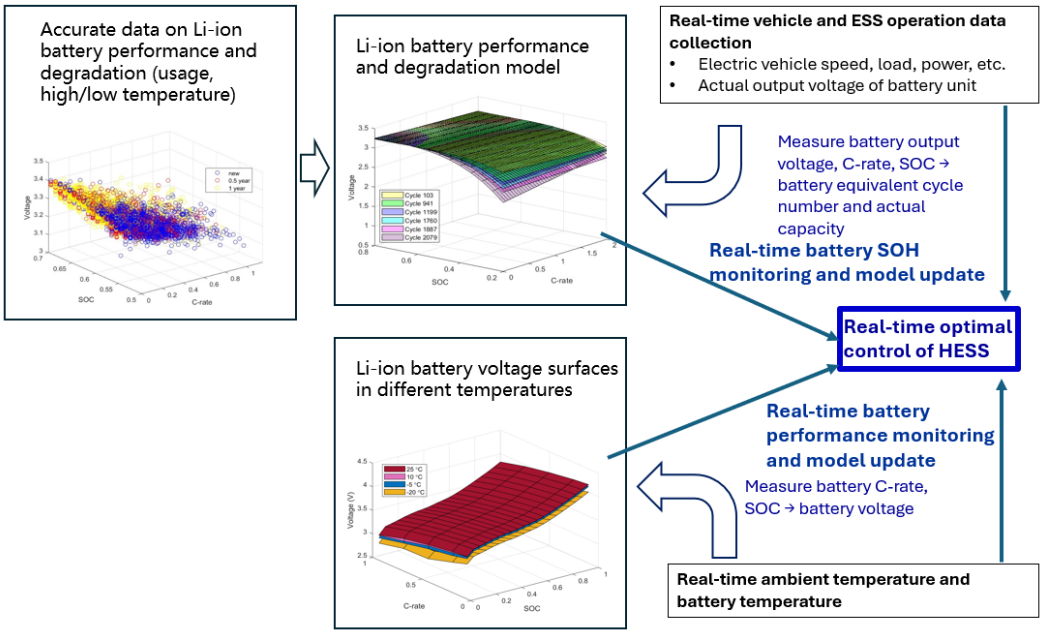

Figure 25. Real-time optimal control method of HESS.

The performance model of the battery incorporates factors such as charging and discharging efficiency, capacity, and power output under varying conditions. By applying this model, the system can predict how the battery will perform based on real-time operational data. Simultaneously, the degradation model tracks the battery's wear and tear over time, incorporating data on cycles, usage patterns, and environmental factors. This model helps to estimate how degradation impacts the battery's capacity and efficiency. Real-time updates to this model are based on actual performance data, allowing for precise tracking of the battery's health and forecasting its remaining useful life.

Temperature plays a critical role in battery performance and degradation. The system incorporates a performance model that accounts for temperature variations, as both ambient and battery temperatures affect the battery's efficiency and longevity. By continuously monitoring the real-time temperature of the battery and its surroundings, the system can adjust its operational parameters to mitigate the effects of temperature fluctuations. This adjustment might involve modifying charging rates or activating cooling/heating mechanisms to maintain optimal operating conditions.

Together, these models enable real-time updates to the battery's status, allowing the energy storage system to perform dynamic adjustments. This approach ensures the battery operates within its optimal range, enhancing efficiency, extending its lifespan, and maintaining overall system reliability. The energy management system can adapt to changing conditions and demands through this approach, providing a robust solution for managing energy storage in ships or vehicles.

Section 3.3 discusses the detailed method for updating the battery's performance and degradation models using real-time battery operation data.

5.5. A new MPC real-time optimal control method

5.5.1. Purpose of the New MPC Method

The purpose of the new MPC real-time optimal control method is to overcome the shortcomings of traditional real-time optimal control methods that can be classified into two major categories with associated shortcomings:

1) Optimal EMS based on known standard vehicle velocity cycles and DP
    - When the vehicle/vessel velocity is known for the entire operation period, this approach can obtain the optimal solution accurately.
    - The actual vehicle/vessel operating velocity deviates from the standard vehicle velocity cycle, resulting in errors if this approach is used for real-time optimal control.
    - DP for the entire operating period requires a lot of calculations and cannot be solved in real-time.

- Difficulty in translating results into codified control rules

2) Real-time optimal control based on the vehicle/vessel's operating velocity at each instant time
    - The approach only requires a small amount of calculation and is easy to solve in real-time.
    - The predicted vehicle/vessel velocity cannot be accurate as the approach lacks a global view of the vehicle/vessel's "trip."

5.5.2. Components of the New MPC Method

The newly introduced MPC real-time optimal control method uses more accurate velocity prediction to solve small DP problems piecewise over a short forthcoming period. The approach consists of the following three elements:

a) Making a more precise vehicle/vessel velocity prediction using model prediction over a short period following, using EKF on the present and past vehicle/vessel velocity on the standard driving cycle and the measured velocity;
b) Using the propulsion system model and vehicle/vessel dynamics model to find the required propulsion power based on the predicted vehicle/vessel velocity;
c) Carrying out DP optimization search to quickly identify the optimal energy management solution.

Optimal control of the vehicle/vessel over the entire operation cycle is done segment by segment. The prediction and optimization accuracy can be selected according to the computing capability of the controller.

5.5.3. Algorithm Implementation

Implementing real-time optimal control is completed through power demand prediction and energy management. Power demand prediction is to generate power demand in a short period, and optimal EMS solves the optimal energy allocation in this short period based on the predicted power demand. The time sampling points of the entire journey are respectively $t_0, t_1, \dots, t_n$, and we perform real-time control on each time interval t_s, t_{s+1}, … , t_{s+p} .

1) Short-term prediction of vehicle velocity and power demand:

    First, the vehicle velocity in the time interval $t_s, t_{s+1}, \dots, t_{s+p}$ is predicted. The deviated velocity is the deviation between the measured real and standard velocities. The standard velocity is the velocity at the corresponding time according to the standard velocity cycle.

    Using the Kalman filtering method, for time t_s, the state of the previous moment is corrected according to the difference between the actual velocity of the vehicle at the moment and the standard velocity, and the velocities at $t_s, t_{s+1}, \dots, t_{s+p}$ are

predicted. The predicted velocity can be obtained by adding the predicted value to the standard velocity.

Then, the power demand of the vehicle in the time interval, $t_s, t_{s+1}, \dots, t_{s+p}$, needs to be predicted. The predicted velocity is input into the vehicle/vessel dynamics and propulsion system models to obtain the power demand in the interval.

2) Time interval control strategy:

At time t_s, we have obtained the predicted power demand at $t_s, t_{s+1}, \dots, t_{s+p}$, battery temperature, battery health status, and ambient temperature for the time interval. We use these as inputs to calculate the optimal control strategy for a short period. $t_s, t_{s+1}, \dots, t_{s+p}$ using DP to obtain the specific energy allocation at each moment. We only take the first moment, t_s. The control strategy at the moment is used as the real-time control strategy at that moment, and $t_{s+1}, \dots, t_{s+p}$. The results of the previous stage are discarded.

3) Overall real-time control strategy:

At time t_{s+1}, we repeat steps 1) and 2), that is, first predict and calculate t_{s+1}, t_{s+2}, … , $t_{s+p+1}$the vehicle power demand in the time interval, then use DP to calculate the control strategy/energy distribution in the time interval and take t_{s+1} the control strategy at the time, the real-time control strategy, and so on.

5.5.4. Adjustment Methods for Computing Time/Capacity

- When the grid is SOC=0.0002 *and p+1* = 2 0, the calculation time on a PC is about 10 seconds.
- When computing power is insufficient, two methods can be used to achieve real-time optimal control.
    - Shorten the period and widen the grid.
    - Use the more real-time control results obtained from each calculation. That is, take the control strategy at $t_s, \dots, t_{s+q}$ as the real-time control strategy at time *s, …, s+q,* and discard the results of the previous stage at $t_{s+q+1}, \dots, t_{s+p}$. The time interval of the next calculation is changed to $t_{s+q+1}, \dots, t_{s+q+p+1}$.

When using the given MPC-based real-time optimal control method and MATLAB program, you can choose between improving the quality of real-time optimal control and the required real-time control strategy calculation time. The smaller the calculation step size, the higher the accuracy, but more calculations are required.

We used a PC with a 13th Gen Intel(R) Core (TM) i7-13700HX, 2100 Mhz, 16 Cores, 24 Logical Processors. For vehicle controllers with different computing power, corresponding choices can be made, as discussed at the end of Chapter 8.

5.6. Testing and Applications of the Introduced New Methods

The following three chapters will explore three distinct case studies demonstrating advanced approaches to optimizing energy management systems. Chapter 6 delves into the performance and degradation models of a Li-ion battery and a hydrogen fuel cell. We adjust the dynamic degradation model based on operational data and SOH updates to enhance optimal control and energy management strategies. This adjustment aims to improve system performance and efficiency by continually refining the control algorithms.

In Chapter 7, we analyze the impact of fuel efficiency alongside emissions of hydrocarbons (HC), carbon monoxide (CO), and nitrogen oxides (NOx), factoring in the effects of battery aging, such as capacity reduction and increased internal resistance. By real-time adjustment of the control strategy, we assess how varying degrees of battery aging affect greenhouse gas emissions and overall battery performance. This case study provides insights into managing battery degradation and emissions to minimize environmental impact and operational losses.

Chapter 8 extends the analysis to consider the influence of temperature on battery performance. We employ real-time operational data to develop and implement optimal control and thermal management strategies by utilizing the attenuation model of lithium batteries and performance models at various temperatures. This approach aims to mitigate battery damage from extreme temperatures and minimize LLC. The focus is on achieving efficient thermal management and maintaining optimal battery performance, even under challenging environmental conditions.

Chapter 6. Case Study on Fuel Cell and Battery Hybrid Electric Marine Propulsion System

6.1. Literature and Motivation

PEMFC offer numerous advantages in heavy-duty marine propulsion systems, including zero tailpipe emissions, high efficiency and high power. However, they mainly excel at providing stable power output and struggle with extremely low or high loads and rapid load fluctuations common in vehicle and ship propulsion. To address this issue, integrating an additional BESS or hybridizing with batteries can bolster the propulsion system responsiveness, capitalizing on fuel cells' benefits while mitigating their limitations and extending their operation life with reduced LCCs.

Despite their advantages, PEMFCs and the commonly used Li-ion batteries have costs and degradation issues. Accurate performance degradation models are pivotal for the hybrid propulsion system's optimal EMS to avoid poor performance and life-shortening deteriorations that lead to high LCCs [5][8][118][119]. Given their different degradation rates, balanced propulsion system design and controls are vital, ensuring optimal propulsion performance and system longevity.

Over the past years, considerable efforts have been devoted to PEMFC performance and degradation modelling. Frequently changing load conditions are the main cause of PEMFCs' degradation. Due to the dynamically shifting operation conditions, voltage fluctuations on PEMFC outputs negatively impact PEMFC materials and composing elements. The starting, stopping, idling, and dynamically varying load operation modes are found to be closely associated with accelerated PEMFC performance degradation [120]. These transient changes in the current load on the PEMFCs will cause frequent fluctuations in the reactant gas pressure, temperature, humidity, etc., resulting in mechanical damage to the fuel cells. More robust materials may improve PEMFC life, but it becomes difficult to see progress after decades of research and development. Optimizing the PEMFC system and FCEV power control and energy management to avoid or reduce these unfavourable operation conditions, on the other hand, will delay the attenuation and prolong PEMFC life. These optimizations can only be achieved by knowing exactly how the PEMFC performance degrades under different operation conditions. Widely studied in recent years, the data-driven modelling approach often has difficulty adapting to the degenerating behaviour of the PEMFC due to poor algorithm consistency. The lack of data requires more complex models to adapt to changing observations, resulting in large uncertainties and extensive computational costs. A data-driven prediction method has been proposed in [47], with less learning data fitting. As a result, the PEMFC aging prediction was more robust, making the application easier. Based on the analysis of the variance method, the influence of different parameters of a novel ANN paradigm was analyzed in [10], and three sets of parameters with greater impact on fuel

cell voltage were identified. A method based on an adaptive neuro-fuzzy inference system has been proposed in [49] to construct a prediction of the PEMFC's output voltage.

The performance and degradation modelling of the Li-ion battery share considerable similarities to the PEMFC system performance and degradation modelling. The latest Li-ion battery health monitoring and prediction research was reviewed in [48], summarizing the technologies, algorithms, and projections of the RUL, SOC, current and voltage, energy capacity, and power of the BESS. The monitoring methods of battery charge status, capacity, impedance parameters, available power, health status, and remaining service life were reviewed in [49], and the advantages and disadvantages of these online or real-time methods were compared. Various estimation methods were classified [15] according to their underlying models and algorithms of big data analysis and related computing tools. The advantages and limitations of these estimation methods were also discussed. The battery SOH assessment methods were classified according to the signals used to extract health indicators and the supporting theories [16], with further discussions on their advantages and disadvantages. Model-based battery performance and SOH prediction methods use a combined equivalent circuit and electrochemical models to improve prediction accuracy [28]. Establishing the form of the performance and degradation models and determining the parameters of these models using experimental or operation data are two essential tasks. Furthermore, dynamically updating the identified model parameters using continuously acquired operation data is critical to ensure accurate real-time optimal power control and energy management.

The fuel cell and battery hybrid propulsion system and its EMS can be optimized offline for a given statistical data-derived driving cycle or operation profile using an extensive global optimization search, such as DP. Recent research has tried to balance the propulsion system's energy efficiency and overall LCCs using the PEMFC's fuel efficiency and either the PEMFC's or Li-ion battery's degradation model. The main causes of PEMFC degradation were identified in [121], and a model was generated to estimate the impact of EMS on PEMFC degradation. A stochastic DP controller minimized the PEMFC system's hydrogen fuel consumption and degradation costs by avoiding transient loads on the PEMFC system. Due to the difficulty in capturing the PEMFC's and Li-ion battery's performance and capacity degradation behaviours, simple and less accurate models were adopted. An EMS that simultaneously considers fuel consumption and degradations of PEMFC and Li-ion battery ESS was introduced in [122] to optimize fuel cell/battery hybrid powertrains using a simplified PEMFC electrochemical model and an empirical model of Li-ion batteries. The propulsion system's EMS and size of the PEMFC system and BESS in a hybrid electric bus were optimized, and the influence of driving mode on the bus optimization results was investigated [123]. Our team's recent work formulated a nested two-level optimization problem to determine the optimal powertrain component size and energy management parameters by combining powertrain system design and control optimization. An advanced agent-based global optimization method was used to solve

complex optimization problems to improve energy efficiency and reduce pollutants and LCCs of PEMFCs [124]. However, the offline pre-optimized PEMFC and BESS hybrid propulsion system and its EMS cannot achieve the true optimal system efficiency or minimum LCCs, as the actual operations of the PEMFC-BESS hybrid system depart from the statistical driving cycle or operation profile. Extensive research has been devoted to various real-time optimal control strategies, including ECM, PMP, MPC, Reinforcement Learning (RL), etc., to improve the fuel cell hybrid electric propulsion system's performance and fuel economy. However, the PEMFC and Li-ion BESS degrade differently under varying operations compared to the offline results. Although research has been devoted to monitoring their changing SOH, the observed changes have not been incorporated to dynamically update the degradation models to improve the real-time optimal control and EMS, causing less than ideal system performance and harm to PEMFC and BESS operation life, resulting in increased LCCs of the FCEV's propulsion system.

This research aims to address the challenges in optimizing the design and controls of a complex PEMFC and BESS hybrid propulsion system, using a medium-sized vehicle and passenger ferry as the research platform and design example. Specific contributions in this test case study included the following.

- Firstly, an innovative and comprehensive approach was developed to integrate the global design optimization and optimal energy management of PEMFC and BESS hybrid electric propulsion system, considering system performance, fuel economy, PEMFC system and Li-ion BESS degradations jointly to minimize the system's LCCs.
- Secondly, more accurate models of Li-ion battery's performance and capacity degradations were introduced using extensive laboratory degradation test data and dynamic degradation model adjustment using real-time battery operation data and SOH update to improve real-time optimal control and energy management.
- Thirdly, the amendment to the lab-derived PEMFC performance degradation model using real-time fuel cell operation data and SOH update to improve real-time optimal control and energy management was added.
- Fourthly, our work addressed the challenge of conflicting hybrid propulsion system's component-sizing design optimization and real-time optimal power control and energy management. A nested global optimization covering the optimal sizing of the PEMFC and BESS and the baseline optimal EMS under the vessels' statistical operation profile for generic use is introduced as the first step. The real-time optimal control of the ship improved the baseline optimal EMS by considering the PEMFC's and BESS's SOH variations induced during the vessel's actual operations.
- At last, this work applied the new integrated component size design optimization and real-time optimal control and energy management of a PEMFC-BESS hybrid electric propulsion system to the example ferry ship based on the vessel's technical

specifications and operation data to demonstrate the feasibility and benefits of the clean propulsion solution.

6.2. Hybrid Electric Fuel Cell Vessel

The PEMFC system and BESS are the two key components of the hybrid electric propulsion system. With the accurate and updated performance and degradation models of the BESS and PEMFC, their actual operation lives under a specific operating sequence of the hybrid electric vessel (or vehicle) can be precisely predicted. The optimal propulsion system design and its optimal EMS can be obtained by identifying the best powertrain configuration, component sizes, and, most importantly, the well-coordinated PEMFC and BESS system operations. As a result, the best balance between fuel consumption reduction and low impact on PEMFC and BESS operation life can be obtained to achieve the minimum LCC of the FCEV. This section uses the optimal EMS development of a PEMFC hybrid electric ferry to demonstrate the application of the newly introduced BESS and PEMFC system performance and capacity degradation models in FCEV propulsion system design and control optimizations.

6.2.1. Vessel Operation Profile

The PEMFC and BESS hybrid electric propulsion system of a medium-sized vehicle and passenger ferry operated by BC Ferries in British Columbia, Canada, was used as a test bed. The ship travels between Salt Spring Island (Fulford Harbour) and Victoria (Swartz Bay), with the technical specifications in Table 6. The representative required propulsion power of the ferry during the round-trip voyage is shown in Figure 27.

Figure 26. Skeena Queen Ferry of BC Ferry Services.

Table 6. Technical Specifications of Skeena Queen Ferry

Max speed	Length	Displacement	Vehicle/Passenger capacity
15.3 knots	110 meters	2942 tones	92/450

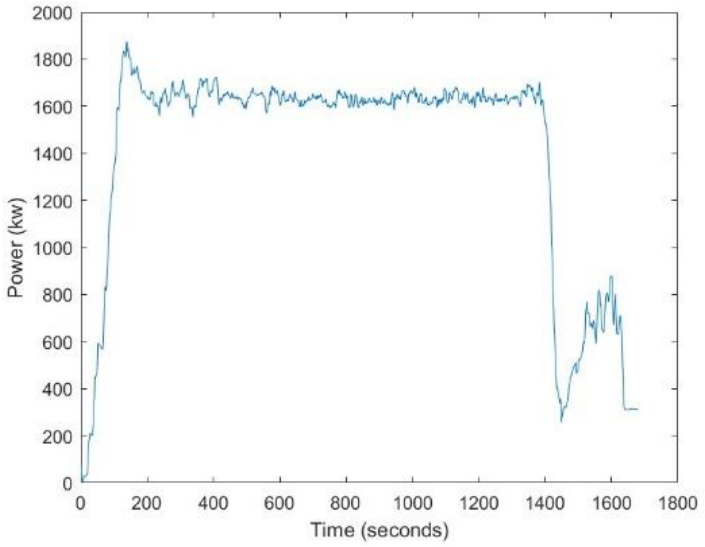

Figure 27. Power demand from Salt Spring Island and Victoria.

6.2.2. Vessel Technical Specification

The hybrid electric propulsion system of the proposed PEMFC-BESS ferry is shown in Figure 28. Hybrid electric propulsion improves fuel economy and propulsion efficiency with zero-tailpipe emissions.

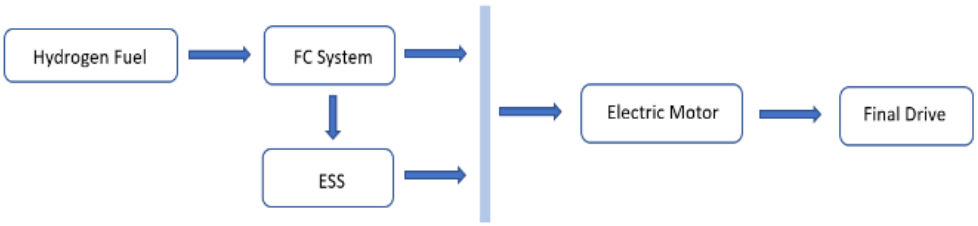

Figure 28. PEMFC propulsion system.

This research aims to improve the optimal EMS of the hybrid electric propulsion system to more precisely count the BESS and PEMFC performance and capability degradations and resulting operation life loss under the ship's specific operation on this route. Improving the globally optimal EMS aims to improve fuel efficiency and extend the BESS and PEMFC systems' operation lives simultaneously to achieve the minimum LCC of the ferry's hybrid electric propulsion system. Furthermore, building on top of the EMS

optimization, the optimal sizing of the propulsion system's key components can also be conducted, as in our team's recent work [107][124].

The LCC minimization problem is formulated as:

$$\min_{x} f(x) = \omega_1 C_{Batt}(x) + \omega_2 C_{FC}(x) + \omega_3 C_{H_2}(x) \quad (23)$$

where $x = [x_1, x_2, x_3]'$, x_1 is the number of batteries in series, x_2 is the number of batteries in parallels, x_3 is the number of PEMFC. $C_{Batt} = x_1 x_2 p_{Batt}(Q_{max} - Q_{cap})/(20\% Q_{max})$ is the degradation-induced costs for the BESS, p_{Batt} is battery projected cost per kwh, $C_{FC} = x_3 p_{FC}(V_{new} - V_{cell})/(10\% V_{new})$ is the degradation-induced costs for the PEMFC systems, p_{FC} is FC projected cost per kw, V_{new} is the output voltage of the new fuel cell, $C_{H_2} = p_{H_2} H_2^{con}$ is the hydrogen fuel cost, p_{H_2} is H_2 projected cost per kg, and H_2^{con} is the hydrogen consumption, which can be obtained from the fuel cell model. $\omega_1, \omega_2, \omega_3$ are weighting factors in the costs of PEMFC systems, BESS, and hydrogen fuels based on design and operation considerations.

The LCC minimization formulation of Eq. (24) determined the optimal PEMFC system and BESS sizes in the hybrid electric ship propulsion system and the system's baseline optimal EMS. The global optimization problem is formulated with two levels and solved simultaneously, with the component size design optimization at the top and the EMS optimization using DP at the bottom. Our earlier work in [119][124] discussed details on the implementation and solution method. This work primarily focuses on the dynamic updates of the BESS and PEMFC system's performance and degradation models and the use of these models to update the optimal EMS of the FCEV to support this global optimization with considerably improved results.

The PSO algorithm was used to solve the formulated global optimization problem. The resulting optimally sized LFP BESS has a nominal capacity of 18Ah, 270 cells in series and 100 cells in parallel, and the PEMFC system has five 400kW sub-system modules.

6.3. Optimal Vessel EMS Considering Life Cycle Costs

6.3.1. Battery and PEMFC Degradation and Life Cycle Cost

To meet the need to accurately predict battery performance degradation under various operating conditions and allow the model to be used for real-time optimal energy management with moderate computational requirements. Battery capacity loss is a function of operation conditions, including operating temperature, overall amp-hours, and discharge rate. This work uses the semi-empirical performance degradation and operation life model for LFP batteries [22][109], as indicated in Eq (4).

The model parameters A, B, C and D influence the propulsion system's performance and warrant adjustments to achieve and maintain optimal power control and EMS. These data-fitted parameters are updated through the KF using continuously acquired operation data

in this work. Our modelling and simulations proved the necessity of updating the PEMFC system and BESS's degradation model parameters. In Figure 29 and Figure 30, the power allocations to the PEMFC system and BESS in the fuel cell hybrid electric system are shown by the blue solid curves. The red-dotted curves, on the other hand, presented different optimal power allocation results using the dynamically adjusted degradation model parameters. The optimal power control and distribution using degradation models with dynamically adjusted parameters can reduce the top-level LCC by 1.03%. For different vehicles or vessels under variant operations, updates of the performance and degradation model parameters as their PEMFC and BESS age with different SOH become essential.

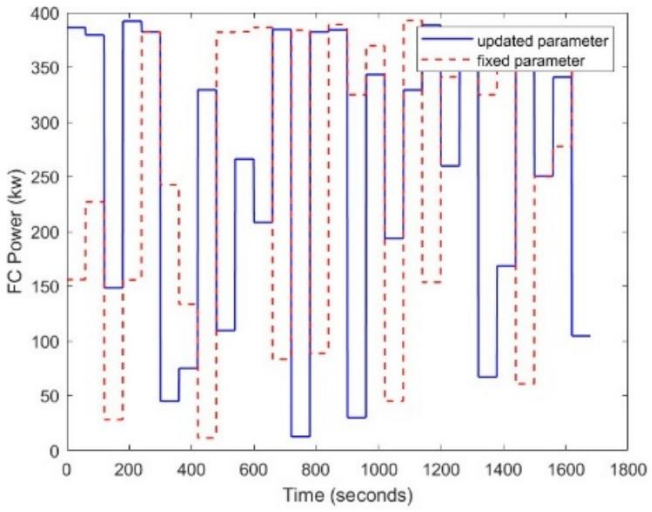

Figure 29. PEMFC power in different degradation models.

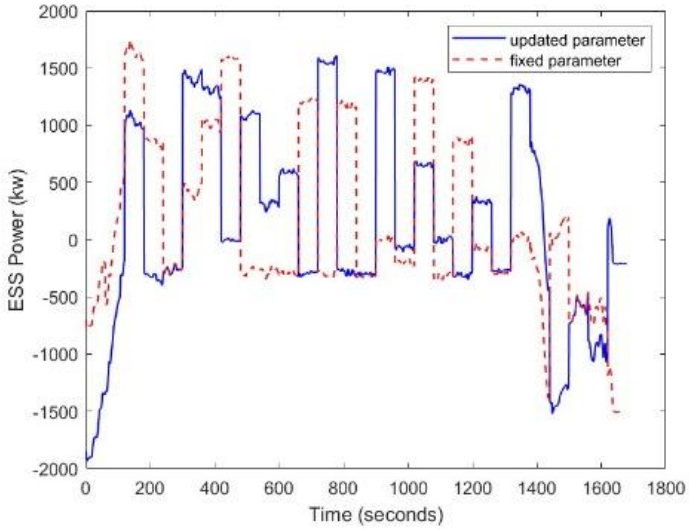

Figure 30. ESS power in different degradation models.

6.3.2. Fuel Efficiency

Normally, the objective of optimal power control and EMS for a vessel operated on fixed routes is to minimize fuel consumption. Reducing fuel consumption without causing more costly PEMFC and BESS life degradation is important and challenging. The best balance can be achieved through a global optimization, considering all three factors jointly, as introduced in the general formulation of Eq. (24). For this FCEV application, the objective function of the global optimization for one sailing operation cycle is detailed as:

$$\min_{u} \int_{t_0}^{t_1} (FC_{op}(u(t)) + FC_{deg}(u(t)) + ESS_{deg}(u(t))dt \tag{24}$$

where t_0 and t_1 are the start time and finish time; $u(t)$ is the control variable; FC_{op} is the hydrogen fuel consumption cost of the vessel obtained using vessel operation simulations; FC_{deg} is the degradation model of the PEMFC system [125]; ESS_{deg} is the degradation model of the BESS. The weighting factors, $\omega_1, \omega_2, \omega_3$, are assumed to be 1 in this work.

6.3.3. Globally Optimal System Design and Operation

The energy management system must properly distribute the propulsion power demand to the PEMFC system and the BESS, and the battery current is used as the control variable. The battery SOC is as follows:

$$\dot{SOC}(t) = -\frac{I_{batt}(t)}{Q_{norm}} \tag{25}$$

where $I_{batt}(t)$ is the battery current and Q_{norm} is the battery capacity.

The PEMFC system's operating voltage and current determine the instantaneous hydrogen fuel consumption.

$$P_{dmd} = P_{fc} \cdot \eta_{fc} + P_{batt} \tag{26}$$

The following constraints on the state and control variables that typically vary over time must be enforced:

$$\begin{gathered} SOC_{min} \le SOC \le SOC_{max} \\ P_{min}^{fc} \le P_{fc} \le P_{max}^{fc} \\ P_{min}^{batt} \le P_{batt} \le P_{max}^{batt} \end{gathered} \tag{27}$$

where, the max and min are the maximal and minimal values, and the upper and lower bounds of the BESS' SOC are set to 0.65 and 0.5, respectively, based on system design experience.

The optimal EMS seeks to minimize the overall costs, including hydrogen fuel consumption and degradations of both the PEMFC system and BESS, over the operation cycle while satisfying given constraints. During the ferry operation, the SOH of the PEMFC and BESS are adjusted regularly. When the SOH changes, the control and EMS will be modified accordingly.

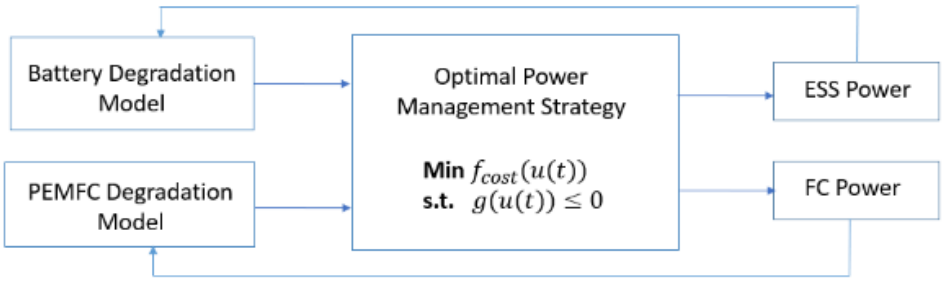

Figure 31. Illustration of optimal EMS for an electrified propulsion system

When a ferry operates on the same route, its propulsion power is assumed to largely follow a statistical operation profile, and the optimal sizes of the PEMFC system and BESS and the baseline optimal EMS of the propulsion system can be identified through the global optimization solved using PSO. However, during the actual vessel operations, the instant ship operation profile will slightly depart from its norm; the PEMFC system and BSS will thus work differently, leading to various performance and capacity degradations. Therefore, the optimal EMS must be adjusted using the dynamically updated degradation models. Not updating these models and using the same baseline optimal EMS will likely accelerate BESS and PEMFC system degradations due to their overuse and increase hydrogen fuel consumption due to departing from the true optimal system efficiency.

For the new and one-year-old BESS and PEMFC systems, the amount of propulsion power provided by the BESS under the optimal EMS is shown in Figure 32. There is a marked difference in how the energy is distributed. When the ESS and PEMFC systems are new, the PEMFC has excellent SOH and strong performance capability. When there is a high propulsion power demand, the PEMFC system can independently supply power at a higher efficiency without battery assistance (for example, 500-650s in Figure 32). After one year of use, the performance of PEMFC declined. If the PEMFC system provides the same high power, it will have accelerated performance degradation. Therefore, a reduced PEMFC power allocation with more battery power assistance can produce less system LCC, resulting in a minor accelerated degradation of the BESS. This needed shift is due to the different contributing costs and cost sensitivities of the PEMFC system and BESS. The global optimization automatically identifies the best balance to achieve a minimum LCC.

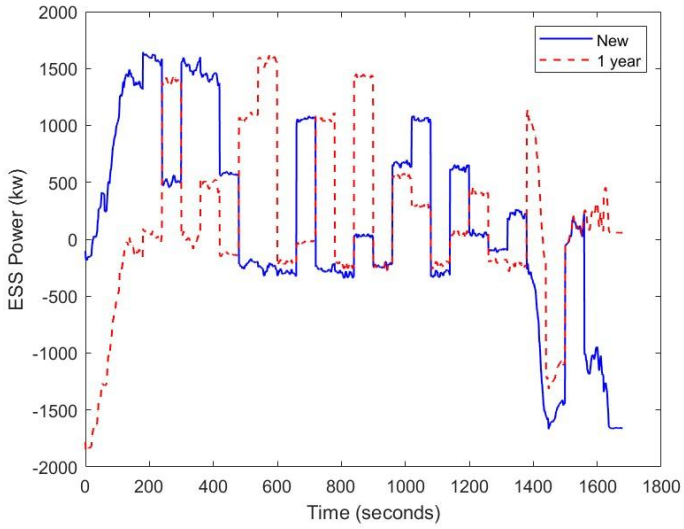

Figure 32. ESS power in different SOH.

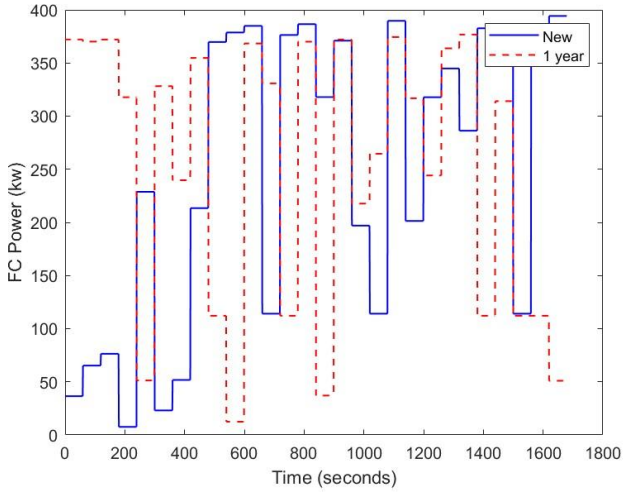

Figure 33. PEMFC power in different SOH.

To better illustrate the effects of the optimal EMS, considering different contributing factors, incorporating or ignoring the PEMFC system and BESS aging, and dynamically updating the aging parameters, the costs of five different cases are shown in Table 7. The crossing cost consideration is limited to the fuel consumption cost of the PEMFC, FC_{op}, the cost associated with the degradation of the PEMFC system, FC_{deg}, and the cost associated with the degradation of the BESS, ESS_{deg}.

Table 7. Crossing cost comparison in different SOH (US$)

SOH	Case 1	Case 2	Case 3 and SOH		
	New	New	New	$1Yr_{OPT}$	$1Yr_{NDC}$
FC_{op}	161.06	179.95	180.09	186.68	241.00
FC_{deg}	434.47	68.93	68.66	83.93	279.32
ESS_{deg}	18.64	20.14	19.92	28.00	29.70
Total	614.16	269.01	268.67	298.61	550.00
Rel. Value	2.290	1.001	1	1.111	2.047

- In *Case 1*, only hydrogen fuel consumption is minimized, as in the past research.
- In *Case 2*, as in many recent publications, hydrogen fuel consumption and PEMFC degradation are considered simultaneously without considering BESS degradation.
- In *Case 3*, balanced hydrogen fuel consumption, PEMFC degradation and battery degradation were found. Furthermore,
    - The *New* condition means that both the PEMFC system and BESS are new.
    - The $1Yr_{OPT}$ condition means the PEMFC system and BESS have been used for one year.
    - The $1Yr_{NDC}$ condition means the performance and capacity degradation model parameters of the PEMFC system and BESS are not considered. After being used for one year, the propulsion system's optimal EMS is still based on the same static PEMFC system and BESS performance and degradation models.

In Case 1, substantial harm is inflicted upon the PEMFC system despite significantly reducing hydrogen consumption, emphasizing the pivotal importance of PEMFC degradation considerations. In Case 2, although hydrogen consumption slightly increased, the PEMFC decay diminished to 16%, leading to a 56.2% reduction in crossing cost. Case 3 incorporates additional battery attenuation, curbing LCC by 56.3%.

Upon one year of PEMFC system and BESS usage, notable attenuation emerges, as shown by the three conditions of Case 3. If control strategies remain static post-aging, crossing cost surges to over twice the PEMFC system and BESS' initial state from $268.67 to $550 or 205%, hastening system aging. However, by proactively accounting for the PEMFC system and BESS degradation dynamics, crossing costs only increased by 11% of the original value after one year of use. The crossing cost was reduced by 45.7% compared to the unadjusted attenuation parameter scenario. According to industry standards, automotive fuel cells are expected to have a service life of approximately 5,000 hours under typical vehicle operating conditions [120]. Adhering to this criterion, it is reasonable to calculate the LLC of PEMFC systems and BESS based on a two-year operational period. The method in this study has demonstrated its effectiveness in reducing the LLC of PEMFC systems and BESS. Our results show that the LLC can be reduced by at least $2,936,235

over the two-year operational period, meeting commercial requirements while maximizing cost savings.

For the new PEMFC system and BESS, the amount of propulsion power provided by the BESS under the optimal EMS in different cases is shown in Figure 34 and Figure 35. In Case 1, since only the hydrogen fuel consumption is considered, the PEMFC has been operating near the highest efficiency point to minimize the fuel consumption, and the decay of PEMFC is fast. In Case 2, since the degradation of the BESS is ignored, the power fluctuation on the battery is larger compared to Case 3, resulting in a larger attenuation. The best result with the minimum crossing cost after one year of use is $298.61, as shown under the "1YrOPT" condition of Case 3 in Table 7. The corresponding BESS and PEMFC system power outputs, controlled by the dynamically optimized EMS, are shown in Figure 34 and Figure 35 under Case 3.

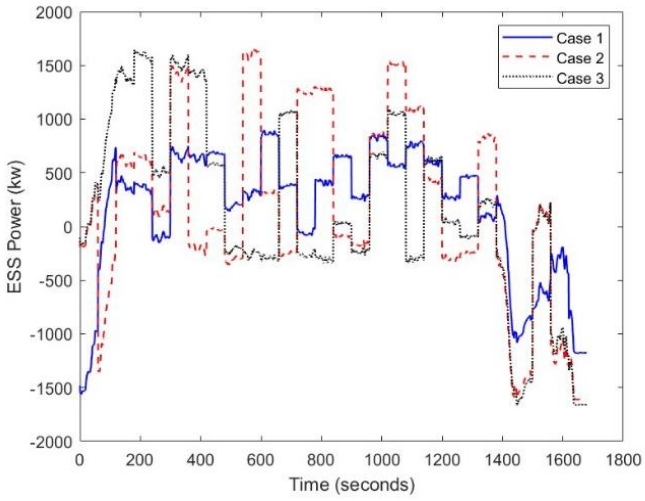

Figure 34. ESS power in different cases.

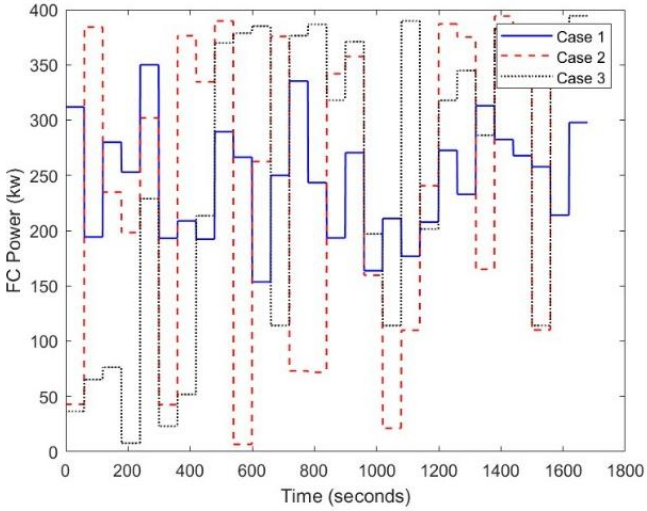

Figure 35. PEMFC power in different cases.

Chapter 7. Case Study on NG-Engine Hybrid Electric Marine Propulsion System Design

7.1. Literature and Motivation

Large marine vessels that transport goods over long distances emit substantial amounts of GHGs [126][127][128]. These emissions arise from the combustion of fossil fuels, primarily heavy fuel oil or marine diesel, in the ships' ICEs. The International Maritime Organization (IMO) has introduced regulations to improve ships' energy efficiency and reduce GHG emissions. Adopting alternative fuels [129] and using hybrid-electric and all-electric marine propulsion systems [130] have great potential to considerably reduce harmful emissions, improve air quality, and promote sustainability in marine transportation.

The global warming potential (GWP) is a metric that compares the climate impact of different GHGs based on their ability to trap heat in the atmosphere over a specific time horizon. GWP provides a way to convert the instantaneous emissions of GHGs, such as hydrocarbons (HC), carbon monoxide (CO), and nitrogen oxides (NOx), into an equivalent value of carbon dioxide equivalent (CDE, or CO2e) emissions.

Liquefied natural gas (LNG) is a promising low-carbon alternative fuel option for replacing diesel in heavy-duty marine propulsion systems with substantial cost savings over diesel fuel, reducing the operational costs for marine vessels. LNG has lower carbon content [131][132], reducing CO2 emissions per unit of energy used and producing fewer air pollutants than other fossil fuels. Retrofitting existing marine vessels to run on LNG can often be achieved with relatively minor modifications to the propulsion systems, making the transition to cleaner natural gas (NG) fuel straightforward [133]. An assessment was made based on the environmental impact, economic viability, and inherent safety of LNG fuel use, showing better sustainability than conventional marine fuel technologies [134]. The NG-fuelled engines also produce less NOx except under light engine load. However, the leak of incompletely combusted NG or methane, mainly HC and increased CO emission from an NG engine contribute to severe environmental impact, measured by the CO2e emissions, and another concern is the surge of NOx emission of an NG engine at low load [135][136]. Our earlier work addressed the dramatic increase in HCs and CO emissions by simultaneously considering vehicle performance, fuel efficiency, and CO2/HC/CO/NOx emissions [136].

Hybrid-electric propulsion systems are widely adopted in various applications, including automotive, maritime, and aviation, because they reduce emissions and enhance energy efficiency [51][137]. The system can leverage the strengths of each power source, allowing intelligent control and optimization of power-sharing based on demand, efficiency, and emissions considerations, resulting in improved overall energy efficiency. Hybridizing

heavy-duty marine vessels and commercial trucks requires a large electric ESS. The widely and commonly used Li-ion BESS poses a key and high-cost component in the hybrid propulsion system. However, the BESS also suffers from performance degradation and shortened operating life under undesirable use patterns, considerably increasing the hybrid electric propulsion system's LCC. A major challenge in hybrid electric propulsion systems' design and control optimizations is to find ways to avoid improper battery sizing and operations to avoid or delay costly BESS replacement. Accurate predictions of BESS performance and capacity degradations are thus essential for optimal BESS sizing and propulsion system energy management.

Numerous research efforts have been made to develop Li-ion battery life prediction models. These models estimate the batteries' degradation and remaining useful life based on various factors such as operating conditions, SOC, operating temperature, cycling rates, DOD, etc. Physics-based models use fundamental electrochemical and thermal principles to simulate the behaviour of Li-ion batteries. [138] presented a framework for aging diagnostic tools based on identifying and tracking the evolution of model parameters of fundamental electrochemistry-based battery models from non-invasive voltage/current cycling tests. [139] described a new method for in situ monitoring of the internal degradation of Li-ion batteries using electrochemical modelling, and the predicted trends show a strong correlation with the experimentally observed degradation. Electrical impedance spectroscopy (EIS)-based models use impedance measurements to monitor battery aging and degradation. These models can estimate Li-ion batteries' internal resistance and capacity degradation by analyzing impedance changes. [140] combined EIS with Gaussian process-based machine learning to build an accurate prediction mechanism that inputs the entire data spectrum to accurately predict the remaining service life. [141] provided a critical overview of the rapidly developing impedance techniques for Li-ion battery degradation and aging studies and summarized the working principles, data validation, and modelling methods of classical EIS and dynamic EIS in detail. Machine learning techniques have been applied to develop data-driven battery life prediction models. These models learn from large datasets of battery degradation and operating conditions to make accurate predictions. [142] proposed and extensively tested two physics-based machine learning methods for estimating a battery's capacity online and diagnosing its dominant degradation modes using only limited early-stage experimental degradation data. [143] surveyed the state-of-the-art degradation research and highlighted the role of machine learning in achieving greater accuracy through accelerated computation.

Hybridizing ship propulsion systems requires sophisticated control to optimize the coordination of multiple power sources at each instance, besides storing and retrieving energy in the BESS. One common approach for generating the optimal EMS is applying DP to thoroughly search for the best solution over the entire operation cycle. This computation-intensive approach provides the best optimal EMS benchmark for a given

operation cycle. However, the method is unsuitable for changing vessel operation profiles and generating real-time optimal control solutions. Real-time optimal control and energy management ensure the propulsion system operates optimally, responding to varying operating conditions or the environment. [144] improved the ECMS to achieve an improved near-optimal control solution through DP-based feedback controllers. [97] explored an EMS based on real-time MPC to mitigate all-electric ships' load fluctuations. The proposed real-time MPC method showed superior performance with enhanced system reliability, improved HESS efficiency, longed self-sustainment time, and extended battery life. [145] investigated a neural network-based real-time EMS for optimal current distribution between the battery and ultracapacitor of the HESS in electric vehicle applications by reducing the batteries' peak current. These research efforts are based on lab-data-based static battery performance and degradation models, limiting their ability to produce the optimal power control and EMS for the electrified propulsion system.

In this work, ships are exposed to various factors that can cause fluctuations in energy demand during their voyages. External conditions such as wind speed, water flow, sea currents, wave height, and weather can significantly impact a ship's performance and energy requirements. At the same time, as Li-ion batteries age, their ability to provide energy gradually weakens, reducing their capacity and overall performance. Implementing safety measures to prevent overcharging and over-discharging can help mitigate capacity fade and prolong battery life. Real-time control strategies are essential to effectively manage the changing energy demand and ensure optimal ship performance. First, the degradation model of the battery is given. The model shows that voltage decreases in different SOC and C-rates as the battery ages. Then, according to the fuel efficiency and HC/CO/NOx emissions maps, we use the DP method to design a control strategy for fixed energy demand to reduce GHG emissions and avoid battery overcharging and discharging. Considering the impact of the environment on energy demand, we use the KF method to predict the energy demand for a short period in the future. At the same time, considering the decrease in capacity and increase in resistance due to the gradual aging of the battery, we use MPC to adjust the control strategy in real-time. Finally, the GHGs and battery loss generated in the ship's operation are given under different environmental changes and battery aging degrees, and real-time control shows a strong advantage.

7.2. NG-diesel Engine Hybrid Electric Marine Propulsion System

This research introduces a dedicated MPC technique for the real-time optimal control of an NG-engine hybrid electric marine propulsion system. The optimal control aims to achieve high fuel efficiency, address the CO_{2e} emissions problem of NG-fuelled engines, and extend the operation life of the BESS to reach the minimum LCC of the hybrid electric propulsion system.

A representative vehicle and passenger ferry, Skeena Queen, operated by the BC Ferries in British Columbia, Canada, is used to demonstrate the newly introduced real-time optimal control methods. The technical specifications of the ferry are given in Table 8.

Table 8. General information about the ferry ship Skeen

	Max speed	Length	Displacement	Vehicle/Passenger capacity
	15.3 knots	110 metres	2942 tonnes	92/450

7.2.1. Example Marine Vessel and Hybrid Electric Propulsion System Design

An LNG-fueled combustion ignition (CI) engine-based series hybrid electric propulsion system, as shown in Figure 36, is proposed to retrofit the present diesel-electric marine propulsion system. Two new LNG-fueled generator sets produce electric power. Four existing electric motors propel the vessel on the port and starboard sides of the bow and stern. The added BESS is the energy buffer that allows the hybrid electric propulsion system to work more efficiently under varying propulsion power loads by ensuring the LNG engines operate at high efficiency with minimum CO2e emissions. This work only considers the LNG fuel use for these NG-diesel dual-fuel CI engines due to the small portion of diesel pilot fuel use.

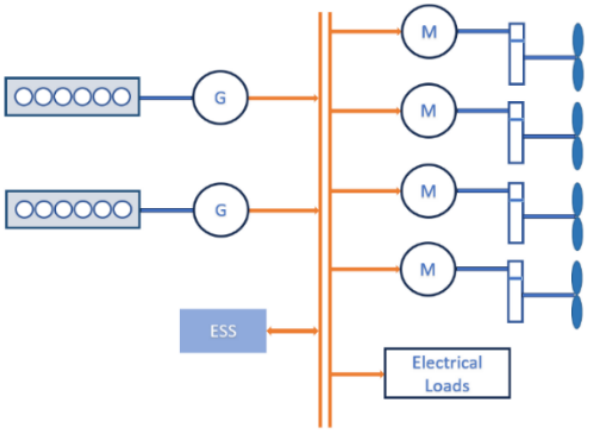

Figure 36. Proposed hybrid electric ferry propulsion system.

7.2.2. Stochastic Vessel Operation Profile

Vessel operation profiles are based on statistical data, providing a general guideline for what to expect under normal vessel operating conditions. The ferry studied in this work travels between Fulford Harbour at Salt Spring Island and Swartz Bay of Victoria, British

Columbia, Canada. Figure 37 shows the typical propulsion power demand during a ferry crossing voyage.

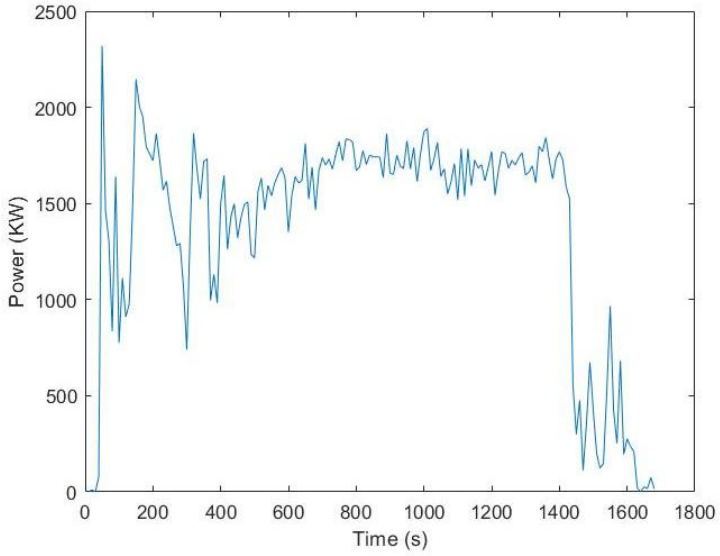

Figure 37. Power demand of Skeena Queen Ferry during a trip.

7.2.3. NG-diesel Dual-fuel CI Engine Fuel Efficiency and Emission Models

Accurate and detailed engine performance, NG fuel consumption, and emissions models are crucial for meeting the propulsion power demand, evaluating fuel efficiency and emissions, and designing an efficient propulsion system and control strategies. These models form fuel consumption and emission maps indexed by the engine's speed and torque, allowing fuel consumption and emissions calculations at different engine operating conditions. Extensive dynamometer test data from a specific engine is gathered to construct these maps, which can be scaled up or down to different engine sizes due to their similar operating characteristics.

The fuel consumption and emissions of the LNG-fueled CI engines are modelled, as shown in Figure 3 (a)-(d) [126]. An engine's carbon dioxide (CO2) emission is directly proportional to its fuel consumption, modelled in Figure (a) and is not modelled separately. On the other hand, HC/CO/NOx emissions, shown in Figures (b), (c) and (d), warrant separate consideration due to their complex formation mechanisms.

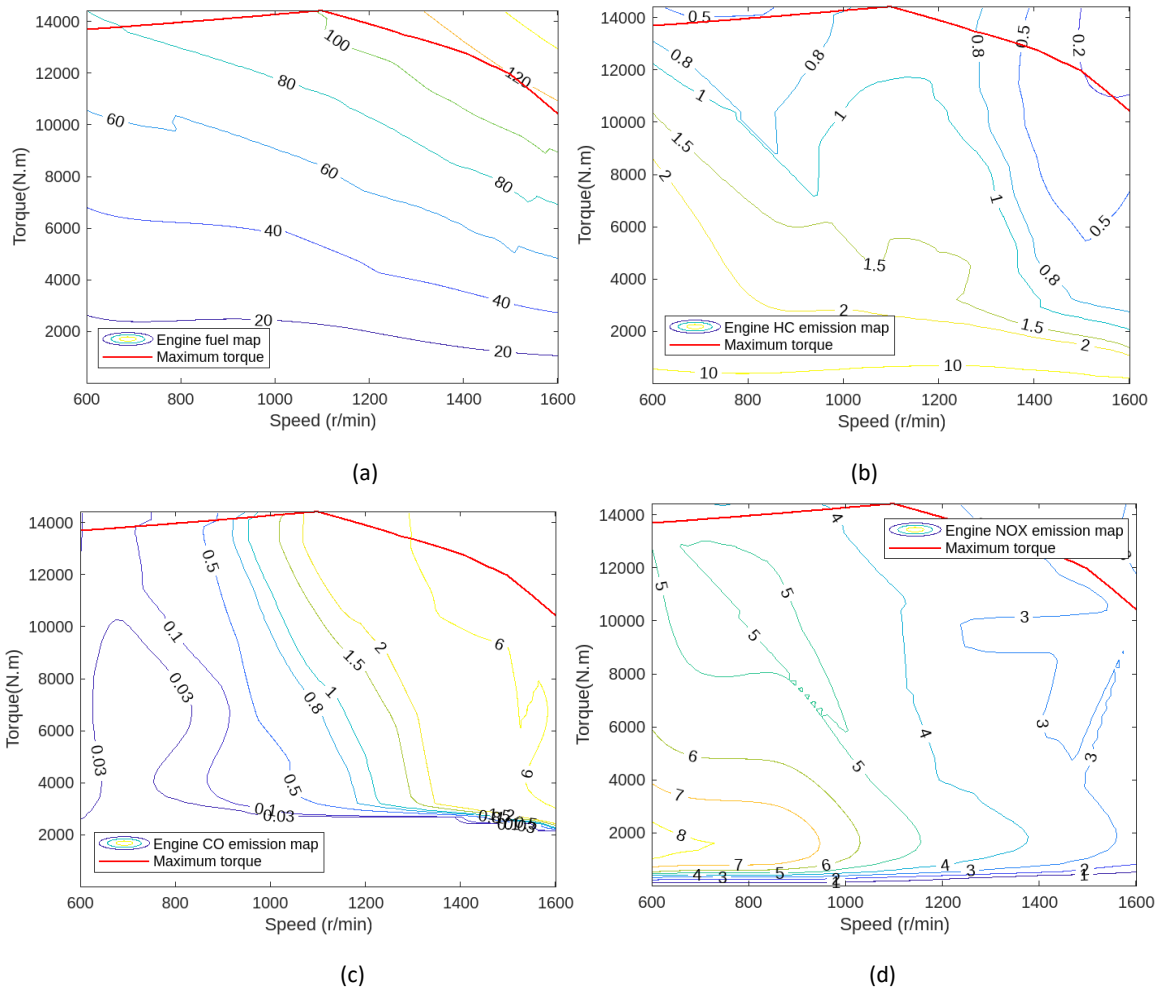

Figure 38. Engine fuel efficiency and HC/CO/NOx emissions maps.

7.2.4. Integrated Hybrid System Design Optimization and Baseline Optimal EMS

This work aims to find optimal propulsion system design and control solutions globally. The optimal sizing of the hybrid propulsion system components and the baseline optimal EMS are determined based on the vessel's statistical operation profile. Real-time optimal power control and energy management are conducted by improving the generic baseline optimal EMS using MPC later to improve the optimal control based on the actual vessel operation data.

The laboratory test data-derived battery performance and degradation models facilitate the selection of an optimally sized NG engine and the BESS. An oversized BESS can lead to unnecessary initial expenditures, while undersized ones may necessitate frequent replacements and higher long-term costs. The overarching goal of the optimal baseline EMS is to concurrently enhance fuel efficiency and extend the BESS's operational lifespan, ultimately achieving the minimum LCC for the ferry's hybrid electric propulsion system.

In the proposed hybrid propulsion system, NG gensets are the primary, and BESS is the supplemental power source. When the vessel requires high propulsion power, the NG gensets operate optimally at full capacity to drive the propulsion motors, and the BESS provides additional power to meet peak power demand. When the propulsion power demand is low, the NG gensets operate at a more efficient working point, and the excess electrical energy is stored in the BESS for future use. The BESS power, $P_{BESS}(k)$ (kW) can be calculated as

$$P_{BESS}(k) = V_{cell}(k) n_s I_{cell}(k) n_p / 1000 \tag{28}$$

where n_s and n_p are the number of battery cells in series and parallel. $P_{dmd}(k)$ is the total power demand at each instant k,

$$P_{dmd}(k) = P_{eng}(k)\,\eta_{eng} + P_{ESS}(k)\,\eta_{ESS} \tag{29}$$

where P_{eng} and P_{ESS} are the engine and ESS power, respectively, and η_{eng} and η_{ESS} are the generator's efficiency of the engine and ESS, respectively.

The measurement of the CO_{2e} emissions can be represented as:

$$CDE(k) = \alpha_1 FC(k) + \alpha_2 HC(k) + \alpha_3 CO(k) + \alpha_4 NO(k) \tag{30}$$

where α_1 is the factor for converting the instantaneous fuel consumption into equivalent CO_2 emissions, α_2 α_3 and α_4 are used for converting the instantaneous emissions of HC, CO and NO_x into equivalent values of CO_2.

Traditional engine power control strategies aim to find the ideal combination of engine speed ω_{opt} and torque T_{opt} to maximize the engine's energy conversion efficiency, improving fuel economy and reducing CO_2 emissions. This work considers more contributing factors in the optimization to determine the optimal engine speed and torque, including fuel consumption and associated CO_2 emission and additional HC, CO, and NO_x discharges. The CDE measure of all contributing emissions is used.

$$\begin{aligned} &(\omega_{opt}, T_{opt}) = argmin(CDE(k)) \\ &P_{eng}(k) = \omega_{opt}\, T_{opt} \end{aligned} \tag{31}$$

In addition, the cost associated with the battery degradation is added to the objective function for each operation cycle and formulated as follows:

$$\min_u \sum_{k=m_s}^{m_f} \omega_{CDE} CDE(u(k)) + \omega_Q Q_{loss}(u(k)) \tag{32}$$

where m_s and m_f are the operation start time and finish time; *u(k)* is the control variable; ω_{CDE} and ω_Q are the weight factors of CO_{2e} emissions and battery degradation cost, respectively.

Constraints on hybrid electric propulsion systems and the BESS's SOC, current, and power limitations include:

$$\begin{aligned} &|SOC_{ini} - SOC_{end}| \le \Delta \\ &SOC_L \le SOC(k) \le SOC_U \\ &I_L \le I(k) \le I_U \\ &P_{ESS_L} \le P_{ESS}(k) \le P_{ESS_U} \end{aligned} \tag{33}$$

where SOC_{ini} and SOC_{end} are the BESS's initial and end SOC, respectively, and Δ is the desired SOC difference between the initial and end values. $*_L$ and $*_U$ are the lower and upper boundaries of each item.

Engine speed, torque, and energy are subject to various mechanical and operational limitations for running NG engines and hybrid propulsion systems.

$$\begin{aligned} &\omega_L \le \omega(k) \le \omega_U \\ &T_L \le T(k) \le T_U \\ &P_{eng_L} \le P_{eng}(k) \le P_{eng_U} \end{aligned} \tag{34}$$

The LCC minimization problem is thus formulated as:

$$\min_x f(x) = \omega_1 C_{inv}(x) + \omega_2 C_{NG}(x) + \omega_3 C_{deg}(x) + \omega_4 C_{CO2e}\,(x) \tag{35}$$

where $x = [x_1, x_2, x_3]'$, x_1 is the size of the NG engine, x_2 is the number of batteries in series, x_3 is the number of batteries in parallel. C_{inv} is the investment cost of the BESS and the NG engine, C_{NG} is the NG fuel consumption costs, C_{deg} is the degradation-induced costs for the BESS, C_{CO2e} is the tailpipe CO_{2e} emissions of the NG engine. $\omega_1, \omega_2, \omega_3, \omega_4$ are weighting factors determined according to the costs of battery and LNG and design/operation considerations. The sizes of the engine and battery will influence the investment costs. The cost associated with battery degradation determines operational life and depends upon the number of charge and discharge cycles, DOD, and operating current. The optimal design of the propulsion system covers all four terms in Eq. 36, while the real-time optimal control only concerns the last three terms. The propulsion system design and control optimizations aim to find a balanced solution considering the system's investment, operation and degradation-induced costs, and tailpipe emissions.

The LCC minimization formulation ascertained optimal engine/BESS sizes and initial EMS/power allocation schemes for the hybrid electric ship propulsion system. The optimization problem is solved using a generic algorithm-based global optimization. The LFP BESS features a nominal capacity of 18Ah and comprises 160 cells in series and three cells in parallel. A baseline optimal EMS is also obtained through the global optimization for the optimized BESS and NG engine sizes.

7.3. Optimal Control Schemes for Hybrid Electric Propulsion

Different optimal power control and EMS schemes can operate a hybrid electric marine vessel under a specific operation profile, from the generic approach for all ICE hybrid propulsion systems to the advanced solution for the NG engine hybrid propulsion system used in this work.

7.3.1. CO_2 Emissions for Pure NG-Fueled Electric Propulsion System

Acknowledging the potential for excessive CO_{2e} emissions stemming from the methane leakage in certain operating conditions of a pure NG-fueled electric propulsion system, we introduce a BESS to enhance overall energy efficiency. Figure 39 illustrates the optimized engine operating point of the pure LNG-fueled electric propulsion system. Upon integrating BESS and advanced real-time optimal control, a notable reduction of approximately 12.28% in CO2e emissions is observed.

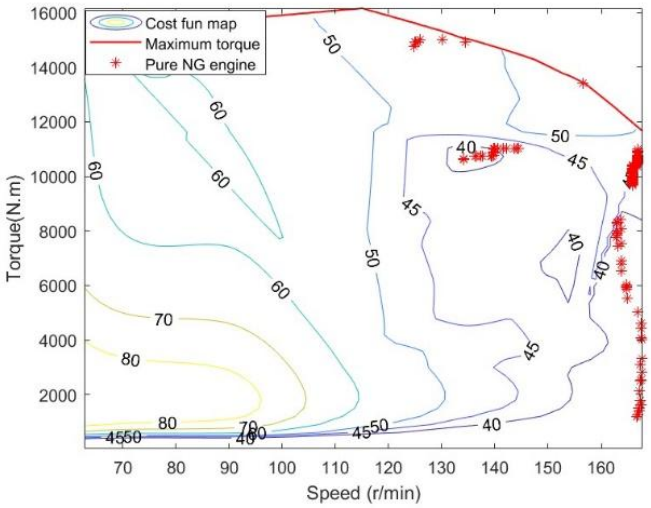

Figure 39. Engine operating points for pure NG-fueled electric propulsion systems.

7.3.2. Minimum Fuel Consumption and Associated CO_2 Emissions

The general and conventional real-time optimal control scheme for ICE hybrid electric propulsion systems uses fuel efficiency as the objective function to minimize fuel consumption and its associated CO2 emissions. The engine's fuel efficiency map (Figure 38(a)) is used to guide engine speed and torque controls. A trace of the engine operating points can indicate the effectiveness of the EMS. The optimized engine operating points, traced by varying engine speed and torque, are depicted as red points in Figure 40.

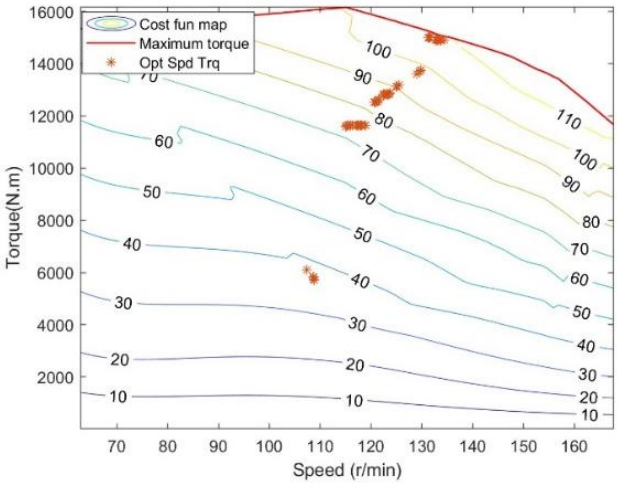

Figure 40. Engine operating points on fuel efficiency map.

7.3.3. Minimum NG Fuel Consumption and CO2e Emissions

The NG CI engine presents lower fuel costs and CO_2 emissions but increased HC and CO emissions due to incompletely combusted methane and NO_x emissions under low load. To address this unique issue associated with the NG-fuelled engine, the CO_{2e} emissions, covering CO_2, HC, CO and NO_x, are considered together with the NG fuel consumption in the optimal control and EMS of the ferry's hybrid electric propulsion system. The blue points in Figure 41 indicate the NG engine operating points derived from the CO_{2e} measure, introduced to optimize fuel efficiency while minimizing CO_{2e} emissions, striking the ideal balance between the two, which reduces approximately 5.75% in CO_{2e} emissions.

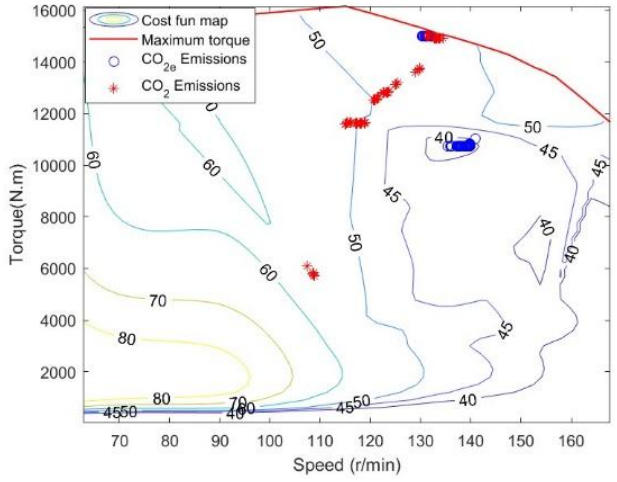

Figure 41. Engine operating points based on CDE map.

7.3.4. Minimum NG Fuel Consumption, CO_{2e} Emissions and LCC

Furthermore, lowering the LCC of the new NG-fueled CI engine hybrid electric propulsion system is critical for the wide commercialization of the new clean marine propulsion

technology. The hybrid electric propulsion system's design and control optimizations should embrace all key aspects, including the system's LCC.

Figure 42 presents the NG engine power and the BESS SOC over one ferry operation cycle using new batteries. Case 1 and Case 2 depict the optimal control strategies with and without considering battery degradation. Incorporating the battery degradation consideration into the optimal power control and EMS of the ferry led to a minor 0.75% increase in fuel consumption but more than 8% of battery decay-related LCC reduction. As the battery ages, excessive usage accelerates aging, significantly increasing the LCC.

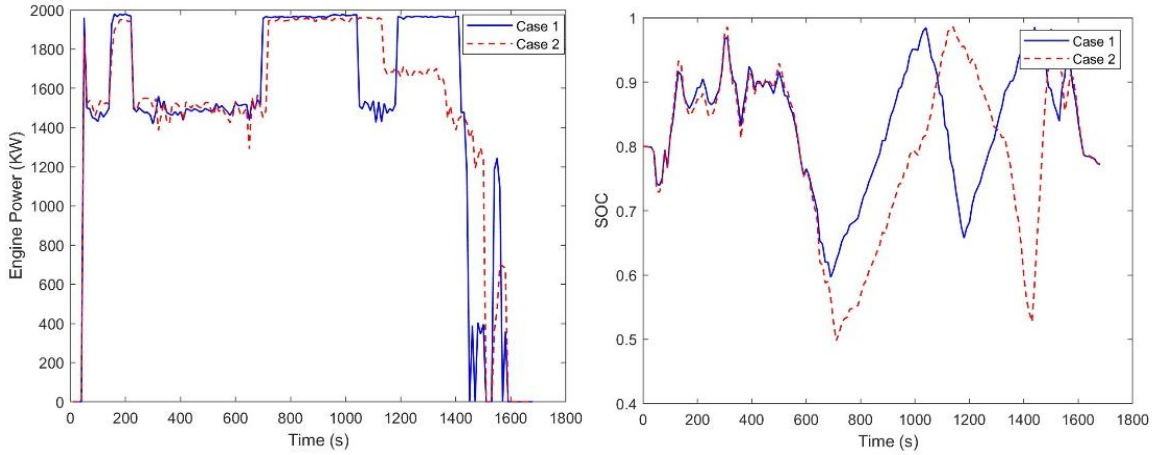

Figure 42. Engine power and SOC in different cases.

During operation, the vessel's power load changes dynamically, slightly departing from its standard operation profile, as assumed in this section, due to weather, ocean conditions, and cargo loads. The SOH of the BESS will also slightly depart from the laboratory data-based prediction due to the accumulated minor operation changes. This research introduces dynamic BESS performance and degradation model updates based on the vessel operation data to produce the real-time optimal EMS of the hybrid electric marine propulsion system, which will be discussed in the following section.

7.4. Real-time Propulsion Power and ESS SOH Predictions

The propulsion power demand of marine vessels fluctuates during their voyages due to variations in sailing routes, payloads, ocean currents, winds, tides, waves, etc. The optimal operation of the hybrid electric propulsion system is conducted by dynamically controlling the power flow and allocation between the gensets and the BESS. The real-time optimal power control and EMS of the NG-fuelled hybrid electric marine propulsion system are based on the minimum NG fuel consumption, CO_{2e} emissions and LCC, induced in Section 7.3.4, and additional improvement of the baseline optimal EMS using a dedicated MPC method. The enhancement is made using the vessel's real-time operation data and the more accurate and dynamically updated BESS performance and degradation models based on the vessel's real-time operation data.

7.4.1. Dynamic Change of Battery SOH and Degradation Model Updates

A vessel's statistical data-based, static operation profile provides a retrospective view of how the ship has been operating over a defined period. On the other hand, the dynamic operation profile is obtained by continuously monitoring and collecting real-time data from various sensors and data acquisition systems on board the ship for operation monitoring and adjustments and for ensuring safety and efficiency. In this work, we considered the most influencing wind load variation on the ferry's power demand and implemented real-time updates to the ferry's control strategy.

7.4.2. Accurate Propulsion Power Prediction Using Real-time Operation Data

Real-time optimal power control and EMS rely on accurately predicting varying propulsion power demand using instantly acquired vessel operation data. The KF is used in this work as the power demand prediction tool to facilitate MPC. KF algorithm uses linear system state equations to estimate the system state optimally through system input and output observation data. This paper uses a cubic polynomial to model the power demand. An EKF is employed to estimate the system state, which involves applying a Taylor series expansion to linearize the nonlinear system.

Given the ferry's fixed route, its power demand exhibits a consistent pattern across various environments. Utilizing historical data to assess the difference in power demand under different wind speeds enables more precise predictions of the ship's propulsion power requirements. This approach surpasses direct energy requirement prediction by incorporating the ship's adaptive response to changing wind conditions, yielding more contextually relevant estimates.

The results of EKF power demand prediction are shown in Figure 43.

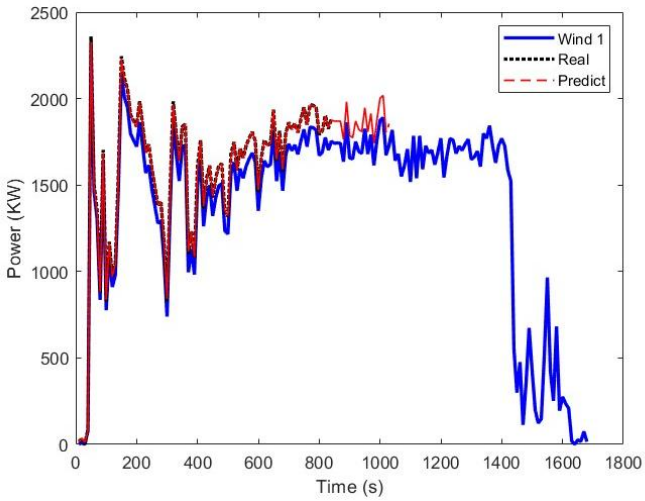

Figure 43. Power demand prediction.

7.5. Real-time Globally Optimal Control of the Propulsion System

7.5.1. Varying Vessel Operating Profile

The power demand for a ship's hybrid propulsion system varies noticeably, and no vessel's voyage follows the same static operation profile exactly. Vessel propulsion power demand differs due to various factors, including weather conditions, cargo types, slight route changes, operational decisions, and unforeseen events.

These changes will impact optimal vessel performance, fuel consumption, maintenance schedules, etc. For instance, the vessel's power demand under different wind speeds is shown in Figure 44. A higher wind speed results in an increase in vessel drag force, demanding more propulsion power.

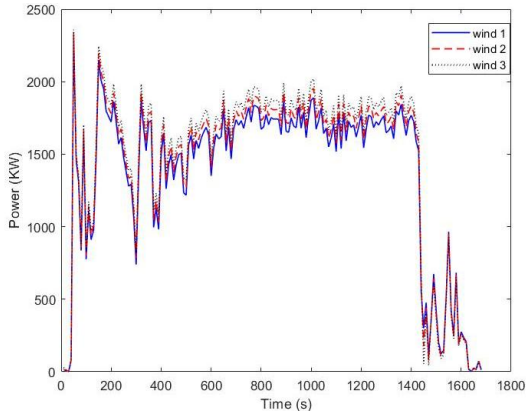

Figure 44. Power demand under different wind speeds.

7.5.2. A Dedicated Adaptive MPC Method

A baseline optimal EMS-guided MPC method is introduced in this work to improve the real-time optimal power control and EMS. The technique utilizes an EKF to forecast vessel propulsion power demand and monitor battery SOH during the ferry's real-time operation, as shown in Figure 45.

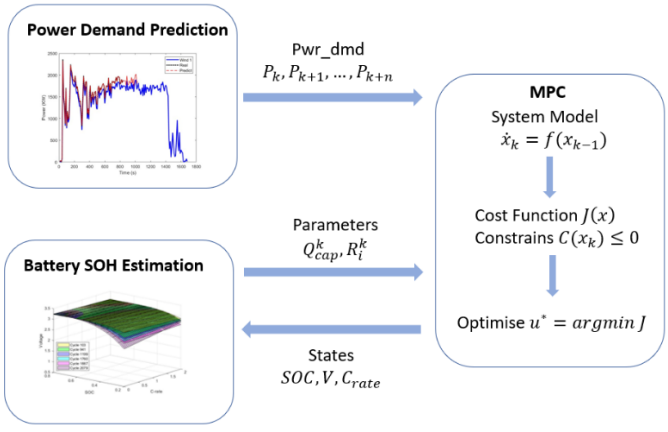

Figure 45. Architecture of the novel adaptive MPC method.

The accurately predicted real-time power demand is compared with the baseline optimal-EMS-associated power demand data to identify discrepancies. The EKF incorporates the current state, historical data, and prediction errors to enhance power supply management for the ferry's propulsion system.

In addition to forecasting power demand, the approach safeguards battery health by continuously monitoring the SOC and SOH parameters. The dynamic adjustments on battery performance and degradation models more accurately reflect the BESS SOH, thus extending battery life and ensuring adequate power output for optimal propulsion system performance. These changes are crucial for sustaining the long-term efficiency and reliability of the ferry's hybrid electric propulsion system.

While MPC is a common choice for optimizing energy consumption in dynamic systems, the KF primarily serves state estimation and prediction. Harmonizing these two strategies creates a comprehensive real-time optimal control approach, encompassing low CO2e emissions and LCC while meeting the vessel's mission. The LCC model defined in Eq. 31 is used in the real-time control optimization, ignoring the first term of the investment costs.

7.6. Results and Discussions

This section presents a comparative analysis of the LCC minimization-oriented real-time optimal control and EMS methods under different vessel operations and BESS SOH conditions. The new techniques for the global design and control optimizations of NG-engine hybrid electric marine propulsion systems were tested in the following four major areas, and conclusive findings are summarized in Table 9 for comparison.

1) The baseline optimal control and EMS approach applied DP to search for the vessel operation solution under the given static, statistical vessel operation profile.

2) The newly introduced EKF-MBC real-time optimal control and EMS method produces dynamic optimal power control and EMS solutions based on real-time vessel operation data during sailing.

3) Three BESS SOHs are considered: brand-new, middle-life, and near-end-life batteries.

4) Dynamic vessel operation condition changes, represented by three different wind speeds during in-the-wind sailing, are considered. Wind1, Wind2 and Wind3 are 1, 6 and 12 km/h, respectively.

The first scenario involves new batteries with the power demand influenced by Wind1. As the wind speed rises, the DP-based optimization produces unchanged BESS SOC, and the NG engine requires additional propulsion power, as shown in Figure 46.

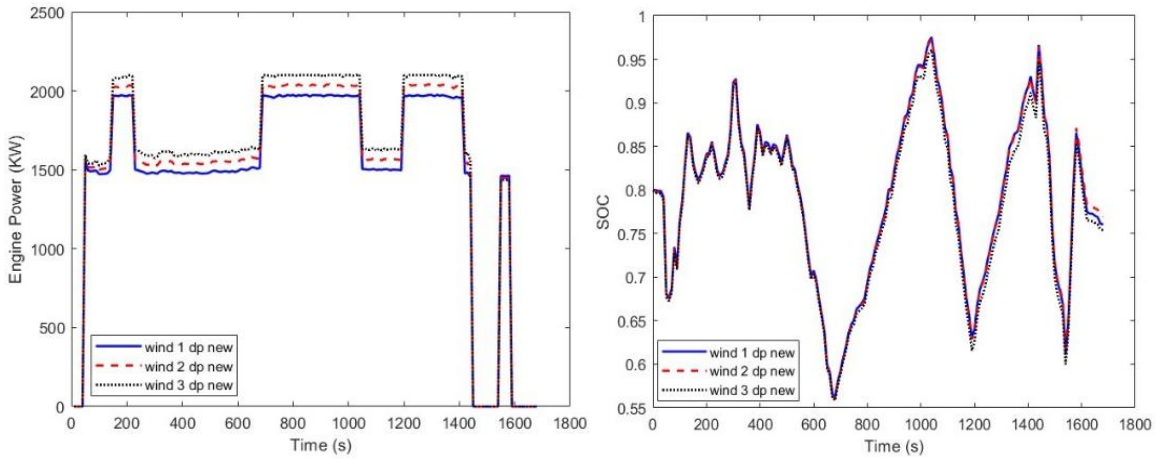

Figure 46. Engine power and SOC based on DP for different wind speeds.

Utilizing the Kalman filter, our new approach predicted a more accurate power demand under different wind speeds and estimated the power demand for the next twenty control steps. Each step covers 10 seconds of vessel operation. The more accurate predictions are then integrated into the MPC optimization algorithm. The EKF-MPC real-time optimal control outcomes are shown in Figure 47.

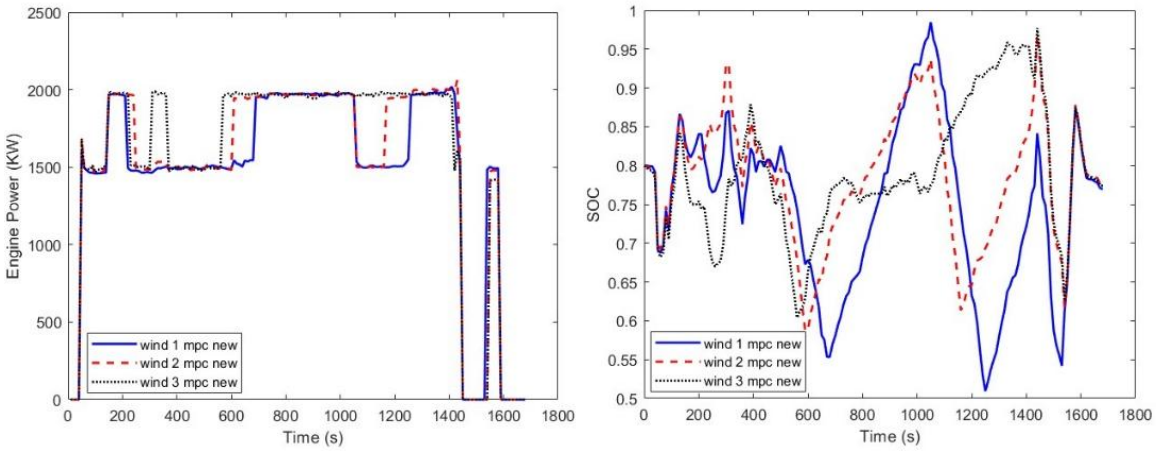

Figure 47. Engine power and SOC based on MPC for different wind speeds.

Figure 48 presents the results of optimal control under Wind1 and BESS degradation variation. The DP-based control optimization relied on fixed vessel power demand and BESS performance and degradation models, ignoring the further weakened battery's energy supply capacity and leading to inadequate power provision, thus increasing reliance on the engine. Consequently, as the battery ages, engine power fluctuates significantly, resulting in a substantial rise in fuel consumption and GHG emissions. Conversely, the BESS SOC management is more gradual in the EKF-MPC real-time optimal control under battery aging, allowing for a slower battery decay rate. This approach helps

to mitigate the impact of BESS decay and contributes to an overall reduction in the battery's deterioration over time.

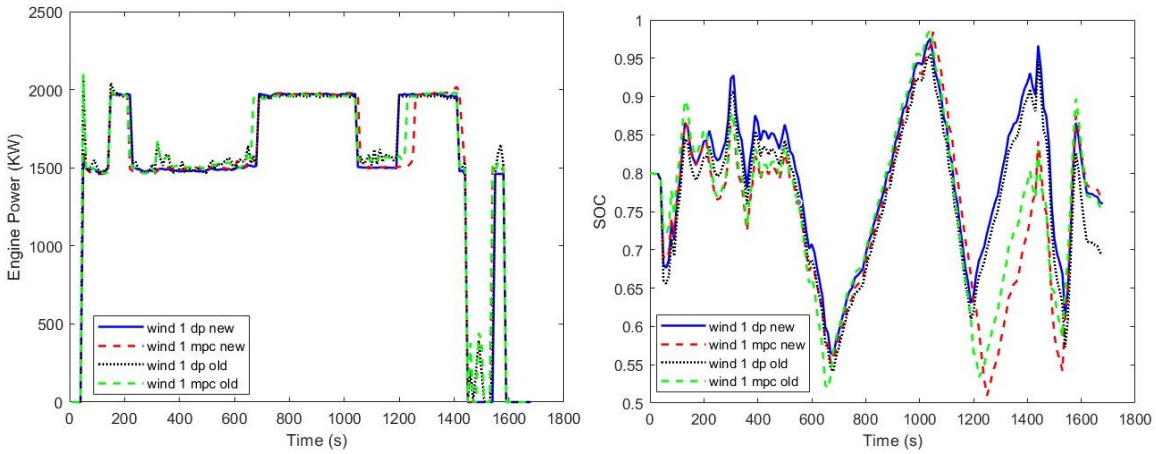

Figure 48. Engine power and SOC in different battery SOH for Wind 1.

Figure 49 illustrates the results of optimal control under Wind3. In the DP-based solution, the NG engine entirely compensates for the increased power demand. Combined with the impact of battery attenuation, the DP-based approach led to a subsequent increase in the LCC cost. On the other hand, the EKF-MPC real-time optimal control struck a better balance between battery degradation, fuel consumption, and CO2e emissions, showcasing the advantages of the new approach and its superiority in managing hybrid propulsion systems efficiently and effectively.

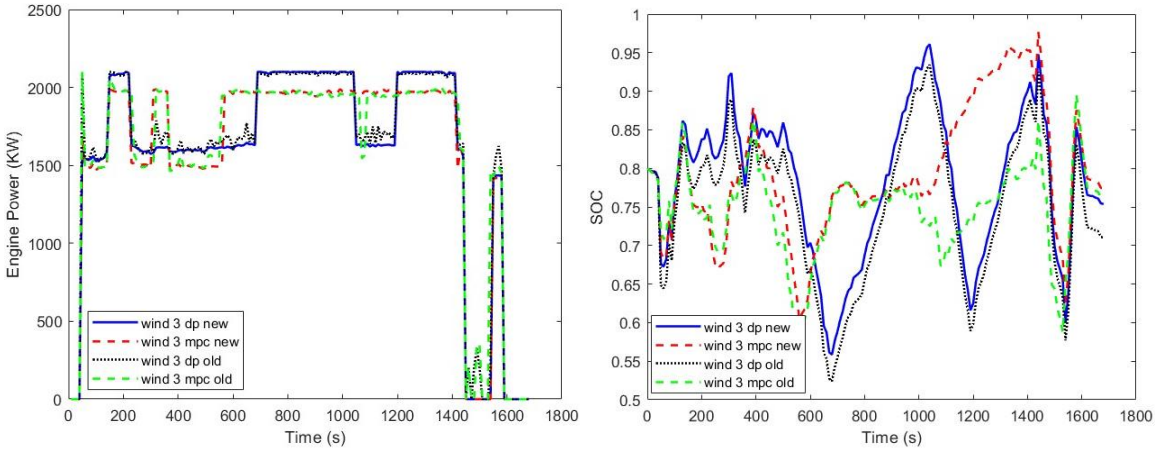

Figure 49. Engine power and SOC in different battery SOHs for the Wind3 Case.

Under the Wind1 load, when the ferry operates under the ideal static operation profile, and the battery has no degradation, the DP-based optimal control produced a better result (lower cost) than the proposed EKF-MPC real-time optimal control method, as expected. However, when there are changes in wind speed and/or battery attenuation, the strength

of the EKF-MPC real-time control strategy becomes evident. Under these dynamically changing loads, the new EKF-MPC real-time optimal control swiftly adapted to the changes and optimized the operation of the hybrid propulsion system, leading to reduced LCC costs.

Table 9. Minimum Overall LCC Measure Results under Different Vessel Operations ($)*

BESS SOH	Wind Condition 1		Wind Condition 2		Wind Condition 3	
	DP-Base	EKF-MPC	DP-Base	EKF-MPC	DP-Base	EKF-MPC
Brand New	6176.8	6189.1	6270.0	6240.2	6395.1	6291.0
Middle life	6272.1	6255.6	6359.9	6306.3	6470.3	6357.1
Near End-life	6293.2	6273.4	6382.6	6319.8	6492.2	6366.6

Table 9 compares the equivalent costs (in CAN$) of the ferry's daily operations under diverse conditions, encompassing factors like fuel consumption, carbon tax linked to CO_2 emissions, and battery depreciation due to degradation. Notably, the efficacy of the real-time control strategy becomes particularly pronounced when faced with fluctuations in wind strength, especially as the remaining battery life drops after extensive use.

The real-time control strategy demonstrates significant advantages, leading to an average reduction in operating costs by $305,286 over a decade of operation. Furthermore, this strategy achieves a noteworthy decrease in overall battery consumption, approximately 12%. These outcomes underscore the tangible economic and environmental benefits derived from the adept application of the real-time control strategy, reinforcing its merit in enhancing ferry systems' operational efficiency and sustainability.

Chapter 8. Case Study on BEV Battery-UC HESS for Low-Temperature Operations

8.1. Literature and Motivation

The surge in the adoption of EVs is driven by a confluence of factors, including heightened environmental awareness, economic considerations tied to fluctuating gasoline prices, the commendable fuel efficiency inherent in EVs, and the compelling need to adhere to evolving pollution standards [147]. Notably, the absence of minimal tailpipe emissions of EVs contributes substantially to enhanced air quality and an overall reduction in the carbon footprint. The superior energy efficiency of EVs, particularly evident in stop-and-go traffic scenarios where regenerative braking enables energy recovery, positions them as pivotal contributors to sustainable transportation. Li-ion batteries are the predominant ESS in EVs. Renowned for their high energy density, Li-ion batteries play a critical role in compactly and effectively storing substantial energy, a vital attribute for optimizing the range and performance of electric vehicles.

BESS is a critical and the costliest powertrain component for BEVs. Applying Li-ion batteries in BEVs introduces certain challenges related to their limited lifespan based on charge/discharge cycles, susceptibility to charge/discharge current and depth, and vulnerability to extreme temperatures. The BESS's power performance and energy storage capacity depend upon its operating temperature and level of degradation. The degradation rate depends upon the battery use pattern and operating temperature. Extreme operating temperatures distort the battery's electrochemical reactions, causing permanent capacity loss, shortening operational life, and increasing LCC. At present, considerable efforts have been made to improve the performance and operational life of the batteries through improved materials and manufacturing processes. A BEV's operation conditions cannot be improved without the assistance of a secondary power source, such as the engine or hydrogen fuel cell system in a HEV.

The battery-ultracapacitor (UC) HESS can address these challenges and enhance the longevity of Li-ion batteries. Most research focuses on reducing BESS's dynamic power loads without improving its operating temperature, particularly at cold and hot starts. A HESS incorporating batteries and UCs has been explored, using the UCs for high-frequency shallow charging and discharging, thereby minimizing the strain on the battery under variable loads and extending its overall service life [148][149]. Effective and economical battery protection within a HESS relies on optimizing the UC’s size and EMS [150]. The early investigations on battery-UC HESS were predominantly directed toward formulating effective control strategies to unlock the full potential of the HESS. These strategies primarily encompass three common control methods: rule-based or reference curves and tables control [151][152], fuzzy logic control [153][154], and closed-loop control [155][156]. Their primary objectives revolved around concurrently addressing the

challenges of delivering high energy and high-power output while minimizing the actual number of working cycles endured by the battery. The optimal power control and EMS of the HESS for a specific vehicle and its conditions are aimed at encompassing the optimal solution for all operating scenarios. DP stands out as the most effective solution method, widely employed in the development of the optimal EMS for vehicles equipped with HESSs [157][158][159]. Relying on the optimal HESS configuration, [13] extracts several control rules derived from DP outcomes and introduces a near-optimal rule-based strategy. The efficacy of UCs in HESS is evident, showcasing a significant reduction in battery life cycle costs, ranging from 47% to 60%, compared to configurations solely reliant on batteries. [160] advocated for adopting optimal control and power allocation strategies of the battery-UC HESSs for PHEVs, introduced a distinctive analytical approach utilizing DP, and presented a tailored optimization framework. The vehicle operation cycle that may constitute repeated standard driving cycles and typical load profile is a statistical representation of the vehicle use pattern. The DP and statistical operation cycle-based global optimization approach is ideal for producing the optimal hybrid powertrain system design and generating the benchmark optimal control solution. However, these DP-based methods can only generate the optimal EMS for vehicles that exactly follow the given operation cycle. As real-time vehicle operations always depart from the statistical driving and load cycle, the DP-based static optimal EMS will not lead to the optimal control solution. On the other hand, conventional real-time optimal control methods produce optimal EMS based on instantly acquired vehicle operation data under dynamically changing vehicle operating and environmental conditions. These include ECMS [161], PMP [162][163] and the most recent developments of MPC [164][165][166]. ECMS identifies the most energy-efficient hybrid powertrain design and control solution through balanced mechanical and electric power flows. The PMP strategy optimizes the power allocation by minimizing the Hamiltonian function at each instant, making it implementable in real time and related to the co-states. Predictive algorithms in [167] leverage weighted Markov processes to forecast propulsion power demands, showcasing real-time control strategies that enhance the operational efficiency of hybrid storage systems and facilitate the capture of surplus regenerative energy. [168] introduced a novel, straightforward, and readily optimized mathematical representation of EMS designed for real-time control of the HESS comprising batteries and UCs in BEVs to minimize energy consumption. [169] established a neural network model trained offline with a dataset derived from wavelet transform decomposition. This model was designed to predict the low-frequency power demand of the battery in real time, calculate the high-frequency power demand online, and subsequently allocate it to the UCs. These research endeavours rely on static battery performance and degradation models derived from laboratory data, constraining their efficacy in formulating optimal power control and EMS for electrified propulsion systems. However, these real-time optimal control methods can only predict the vehicle power demand over a short period, and they cannot foresee the vehicle operation over the entire vehicle operation cycle. The series of local optima do not necessarily lead to the global

optimum. A combination of the DP and statistical operation cycle-based global control optimization and the conventional real-time optimal control methods can potentially minimize the errors caused by the difference between the statistical operational cycle and real-time operation and the inability to predict long-term power demand accurately. This research will introduce a new optimal EMS-generating method to fulfill this need.

Temperature extremes, especially at the lower end of the spectrum, significantly impact the performance and capacity of Li-ion batteries [170][171][172]. Operational temperatures between 15°C and 35°C are deemed optimal, ensuring limited adverse effects on battery performance and capacity [173]. To mitigate the impact of low temperatures, typically ranging from -40°C to 15°C, and high temperatures of above 35°C, active battery thermal management using another onboard power source, such as the engine in a HEV, is employed to bring the operating temperature of the batteries into the desired 15-35°C window to ensure its performance and avoid rapid degradation. For a BEV with a sole energy source, drawing battery power to warm up cold batteries at low operating temperatures is ineffective due to poor battery performance and is harmful to battery life. Cooling down the hot batteries at high operating temperatures using battery power is also detrimental to battery life. The UCs in a HESS, which are resilient to extreme temperatures, can power the active battery thermal management in principle. However, due to the lack of battery performance and degradation data, as well as associated models at extreme temperatures, an effective battery thermal management strategy (TMS) and associated HESS design and control optimization methods have not yet been systematically developed. This work extends the use of the UCs in the HESS to improve the undesirable initial temperature of the batteries, improve their power performance, and reduce long-term capacity degradation. This proactive thermal management ensures that the battery operates within or near the prescribed temperature range, safeguarding optimal performance and preventing irreversible damage.

The core innovation of this work is the optimal thermal management for the batteries using the energy from the UCs in the HESS at cold or hot starts and during operations. The realization of optimal thermal management is embedded into the HESS system design optimization and the HESS optimal EMS stated previously. In this context, temperatures around 25°C represent the ideal operational range, with goals set for the TMS to maintain conditions conducive to prolonged battery life and sustained performance. Considerable efforts have been devoted to collecting Li-ion batteries' performance, temporary and long-term capacity loss, and thermal behaviour data and building their performance, degradation, thermal, and LCC models. These models form the foundations for optimized system design, EMS and TMS of the HESS for a given BEV under a specific operation profile. These vehicles experience diverse operations and extreme starting temperatures, leading to propulsion and operation power demand fluctuations. Particularly, extremely low environmental temperatures significantly impact the aging of Li-ion batteries, temporarily or permanently diminishing the energy they supply, impacting these vehicles' overall

capacity and performance. The extremely high environmental temperatures present a similar case without instant battery performance loss. Battery chilling, instead of heating, can be used. The topic is beyond the scope of this paper.

The new synchronized optimizations of the battery-UC HESS design, EMS and TMS are introduced to address this overlooked issue, ensuring the BEVs' electric ESS power performance and energy storage capability and minimizing the LCC of the BEV. This optimized HESS design and operation improve the batteries' use pattern and performance under low temperatures and reduce the extreme temperatures' impacts on the batteries' operational life. First, performance and degradation data of commonly used Li-ion batteries under extreme temperatures and various use patterns are collected to form advanced battery performance, degradation and thermal models to facilitate the HESS's optimal design and energy management for a BEV under different operations. Effective EMS and TMS are introduced to play the batteries and UCs to their strength to minimize the BEV's LCC. The optimized HESS reduces the harsh use of the batteries and allows the batteries to operate at the preferred temperatures, ensuring performance and longevity while minimizing the added costs. The optimal sizing of the batteries and UCs and the HESS baseline optimal EMS are simultaneously generated using empirical data-based battery performance and degradation models and the BEV's operation cycle using global design optimization and DP-based optimal energy management. The optimal operation of the HESS in real-time incorporates active battery TMS under different temperatures and extends the baseline optimal EMS and battery degradation models according to the vehicle's and the batteries' instant operation data. The accurate prediction of vehicle propulsion power is made through the EKF using both statistical and online data. The batteries' performance and degradation models are improved using the continuously updated SOH model. These rapid updates enable precise control and EMS through MPC. A case study demonstrates the benefits of the newly introduced HESS design and control optimization methods, showcasing the effectiveness of the new EKF-MPC real-time optimal control, EMS and TMS.

8.2. ESS System Design and Energy Management for EVs

The design and EMSs for various types of EVs, including HEVs and BEVs, differ significantly due to their varying propulsion architectures and ESS characteristics.

HEVs feature an ICE and an electric motor/generator, with a smaller battery pack than other EVs. The ESS in HEVs is typically used to supplement the ICE during acceleration and provide regenerative braking capability. Thermal management in HEVs often relies on the engine's waste heat to regulate battery temperature. Energy management focuses on optimizing the coordination between the ICE and the electric motor to achieve fuel efficiency while meeting performance demands.

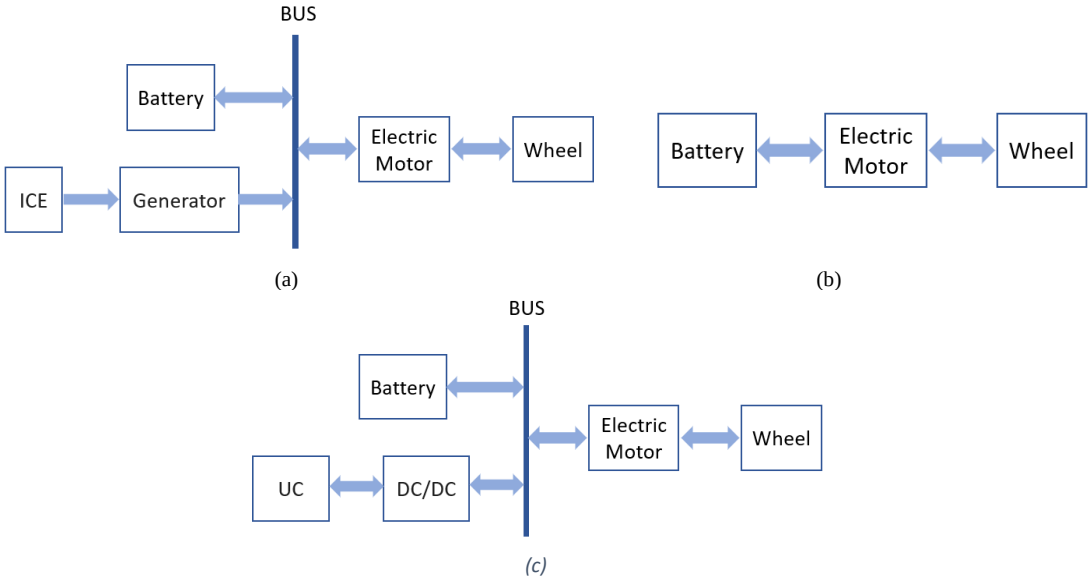

Figure 50. Energy power diagram for (a) HEV, (b) BEV and (c) HESS-EV.

BEVs feature a significantly larger battery pack than HEVs to provide sufficient range. In the design of BESS, battery usage patterns must be carefully considered to avoid excessive degradation. BEVs rely solely on battery power, making battery performance and longevity critical. Advanced BMS is necessary to monitor and regulate factors such as charging/discharging rates, DOD, and temperature to optimize battery life. Thermal management is crucial to maintaining optimal battery temperature, often employing active cooling/heating methods. However, under extremely low temperatures, the effectiveness of thermal systems is usually limited, especially if the vehicle is not actively being driven or if the temperature remains consistently low for an extended period, which could lead to reduced battery efficiency and capacity, limiting the vehicle's range and overall performance.

The batteries and UCs in HESS-EVs are complementary energy storage technologies, potentially offering improved performance, efficiency, and extended lifetime compared to using either technology alone. By integrating UCs, the ESS can optimize the use of both batteries and UCs, reducing strain on the battery and improving overall efficiency. First, UCs can efficiently handle rapid charge and discharge cycles, making them ideal for capturing energy during braking and providing power during acceleration. UCs can provide bursts of power without significant temperature fluctuations. By sharing the workload with UCs, the battery experiences less stress, which can help regulate temperature impacts and improve battery longevity. Secondly, insensitive to extremely low starting temperatures, UCs can provide energy to power the batteries' TMS during cold starts to regulate the battery pack's temperature without putting additional strain on the batteries. However, the latter has not yet been systematically studied due to the lack of adequate battery performance/degradation data and models at low temperatures and the effective

optimal EMS and TMS. This research adds the second part and integrates both to enhance BEV's efficiency, durability, and usability across various operating conditions.

8.3. Modelling of HESS and Its Other Components

8.3.1. Li-ion Battery-UC HESS

Battery-UC HESSs have three different energy management approaches: passive, active and semi-active. The semi-active HESSs are currently used in most applications due to the balance between system performance and complexity, as shown in Figure 51. Here, a bidirectional DC/DC converter adapts to the wide range of voltage changes when the UCs work and controls the energy flow between the battery and UC modules.

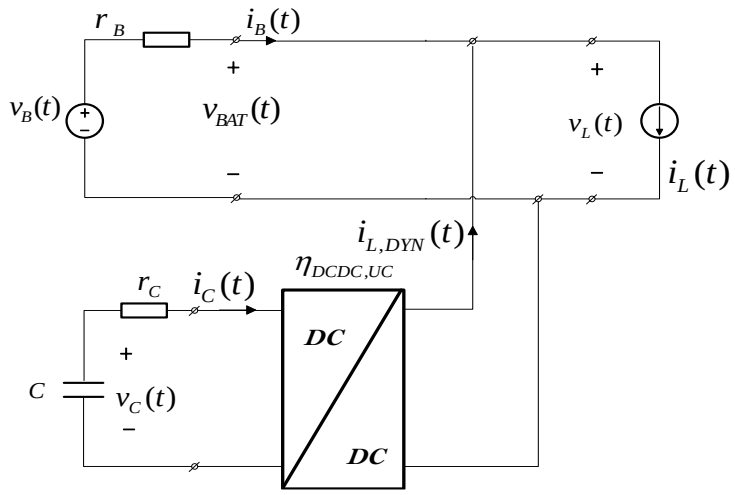

Figure 51. Composite electric energy system structure of Li-ion battery-UC.

8.3.2. UC Model

As UCs are increasingly used in different applications, their modelling is essential for system design, condition monitoring, and performance evaluation. Many UC models have been reported in the literature, and the UC model is shown in Figure 52.

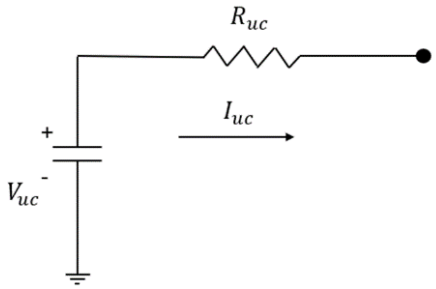

Figure 52. UC equivalent circuit model.

UC packs are organized into groups using n_s^{uc} series and n_p^{uc} parallel connections. The UC models are:

$$C_{uc} = \frac{n_p^{uc} C_M}{n_s^{uc}} \tag{36}$$

$$V_{uc} = V_{uc}^{ocv} n_s^{uc} \tag{37}$$

where C_{uc} is the capacity of the UC pack, C_M is the capacity of UC cells. V_{uc}^{ocv} is the open circuit voltage of the UC module, and V_{uc} is the OCV of the UC pack.

The SOC of the SC is linearly proportional to V_{uc} as follows:

$$SOC_{uc} = \frac{V_{uc}}{V_n} \tag{38}$$

$$E_{uc} = 0.5 C_{uc} V_n^2 (1 - SOC_0^2) \tag{39}$$

where V_n is the UC voltage under fully charged conditions, E_{uc} is the released energy of the UC when its SOC drops to SOC_0.

Since a simplified UC model is used here, the slight influence of temperature is not considered for C_{uc}. Equation (39) shows that when the power in the UC drops from 100% to 50%, the UC can release 75% of its stored energy. The feasible *SOC* of the UCs is normally between 50-100%. Given the long cycle times of UCs of over 500,000 cycles, their capacity loss is not considered in the model.

8.3.3. DC/DC Converter Model

A generic modelling tool for a DC/DC converter, with its example efficiency map shown in Figure 53, has been introduced in earlier research [174] to predict power loss under different operation conditions. The performance and energy efficiency influences of possible DC/DC converters in the electric powertrain and ESS charge systems will be captured using this tool.

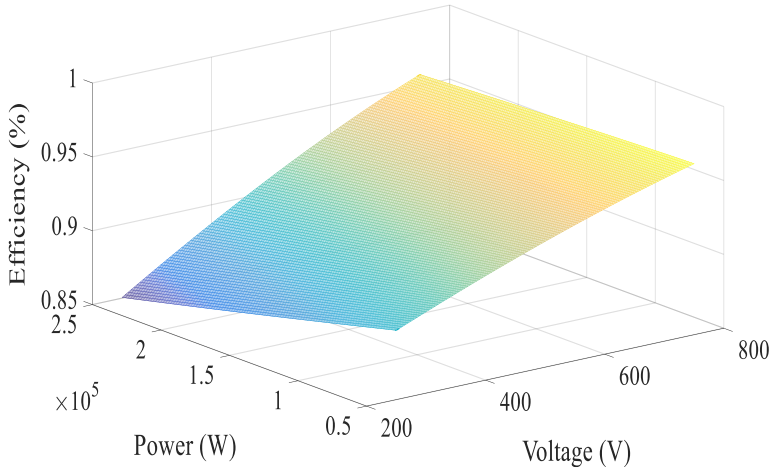

Figure 53. DC/DC converter efficiency map model [174].

8.4. Battery-UC HESS Design and Baseline Optimal EMS

UCs and batteries, distinct yet complementary energy storage technologies, allow the HESS to surpass their individual energy storage capabilities to meet a BEV's power demand and improve battery performance and life, which is unique to this work.

The optimal sizing of the batteries and UCs within the HESS and the baseline optimal EMS are based on the specific BEV and its driving characteristics, represented by the standard driving cycle from statistical operation data. We use a typical BEV with an average payload and the standard driving cycle to derive the vehicle power load profile to be met by the new integrated HESS design and EMS optimizations. The battery TMS is part of the HESS EMS, extending its function beyond providing propulsion power to the BEV as in the conventional approaches.

In addition, a new and more accurate real-time optimal control will be introduced based on instant vehicle and battery operation data for dynamically coordinating battery-UC their charge and discharge.

In this study, we established a vehicle simulation model within the MATLAB/Simulink environment, which reflects the parameters characteristic of typical light trucks (listed in Table 10). The comprehensive setup encompasses battery ESS, propulsion motors, final drive, wheels, vehicle dynamics, power converters, and electrical accessories.

Table 10. Vehicle Design Parameters of Electric Medium-Duty Truck (MDT)

Vehicle	Curb mass/kg	2212
	GVWR/kg	3495
	Wheel base/mm	3030
	Top speed/km/h	131.3
	Tire radius/m	0.3012
Final drive	Ratio/1	5
Motor	Rated power/kW	150
	Maximum speed/r/min	8000
	Maximum efficiency	0.9
Battery	Cell nominal voltage/V	3.7

Figure 54. A typical electric MDT.

A backward-facing, Matlab-based, vehicle-level DP has been modelled to perform the energy analysis of electric vehicles. This vehicle level considers the vehicle as a point mass and studies the insertion with the external environment to compute the power and energy needed to move it at the specified speed. This high-level approach is useful for understanding the vehicle longitudinal dynamics and the energy characteristics of vehicles.

The propulsion system model contains a vehicle dynamic model, which calculates the force due to air drag and tire resistance. It also accounts for the grade force when travelling uphill/downhill. The quadric function to estimate the vehicle dynamic force, which contains wheel force, grade force, and aerodynamic force, and can be summarized as follows:

$$T_{wheel} = F_{wheel} * r_{wheel} \tag{40}$$

$$\begin{aligned} F_{wheel} = & F_{roll} + F_{cd} + F_{grade} + ma \\ = & \alpha + \beta v + \gamma v^2 + m\, g \times sin(\theta) \\ & + \alpha_{cd} A v \times sin(\theta) + ma \end{aligned} \tag{41}$$

where α, β, γ are the tire friction coefficient, v is the vehicle speed; m is the mass of the vehicle; a_{cd} is the air drag coefficient; A is the vehicle frontal area; a is the acceleration. T_{wheel}, F_{wheel}, r_{wheel} is the torque, total force and the radius of the wheel. As shown in Figure 55, the optimal power control code is embedded in the controller model.

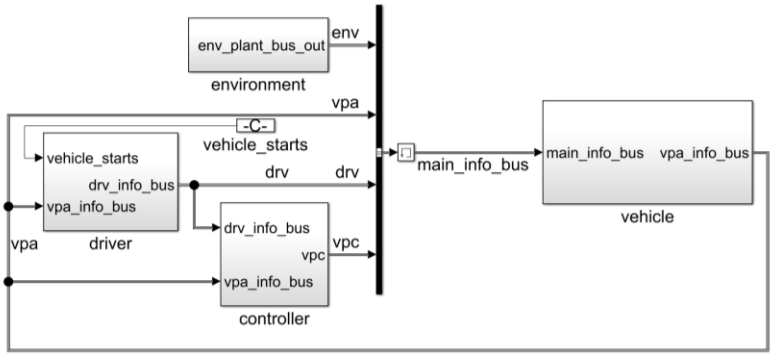

(a) Upper-level model

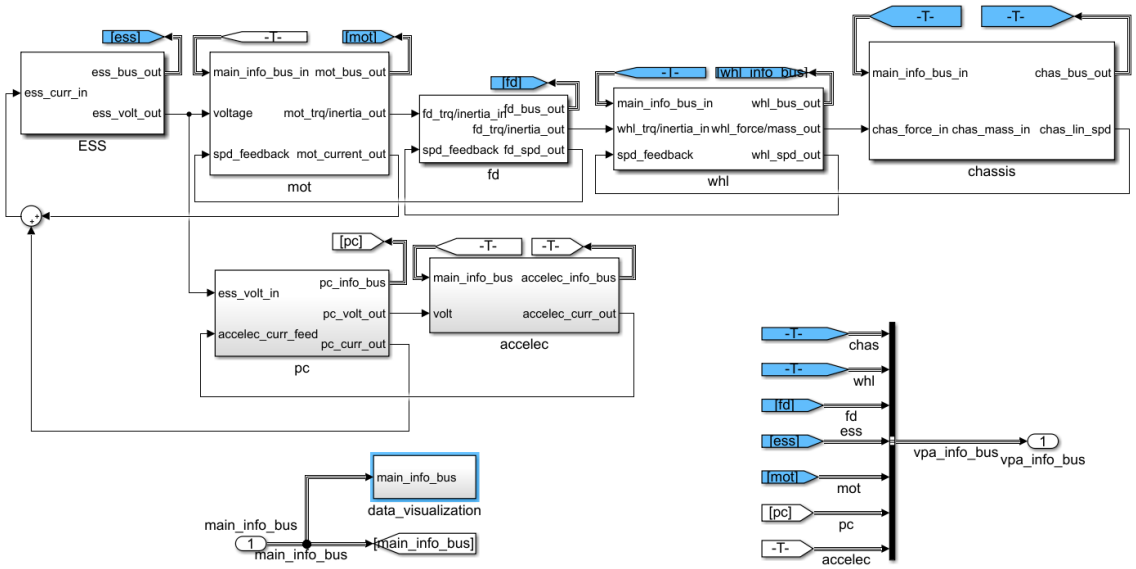

(b) Vehicle plant model.

Figure 55. Vehicle simulation model.

The United Nations Economic Commission developed the worldwide harmonized light vehicles test cycles (WLTC) for Europe, a series of standardized test procedures and driving cycles designed to assess the fuel consumption and emissions of light vehicles, such as passenger cars and light commercial vehicles.

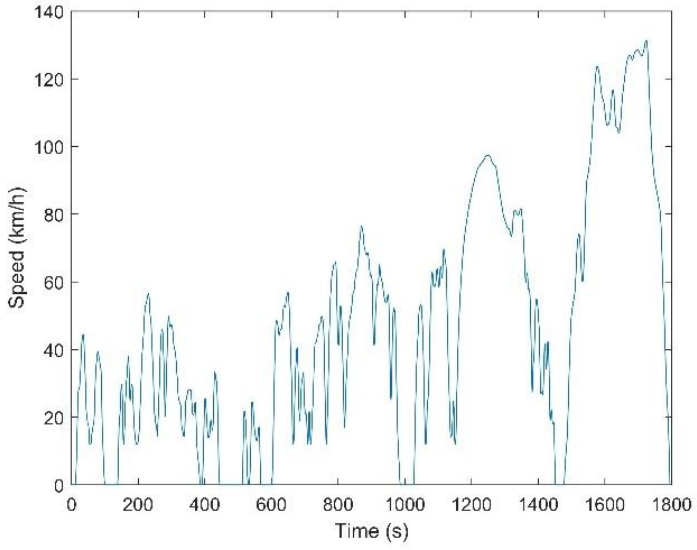

Figure 56. Vehicle speed of WLTC cycle.

The power demand can be obtained using vehicle operation simulations under the WLTC driving cycle.

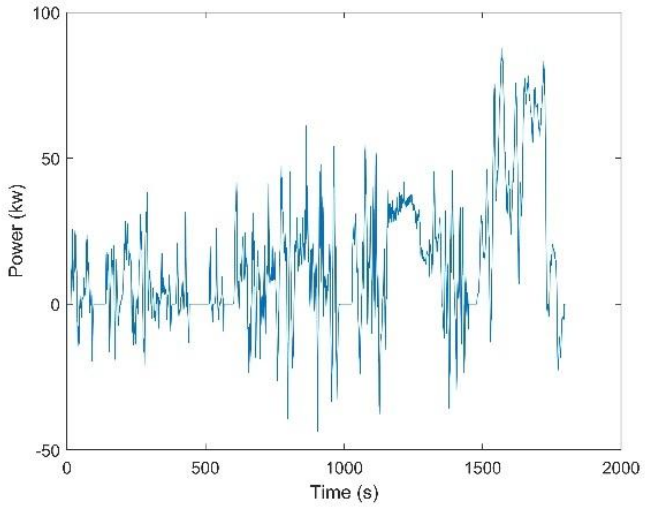

Figure 57. Vehicle propulsion power demand based on the WLTC cycle.

8.5. Optimal Sizing of Battery and UC for Minimum LCC

The design of the HESS and its EMS/TMS are inseparable. The global minimization of the HESS' LCC involves the optimal sizing of the batteries and the UCs and the optimal EMS and TMS of this HESS with the given battery pack and UC pack sizes. This formulation leads to a nested, two-level global optimization problem. The problem consists of the top-level global optimization of the HESS sizing parameters and the bottom-layer optimal EMS and TMS searches using DP over all feasible control operations. These optimizations' objective and constraint functions are based on the numerical simulations of the vehicle performance, energy consumption, system investment costs and battery end-of-life replacement cost using the BEV's MATLAB/Simulink models.

8.5.1. Optimal Sizing of Battery and UC for Minimum LCC

The optimal sizing of batteries and UCs in a HESS incorporates various considerations. First and foremost, it aims to fulfill the BEV's functional requirements, ensuring simultaneous compliance with the high-energy and high-power output demands of the vehicle power system. Utilizing UCs involves taking over or shunting frequent shallow and rapid charging and discharging, thereby diminishing the actual working cycles of the battery in each application. Additionally, leveraging the power stored in UCs enhances electric vehicle battery performance during cold starts or in extremely high temperatures. These requirements dictate the minimum size of UC cells in the HESS. However, this sizing must align with overall ESS constraints such as size, weight, and costs. These requirements and constraints are contingent upon the specific application. Simultaneously, achieving the lowest LLC of the system is imperative. Investing and incorporating UC units into the ESS prolongs the battery's service life and reduces costs. Striking an optimal balance between the investment costs for UC units and system control is crucial, ensuring efficiency gains in the vehicle power system and minimizing expenses related to battery life extension.

Minimizing LLC determines the optimal size of the HESS and devises effective energy management and power allocation schemes for the BEV's powertrain. Overly large HESS, including their UC units, can result in substantial investment costs and added weight for electric vehicles. Conversely, inadequately sized systems may compromise vehicle performance and contribute to the need for costly battery replacements. Striking the right balance is crucial for achieving an optimal and cost-effective BEV's ESS solution.

The LCC model includes capital and operating costs calculated using the following equations:

$$LCC = \omega_1(UC_{cap} + Batt_{cap}) + \omega_2 Q_{cycle} \tag{42}$$

$$UC_{cap} = S_{UC} \cdot P_{UC} \cdot E_{UC_{cell}} \tag{43}$$

$$Batt_{cap} = S_{batt} \cdot P_{batt} \cdot E_{batt_{cell}} \tag{44}$$

$$Q_{cycle} = \sum_{i=1}^{N} Q_{loss(i)} \tag{45}$$

where UC_{cap} and $Batt_{cap}$ are the capital costs of UC and battery, respectively, S_{UC}, P_{UC}, S_{batt}, P_{batt} are the number of UC/battery cells in series and parallel, $E_{UC_{cell}}$ and $E_{batt_{cell}}$ are the cost of UC and battery cells, respectively. Q_{cycle} is the total Q_{loss} in a cycle, which covers the costs related to system efficiency loss.

8.5.2. Optimal HESS Power Control and Baseline EMS Using DP

The DP is widely applied to solve the problem of EMS for HESS-based vehicles [157][158][159]. The approach identifies the global optimal control solution for power allocation and sharing between the batteries and the UCs in the HESS over the entire BEV's power demand cycle or a trip between ESS grid charges. The optimization of HESS baseline EMS is crucial for enhancing the performance and longevity of BEVs. This optimization encompasses three key aspects, each designed to maximize efficiency, extend battery life, and improve overall vehicle performance.

- Optimizing HESS Energy Efficiency: Our optimization strategy focuses on achieving the best possible energy efficiency for the HESS. By precisely matching the energy demand cycle of BEVs with the capabilities of the HESS, we aim to minimize energy wastage and ensure optimal utilization of available resources.
- Extending Battery Life with Improved Usage Patterns: Prolonging the lifespan of BEV batteries is crucial for reducing operational costs and environmental impact. Utilizing UC, we can efficiently manage large and shallow charge/discharge loads, reducing strain on the battery cells.
- Extending Battery Life Using Heating at Cold Start: Cold weather conditions present significant challenges to battery performance, particularly during vehicle startups. By utilizing the energy stored in the UC to power the battery thermal management

system during startup, we can efficiently heat the battery to a more suitable operating temperature. This approach could minimize cold-start-related degradation, extending its lifespan and improving long-term reliability.

The formulation of the DP-based EMS optimization consists of the objective function and constraints listed in Equations 46 and 47. As the DP search is based on the statistical data-based standard driving cycle, the optimal EMS serves the baseline optimal EMS, which needs to be extended for the BEV's real-time operations, as discussed in the following section.

$$min \sum_{k=1}^{T} \omega_E E(k) + \omega_Q Q_{loss}\big(Ah(k), C_{rate}(k), Temp(k)\big), \tag{46}$$

$$\begin{aligned} &P_{dmd}(k) = P_{cycle}(k), k \in [1, T] \\ &SOC_{UC} \in [SOC_{UC_L}, SOC_{UC_H}] \\ &SOC_{UC_0} = SOC_{UC_{end}} \\ &I_{BT} \in [0, I_{BT_{max}}] \\ &P_{UC} \in [P_{UC_{min}}, P_{UC_{max}}] \end{aligned} \tag{47}$$

where E is the energy consumption of the ESS, P_{dem} is the power demand, P_{cycle} is the total power of the driving cycle, SOC_{UC_L} and SOC_{UC_H} are the lower and upper limits of the SOC_{UC}, is the initial SOC_{UC} value, $SOC_{UC_{end}}$ is the end SOC_{UC} value, $SOC_{UC_{min}}$ and $SOC_{UC_{max}}$ are the minimal and maximal power of the UC pack, and $I_{BT_{max}}$ is the maximal discharge current of the battery pack.

The power of the battery and UC needs to satisfy the power demand shown in Equation (48), where P_{BT} and P_{UC} represent the actual output power of the battery and UC packs after considering the efficiency of the DC/DC converter:

$$P_{\text{dem}}(k) = P_{\text{BT}}(k) + P_{\text{UC}}(k) \tag{48}$$

During vehicle operation, the battery's performance is influenced by two key factors. Firstly, temperature fluctuations impact the battery's V_{oc}, with lower temperatures resulting in lower Voc. Additionally, battery aging occurs with usage, leading to diminished SOH, elevated resistance, and reduced capacity. An effective battery decay model continually monitors performance during usage and adjusts parameters to refine the battery model.

Given that low temperatures accelerate battery decay, prompt temperature elevation is crucial. Although the battery generates heat during operation, this process is gradual. Therefore, apart from meeting driving energy demands, supplying energy to the battery thermal management system becomes imperative to maintain optimal temperature levels.

Here, UCs play a pivotal role in aiding vehicle energy supply. Their performance remains largely unaffected by temperature, making them a reliable energy source. Leveraging UC energy, especially when battery temperatures haven't risen, safeguards both the thermal management system and vehicle power supply, augmenting the battery's function.

A crucial step in designing a DP model and search is specifying state and control variables. State variables (such as SOC and temperature) are chosen to maintain consistency throughout the driving cycle. In contrast, the control variables (such as the power split rate between different power sources and the heat power) are chosen to influence the vehicle state at the proceeding step. The state vector, X, is calculated by iterating through the values of each state variable and driving cycle. The control vector, U, is formed by repeating this process. The indices in the respective vectors are used to relate to each distinct state and control. Finally, the DP algorithm can be summarized in Figure 58.

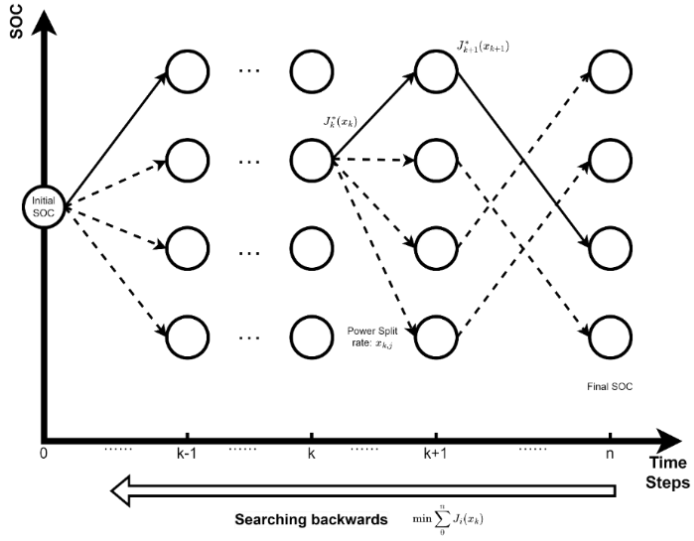

Figure 58. DP algorithm.

8.5.3. Advantages of HESS and Comparison

When cars rely solely on batteries as their primary energy source, the battery's SOC can exhibit significant fluctuations during a driving cycle. This fluctuation is due to the varying energy demands on the battery as the vehicle accelerates, decelerates, and encounters different driving conditions. These fluctuations can impact the vehicle's overall efficiency and performance.

Integrating a UC as an auxiliary energy source in the vehicle's electrical system can help stabilize the battery SOC. UCs are energy storage devices that can quickly store and discharge electrical energy. They are known for their ability to rapidly provide bursts of power, making them well-suited for smoothing out the power demands on the battery in dynamic driving situations.

Figure 59 depicts a DP-based control strategy. Initial parameters are set with the battery's SOC at 0.95, the UC's SOC at 1, and both battery and ambient temperatures at -15 degrees Celsius.

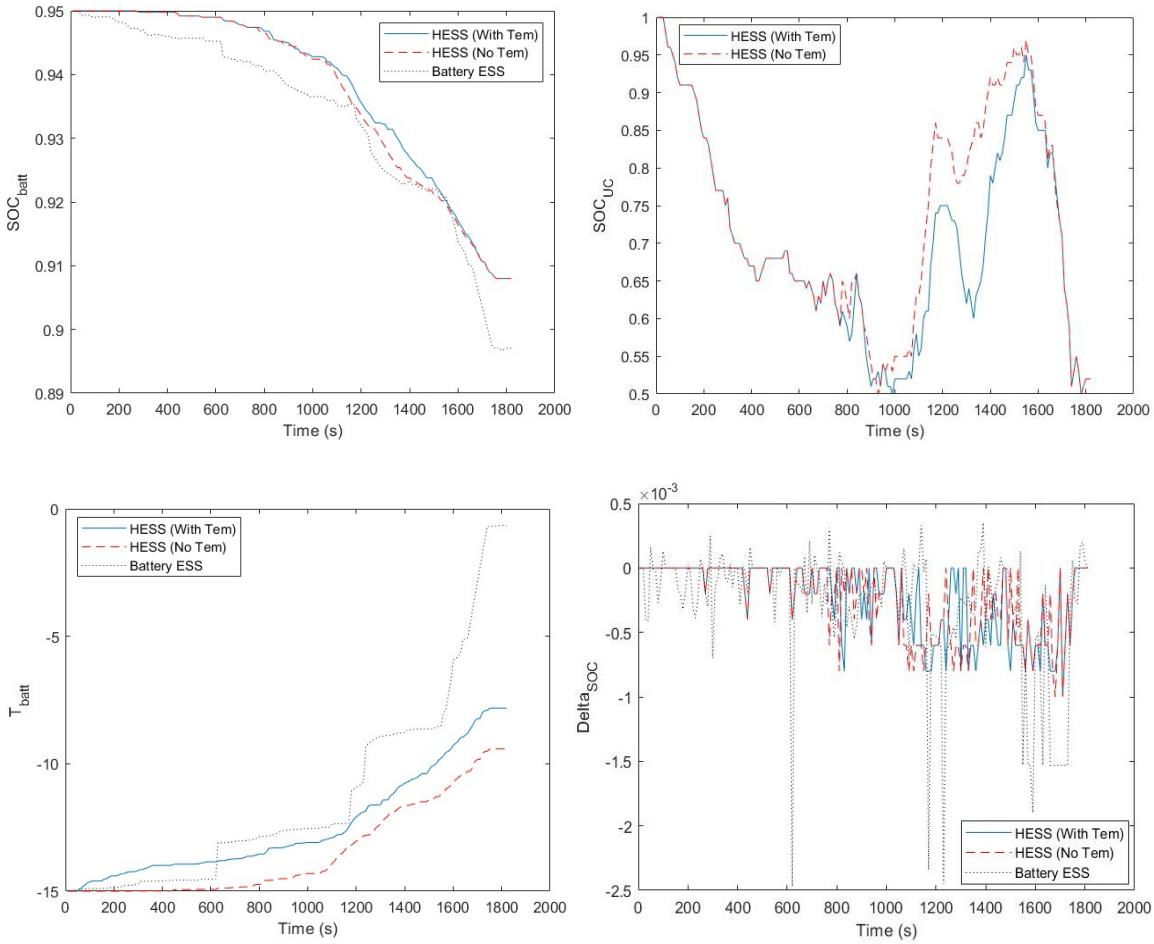

Figure 59. Battery SOC, UC SOC, temperature and delta SOC of both HESS and BESS.

UCs can absorb and release electrical energy rapidly. When the vehicle goes through quick accelerations and decelerations with propulsion and braking-recovery power surges, the UC can provide and absorb the excess energy, reducing strain on the battery with fewer SOC fluctuations and large discharge and charge currents. During regenerative braking, energy generated during deceleration is typically captured and stored. UCs excel in this scenario, quickly absorbing the excess energy and preventing battery overcharging. UCs can operate efficiently at lower temperatures compared to batteries. They are less sensitive to temperature changes, making them suitable for cold environments.

Without considerations for low temperatures, UCs manage the rapid charge and discharge demands within electric ESSs, thereby mitigating stress on lithium batteries. This reduction in charge-discharge cycles and current levels minimizes battery degradation and extends its operational lifespan, thus lowering the overall LLC. Moreover, when factoring

in an initial low temperature of -15°C and employing UCs for battery heating, optimizing energy management within the composite electric ESS undergoes significant changes. This results in distinct operational states for two design configurations: HESS (No Temp) and HESS (With Temp).

The impact on the Li-ion battery's storage capacity loss and the equivalent charge-discharge cycles over a half-hour period is detailed in the table below.

Table 11. Comparison of BESS, HESS (No Temp) and HESS (With Temp)

	BESS	HESS (No Temp)	HESS (With Temp)
Q_{loss}	11.60e-6	8.12e-6	7.89e-6
Equivalent charge-discharge cycles	1.45	1	1

By adjusting the temperature and reducing the DOD on the battery, adding a UC can help extend the battery's overall lifespan by 42.86% and reduce the number of battery cycles by 45% in one cycle. Considering low temperatures, the lifespan can be additionally extended by 2.92%. Integrating a UC as an auxiliary energy source in a BEV can improve energy management and contribute to a more efficient and durable vehicle.

8.5.4. Solution of the Nested Global Optimization Problem

Solving this complex, computation-intensive, black-box global optimization problem requires an efficient global optimization search algorithm. Our test examples compare the commonly used genetic algorithms (GA) with our innovative multi-start space reduction (MSSR) algorithm, leveraging a kriging-based agent model, multi-start scheme, and alternating sampling in global, medium, and local spaces. Table 12 shows the total computation time and the number of computationally demanding DP calculations for both algorithms over 50 iterations. Notably, the MSSR algorithm reduces total time consumption to just 10% of GA, primarily due to a significant reduction in DP calculations. This reduction is crucial, given the time-intensive nature of the DP algorithm. The MSSR algorithm's computation time reduction by an order of magnitude makes the solution of the formulated optimization problem viable on a regular Windows PC workstation. This efficiency paves the way for rapid and effective optimization iterations, ensuring a streamlined approach to achieving the best system design and control integration solution.

Table 12. Comparison of two algorithms

Algorithms	Total time	Times of DP Searches
GA	37.5h	1000
MSSR	3.7h	98

The LCC minimization formulation ascertained optimal HESS sizes and initial EMS/power allocation schemes for the HEV propulsion system, as shown in Table 13.

Table 13. Parameters of energy storage components

Battery	Cell nominal capacity/Ah	40
	Number in series	125
	Number in parallel	10
UC	Nominal capacity/F	140
	Number in series	10
	Number in parallel	15

8.6. Real-time Optimal Control of HESS

The speeds outlined in standardized driving cycles like WLTC are designed to simulate typical driving conditions. However, speeds vary significantly in real-world scenarios due to traffic congestion, road conditions, weather, and driver behaviour. Therefore, actual driving speeds may fluctuate during operation.

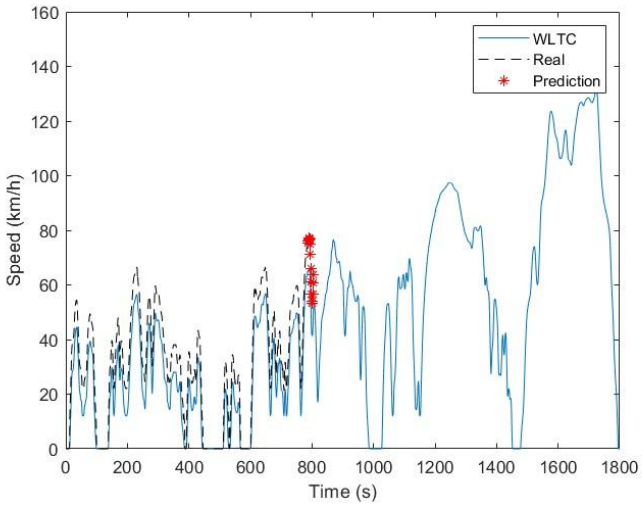

Figure 60. Power demand under different conditions.

A baseline optimal EMS-guided MPC method is introduced in this work to improve the real-time optimal power control and EMS, as shown in Figure 61.

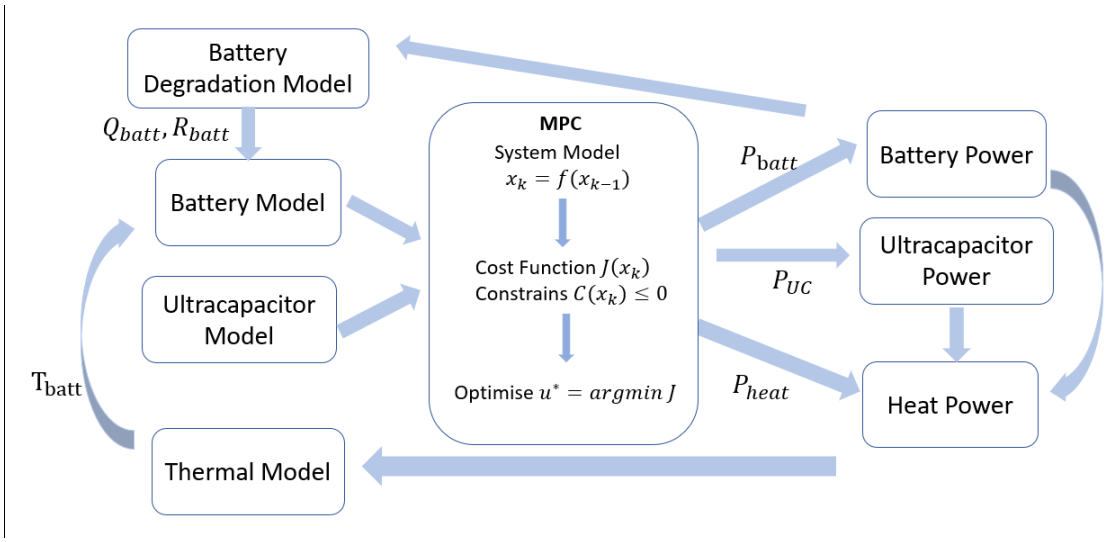

Figure 61. The novel adaptive MPC method.

8.7. Result Discussions

Our study comprehensively compared MPC-based real-time control and the baseline optimal EMS derived from vehicle operation following the standard driving cycle and optimized using DP optimization search. This comparison is illustrated in Figure 62. The results revealed that compared to the baseline optimal EMS, battery degradation based on real-time EMS only increased by 7.10%.

This finding underscores the effectiveness of real-time control strategies in mitigating battery degradation. Unlike traditional approaches, such as DP, which rely on static control strategies, real-time control continuously adapts to changing conditions and battery states. When the battery undergoes decay over time due to usage, the real-time control system dynamically adjusts the battery parameters to optimize performance and extend its lifespan.

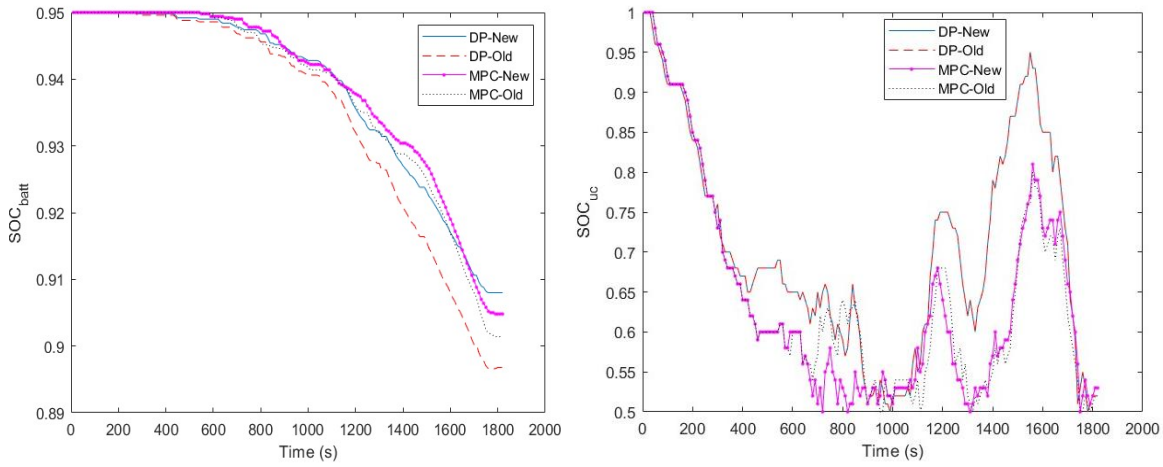

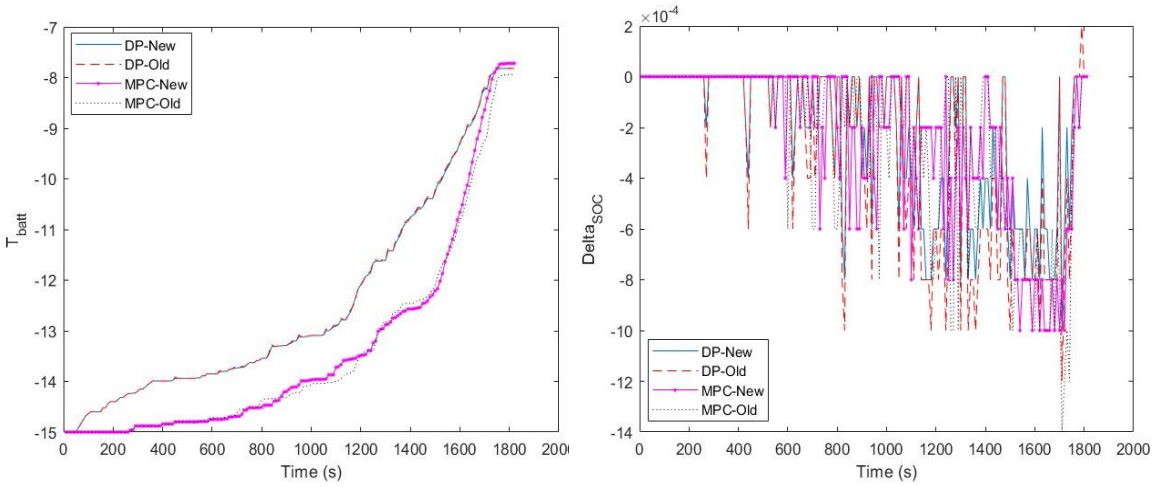

Figure 62. Battery SOC, Temperature and Delta SOC, and UC SOC and SOH (Standard Cycle)

When the battery decays after being used for some time, the control strategy of UC employed in DP remains unchanged, merely adjusting the change in SOC of the battery to compensate for its diminishing power supply capability. However, this approach may lead to faster battery degradation.

Our research demonstrates that real-time control can lead to a remarkable 9.55% reduction in battery degradation compared to the traditional DP approach. By continuously optimizing charging and discharging profiles, managing temperature fluctuations, and adapting to varying usage patterns, real-time control strategies offer a proactive solution to mitigate battery degradation and enhance overall system performance.

Optimizing the HESS with UCs to form the baseline optimal EMS presents a static and ideal approach, as vehicles never exactly follow the standard driving cycles. In actual operation, the vehicle velocity always departs from the statistical driving, showing minor perturbations at least. Under these situations, the battery must meet additional energy demands, highlighting a notable limitation compared to the dynamic adaptability of real-time control algorithms. This deficiency is starkly illustrated in Figure 63, where the shortcomings of the static UC usage become apparent, particularly during significant current fluctuations.

With the UC unable to adequately replenish power, the battery becomes increasingly burdened with high-current discharges, accelerating its degradation process. Furthermore, the heightened activity within the battery generates additional heat, which, while theoretically beneficial for performance, paradoxically hastens the decay rate. This dual effect of increased current stress and elevated temperature underscores the inherent limitations of relying solely on preset UC usage within the baseline optimal EMS.

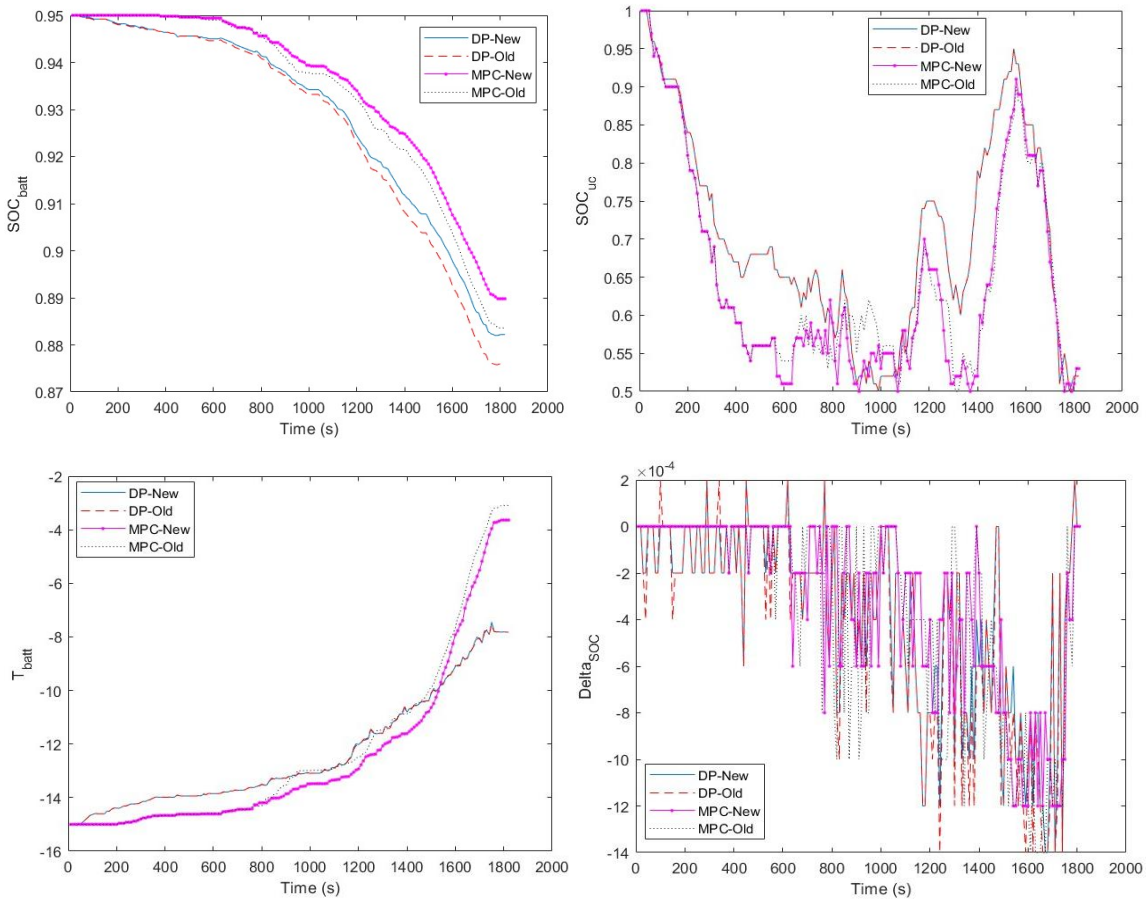

Figure 63. Battery SOC, Temperature and delta SOC, and UC SOC and SOH (Actual Driving).

In contrast, real-time control strategies offer a dynamic solution that effectively mitigates battery degradation. Our analysis reveals a substantial reduction of 22.30% in battery degradation when employing real-time control compared to the conventional DP algorithm. This significant improvement is particularly pronounced as the battery undergoes decay over time, where real-time control demonstrates its ability to reduce the decay rate by an impressive 23.29%.

Table 14. Minimum Overall LCC Measure Results under Different Vehicle Operations

Q_{loss}(%) Operations / SOH	Without speed changes		With speed changes	
	DP-based	MPC-based	DP-based	MPC-based
New	7.89e-6	8.45e-6	13.27e-6	10.85e-6
Old	9.98e-6	9.11e-6	14.61e-6	11.85e-6

These findings underscore the critical importance of dynamic control strategies in optimizing battery performance and extending its operational lifespan. Real-time control

algorithms offer a proactive approach that mitigates degradation and enhances overall system efficiency and reliability by continuously adjusting parameters in response to changing conditions. This new approach represents a fundamental shift from static control methodologies, offering a pathway toward maximizing the potential of ESSs in various applications.

8.8. Real-time implementation

The optimal EMS for power distribution between the battery and UP modules in the HESS using DP after obtaining the vehicle's full-distance velocity data is ideal but impossible. Using the implementation discussed in Sections 5.3 and 5.4, we can implement the new MPC-based real-time optimal control differently based on the controller's computation capability.

The velocity data from the standard driving cycle are then used as references (the battery attenuation is set to 1). The relative battery attenuation and the required calculation time corresponding to the four different real-time control accuracies are listed in the following table.

Option 1 has the best control result. One can choose options 2, 3, or 4 to shorten the calculation time. Option 2 increases the grid width, Option 3 shortens the prediction range, and Option 4 increases the control range.

Table 15. Implementation options of the new MPC method

	Option 1	Option 2	Option 3	Option 4
Battery attenuation	1.13	1.21	1.34	1.65
Computation time required for each step	2.75 s	0.45s	0.25 s	0.14 s

Given that in normal operation, the controller of an electric vehicle typically issues control commands every 1-5 seconds, these real-time optimal controls (strategies) can be achieved.

Chapter 9. Conclusions

9.1. Summary

This research introduced an advanced method for the integrated design and control optimizations of hybrid electric propulsion systems, focusing on maintaining and improving the health and operation life of key system components, Li-ion batteries and PEMFC systems. The study starts with detailed performance and degradation modelling of Li-ion batteries and PEMFCs, both costly and prone to degradation under inadequate use and low temperatures, utilizing over 2,000 cycles of Li-ion battery charge-discharge degradation test data. A novel approach was introduced to track the SOH of Li-ion battery and PEMFC performance and capacity decay and update their performance and degradation models using online data, improving the quality of real-time optimal power control and energy management.

A new Li-ion battery performance and degradation decay model under low temperatures was introduced through an extensive search of available experiment data to quantitatively predict the batteries' potential losses under these conditions and guide the mitigation design and control solutions. The new approach dynamically adjusted model parameters based on actual temperature fluctuations, providing feedback on the effect of active battery thermal management using the energy from UCs and other sources, particularly during cold start and enhancing the accuracy of optimal EMS to extend battery life in cold environments. Similarly, a PEMFC degradation model was developed using a year's worth of PEMFC bus driving data, enabling continuous SOH and performance updates for the PEMFC system based on real-time current and voltage data.

This study proposed optimized design and control methods tailored to each propulsion system component's performance and degradation characteristics to maximize the overall hybrid propulsion system's performance and LCC. Global optimization was conducted to achieve ideal component sizing, ensuring sufficient power output, high energy efficiency and low system LCC. Advanced optimal EMS managed each component to operate within its optimal performance range while preventing accelerated degradation. Three case studies were used to validate the efficacy of the newly introduced methods.

Case 1 incorporated capacity and performance degradation into the PEMFC and BESS models, optimizing propulsion system component sizing, power control, and EMS design for an FCEV, a PEMFC-battery hybrid electric vehicle and passenger ferry in the case study. With the increasing pace of commercialization, the PEMFC system-powered FCEVs present a highly efficient, zero tailpipe emission propulsion solution. A BESS is normally integrated with the PEMFC system to improve its performance, energy efficiency and operational life. However, both the PEMFC system and the BESS suffer from relatively short operation life and high replacement costs. Optimal EMS become essential to improve their working

conditions, thus extending their working life based on their distinct performance degradation behaviours and achieving the minimum LCC. Extending from the present static modelling approach, this research introduces three new methods for dynamically updating the performance and degradation models of Li-ion batteries and PEMFCs using real-time operation data of a fuel cell-battery hybrid electric propulsion system. The combined methods more accurately capture the performance and capability of each specific fuel cell hybrid propulsion system's BESS and PEMFC system. This approach enables precise performance tracking, degradation assessment, and optimal energy management. A new integrated approach to the hybrid electric propulsion system's component-sizing design optimization and optimal energy management is introduced using these new modelling schemes, minimizing the LCC by balancing the propulsion system performance, fuel economy, and the BESS and PEMFC system degradations. These modelling and optimization methods are applied to the hybrid electric ferry to produce the optimal fuel cell-battery hybrid propulsion system design and EMS to strike the best balance between fuel efficiency and the PEMFC and BESS operation life. The embedded degradation model significantly improved the accuracy of the EMS by 54%, resulting in a $2,936,235 reduction in the LCC of the hybrid marine propulsion system over its projected 10-year life. This work presented a systematic FCEV design and control optimization method, facilitating the further development and wide adoption of zero-emission fuel cell technology for marine vessels.

Case 2 tackled two significant issues in LNG-diesel dual-fuel hybrid electric propulsion systems: the methane leakage from NG engines under certain loading conditions, which increased CO_{2e} emissions, and the high costs and reduced lifespan of BESS in this hybrid electric propulsion systems. This research introduced a new approach to combine the LNG-fuelled engine with hybrid electric propulsion and real-time optimal control to maximize fuel efficiency and minimize CO_{2e} emissions. In addition to low-cost LNG fuel, the approach controls and reduces the battery degradation costs to provide a clean and economical marine propulsion solution. An integrated globally optimal propulsion system design and real-time optimal control strategy for the LNG-fueled hybrid electric ships effectively addressed the methane slip-triggered emissions issue of NG engines, reducing CO_{2e} emissions by 12.28% and the high cost and relatively short life of the hybrid propulsion system’s BESS, decreasing battery capacity loss by 12%. The optimal sizing of the NG-diesel dual-fuel compression ignition (CI) engine and BESS and the optimal baseline power control and EMS are jointly created using DP for the vessel’s statistical data-based, normal operation profile. As marine vessels have more variations of propulsion power demand than road vehicles due to varying ocean operation conditions, two new methods are introduced to accurately predict the varying propulsion power demands and dynamically update the BESS’s state of health (SOH) in real-time. The former applies an extended Kalman filter (EKF) on both real-time vessel operation data and the statistical vessel operation cycle to predict vessel power demand more accurately. The

latter compares the instantly measured battery output voltage data with the battery performance and degradation models built using extensive battery test data to capture the state of the BESS more precisely. These two new update schemes lead to an extended model predictive control (MPC) approach for the real-time optimal power control and energy management of the hybrid electric ship operation, considering the NG fuel consumption, CO_2e emissions and BESS degradation associated costs. The newly introduced NG-engine hybrid electric propulsion system component size and EKF-MPC real-time control optimization techniques have been tested using the technical specification and operation data of a real medium-sized vehicle and passenger ferry in operation, with reduced CO_{2e} emissions and battery capacity loss and lowered ferry operating costs by $305,286 over 10 years of operations.

Case 3 presented a strategy to improve battery system resilience under heavy load and extreme temperatures, prolonging battery life and optimizing energy storage efficiency. The BESS is a critical and the costliest powertrain component for BEVs). Heavy loads and extreme operating temperatures distort the battery's electrochemical reactions, causing permanent capacity loss, shortening operational life, and increasing LCC. This work introduces new methods for optimizing battery and UC HESS design and the HESS EMS and TMS. In addition to altering the batteries' use pattern to extend operational life, this combination also improves battery performance and reduces the impacts on the batteries' operational life under low temperatures. First, performance and degradation data of commonly used Li-ion batteries under extreme temperatures and various use patterns are collected to form advanced battery performance, degradation and thermal models to facilitate the HESS's optimal design and energy management for a BEV under different operation conditions. Effective EMS and TMS are introduced to play the batteries and UCs to their strength and to use energy from the UCs to improve the batteries' operating temperature to extend battery life and minimize the BEV's LCC. The optimal sizing of the batteries and UCs and the HESS baseline optimal EMS are simultaneously generated using empirical data-based battery performance and degradation models and the BEV's operation cycle through global design optimization and DP-based optimal energy management. The accurate prediction of vehicle propulsion power over a short period is made through the EKF, considering vehicle velocities from the standard vehicle driving cycle and real-time measurements, vehicle dynamics model and powertrain system model. The batteries' performance and degradation models are dynamically updated using the online battery voltage data and continuously calibrated SOH model. These updates enable precise optimal control and EMS through MPC period by period during actual driving. Utilizing the UC's rapid charge/discharge and thermal adaptability, we extended battery life by 47% and reduced the number of full charge cycles by 45%. In addition, the newly introduced real-time control reduced battery degradation by up to 23%.

9.2. Original Research Contributions

This study addresses critical challenges in the design and control optimizations of hybrid propulsion systems for clean vehicles and ships, using a light-duty commercial vehicle and a medium-sized ferry as research platforms and design examples. The specific contributions of this work are outlined below:

1) Introduced more accurate Li-ion battery performance and degradation models and extended these models to account for the impacts of extreme temperatures

This study established a detailed lithium-ion battery degradation model based on extensive experimental data, correlating performance degradation to the cumulative charge and discharge cycles. The impact of extreme temperatures on battery performance and degradation is quantitatively captured and modelled using low- and high-temperature battery performance and degradation data collected through an extensive literature search. This enhancement makes the model more comprehensive and accurate, offering valuable insights for developing optimal energy and thermal management strategies for hybrid energy storage systems under challenging thermal conditions.

2) Introduced a dynamic PEMFC degradation modelling method using real-time data

Building upon existing static, lab-based PEMFC degradation models, this study introduces a dynamic method to update a key model parameter, the active area, using real-time PEMFC operational data. Three machine learning algorithms—GPR, BP, and SVM—were tested to obtain the updated degradation parameters. Among these, SVM demonstrated the highest prediction accuracy, offering a robust real-time PEMFC health monitoring and model updating tool.

3) Developed a real-time Li-ion battery performance and degradation model updating method

A method to dynamically determine the battery's SOH is introduced using measured battery output voltage under key operating parameters and the static battery performance and degradation models to find the battery’s equivalent charge-discharge cycle number in real time. This approach enables real-time updates and corrections to the battery degradation model, accurately assessing the instantaneous battery energy supply capacity. This refreshed model supports more precise optimal control and energy management in HESS and vehicle propulsion systems, improving system reliability and longevity.

4) Extended integrated design optimization and optimal energy management for hybrid electric propulsion systems

A novel methodology was developed to integrate the sizing optimization of key hybrid electric propulsion system components with the optimal energy management of the

system to eliminate any conflict between design and control optimizations. The nested global optimization approach minimizes the system's LCC while balancing performance, fuel economy, emissions, and PEMFC and Li-ion battery degradations. This methodology was validated across various scenarios, yielding the following significant contributions:

- The methodology was applied to optimize the design and energy management of hybrid propulsion systems for fuel cell-battery hybrid propulsion of a medium-sized vehicles and passenger ferry ship. It achieved an optimal balance between fuel efficiency and the operational lifespans of PEMFCs and BESS, demonstrating the superiority of the proposed approach.
- For LNG-powered hybrid electric vessels, the methodology integrated the NG engine and BESS optimal sizing with a baseline EMS developed using DP. By leveraging statistical operating profiles and real-time data, the NG engine operates at optimal speed and torque, reducing fuel consumption and CO_{2e} emissions while preventing the overuse of BESS. This dynamic SOH-based EMS ensures minimal LCC under varying operational conditions.
- The study extended the design of BEVs by integrating UCs into the energy storage system to form an HESS. The accurate battery performance and degradation models under various loading conditions and extreme temperatures allow the added UCs to improve the operational conditions of the battery using optimal energy and active thermal management. Both of these were conducted using real-time MPC. The EKF is used to predict the vehicle's velocity over a short period precisely, considering the measured vehicle velocity and corresponding standard driving cycle. It effectively manages fluctuating power requirements while mitigating the high current battery charge, discharge, and low temperature, improving system efficiency, reducing battery capacity degradation, and extending battery life.

Chapter 10. Future Work

Our forthcoming investigations entail a comprehensive exploration of varied Li-ion battery and fuel cell performance facets. Data procurement from extensive battery tests conducted under diverse thermal conditions is imperative. These data will serve as the foundation for constructing robust life attenuation models tailored to different Li-ion battery variants and operational temperatures. Subsequently, rigorous validation exercises will be conducted to ascertain the accuracy and efficacy of these models in predicting battery lifespan within practical applications.

Furthermore, our research agenda extends to encompassing an array of PEMFC operational scenarios, including start-stop cycles, idling, load fluctuation, and high-power demands. Each operational condition will undergo meticulous data gathering to facilitate the development of precise PEMFC life decay models. These models will encapsulate the nuanced impact of various operational dynamics on fuel cell longevity, thereby enabling accurate prognostication of their lifespan in real-world settings.

Our comprehensive research agenda spans the spectrum from data acquisition and model development to real-world validation, focusing on enhancing the understanding and predictive capabilities pertaining to the performance and longevity of Li-ion batteries and PEMFCs. Through meticulous execution and validation, we aim to furnish the clean transportation industry with invaluable insights poised to drive advancements in energy storage and clean propulsion technologies.

References

[1] Shaheen S A, Lipman T E. Reducing greenhouse emissions and fuel consumption: Sustainable approaches for surface transportation[J]. IATSS research, 2007, 31(1): 6-20.

[2] Wieczorek M, Lewandowski M, Jefimowski W. Cost comparison of different configurations of a hybrid energy storage system with battery-only and supercapacitor-only storage in an electric city bus[J]. Bulletin of the Polish Academy of Sciences: Technical Sciences, 2019: 1095-1106-1095-1106.

[3] Pollet B G, Kocha S S, Staffell I. Current status of automotive fuel cells for sustainable transport[J]. Current opinion in Electrochemistry, 2019, 16: 90-95.

[4] Lu L, Han X, Li J, et al. A review on the key issues for Li-ion battery management in electric vehicles[J]. Journal of power sources, 2013, 226: 272-288.

[5] Barré A, Deguilhem B, Grolleau S, et al. A review on Li-ion battery ageing mechanisms and estimations for automotive applications[J]. Journal of Power Sources, 2013, 241: 680-689.

[6] Han X, Lu L, Zheng Y, et al. A review on the key issues of the lithium ion battery degradation among the whole life cycle[J]. ETransportation, 2019, 1: 100005.

[7] Kumar B, Khare N, Chaturvedi P K. FPGA-based design of advanced BMS implementing SOC/SOH estimators[J]. Microelectronics Reliability, 2018, 84: 66-74.

[8] Liang K, Zhang Z, Liu P, et al. Data-driven ohmic resistance estimation of battery packs for electric vehicles[J]. Energies, 2019, 12(24): 4772.

[9] Wassiliadis N, Adermann J, Frericks A, et al. Revisiting the dual extended Kalman filter for battery state-of-charge and state-of-health estimation: A use-case life cycle analysis[J]. Journal of Energy Storage, 2018, 19: 73-87.

[10] Zhang J, Lee J. A review on prognostics and health monitoring of Li-ion battery[J]. Journal of power sources, 2011, 196(15): 6007-6014.

[11] Waag W, Fleischer C, Sauer D U. Critical review of the methods for monitoring of Li-ion batteries in electric and hybrid vehicles[J]. Journal of Power Sources, 2014, 258: 321-339.

[12] Berecibar M, Gandiaga I, Villarreal I, et al. Critical review of SOH estimation methods of Li-ion batteries for real applications[J]. Renewable and Sustainable Energy Reviews, 2016, 56: 572-587.

[13] Ungurean L, Cârstoiu G, Micea M V, et al. Battery SOH estimation: a structured review of models, methods and commercial devices[J]. International Journal of Energy Research, 2017, 41(2): 151-181.

[14] Yang S, Zhang C, Jiang J, et al. Review on state-of-health of Li-ion batteries: Characterizations, estimations and applications[J]. Journal of Cleaner Production, 2021: 128015.

[15] Li Y, Liu K, Foley A M, et al. Data-driven health estimation and lifetime prediction of Li-ion batteries: A review[J]. Renewable and sustainable energy reviews, 2019, 113: 109254.

[16] Tian J, Xiong R, Shen W. A review on SOH estimation for Li-ion batteries in photovoltaic systems[J]. ETransportation, 2019, 2: 100028.
[17] Zhang Q, Wang D, Yang B, et al. Electrochemical model of Li-ion battery for wide frequency range applications[J]. Electrochimica Acta, 2020, 343: 136094.
[18] Guha A, Patra A. SOH estimation of Li-ion batteries using capacity fade and internal resistance growth models[J]. IEEE Transactions on Transportation Electrification, 2017, 4(1): 135-146.
[19] Pastor-Fernández C, Uddin K, Chouchelamane G H, et al. A comparison between electrochemical impedance spectroscopy and incremental capacity-differential voltage as Li-ion diagnostic techniques to identify and quantify the effects of degradation modes within battery management systems[J]. Journal of Power Sources, 2017, 360: 301-318.
[20] Howey D A, Mitcheson P D, Yufit V, et al. Online measurement of battery impedance using motor controller excitation[J]. IEEE transactions on vehicular technology, 2013, 63(6): 2557-2566.
[21] Bloom I, Potter B G, Johnson C S, et al. Effect of cathode composition on impedance rise in high-power Li-ion cells: Long-term aging results[J]. Journal of power sources, 2006, 155(2): 415-419.
[22] Wang J, Liu P, Hicks-Garner J, et al. Cycle-life model for graphite-LiFePO4 cells[J]. Journal of power sources, 2011, 196(8): 3942-3948.
[23] Marongiu A, Roscher M, Sauer D U. Influence of the vehicle-to-grid strategy on the aging behavior of Li-ion battery electric vehicles[J]. Applied Energy, 2015, 137: 899-912.
[24] Farmann A, Sauer D U. Comparative study of reduced order equivalent circuit models for on-board state-of-available-power prediction of Li-ion batteries in electric vehicles[J]. Applied Energy, 2018, 225: 1102-1122.
[25] Lai X, Wang S, Ma S, et al. Parameter sensitivity analysis and simplification of equivalent circuit model for the state of charge of Li-ion batteries[J]. Electrochimica Acta, 2020, 330: 135239.
[26] Wei H, Chen X, Zhiqiang L, et al. Online estimation of Li-ion battery SOH using grey neural network[J]. Power Syst. Technol, 2017, 41: 4038-4044.
[27] Wang Y, Li M, Chen Z. Experimental study of fractional-order models for Li-ion battery and ultra-capacitor: Modelling, system identification, and validation[J]. Applied Energy, 2020, 278: 115736.
[28] Chen Z P, Wang Q T. The application of UKF algorithm for 18650-type Li-ion battery SOH estimation[C]Applied Mechanics and Materials. Trans Tech Publications Ltd, 2014, 519: 1079-1084.
[29] Gholizadeh M, Yazdizadeh A. Systematic mixed adaptive observer and EKF approach to estimate SOC and SOH of lithium–ion battery[J]. IET Electrical Systems in Transportation, 2020, 10(2): 135-143.
[30] Zhang J, Liu X, Chen C, et al. An Intelligent Deformation‐Based Approach to the SOH Estimation of Collided Lithium‐Ion Batteries for Facilitating Battery Module Safety Evaluation[J]. Energy Technology, 2020, 8(11): 2000624.

[31] Ungurean L, Micea M V, Carstoiu G. Online SOH prediction method for lithium-ion batteries, based on gated recurrent unit neural networks[J]. International journal of energy research, 2020, 44(8): 6767-6777.
[32] Luo X, Wang J, Dooner M, et al. Overview of current development in electrical energy storage technologies and the application potential in power system operation[J]. Applied energy, 2015, 137: 511-536.
[33] Wang Y, Chen K S, Mishler J, et al. A review of polymer electrolyte membrane fuel cells: Technology, applications, and needs on fundamental research[J]. Applied energy, 2011, 88(4): 981-1007.
[34] Mazloomi, Kaveh & Gomes, Chandima. (2012). Hydrogen as an energy carrier: Prospects and challenges. Renewable and Sustainable Energy Reviews. 16. 3024-3033. 10.1016/j.rser.2012.02.028.
[35] Pei P, Chen H. Main factors affecting the lifetime of Proton Exchange Membrane fuel cells in vehicle applications: A review[J]. Applied Energy, 2014, 125: 60-75.
[36] Zhang T, Wang P, Chen H, et al. A review of automotive proton exchange membrane fuel cell degradation under start-stop operating condition[J]. Applied energy, 2018, 223: 249-262.
[37] Ren P, Pei P, Li Y, et al. Degradation mechanisms of proton exchange membrane fuel cell under typical automotive operating conditions[J]. Progress in Energy and Combustion Science, 2020, 80: 100859.
[38] Hou Y, Hao D, Shen J, et al. Effect of strengthened road vibration on performance degradation of PEM fuel cell stack[J]. International Journal of Hydrogen Energy, 2016, 41(9): 5123-5134.
[39] Bezmalinovic D, Simic B, Barbir F. Characterization of PEM fuel cell degradation by polarization change curves[J]. Journal of Power Sources, 2015, 294: 82-87.
[40] Hou Y, Zhou B, Zhou W, et al. An investigation of characteristic parameter variations of the polarization curve of a proton exchange membrane fuel cell stack under strengthened road vibrating conditions[J]. International journal of hydrogen energy, 2012, 37(16): 11887-11893.
[41] Wu J, Yuan X Z, Martin J J, et al. Proton exchange membrane fuel cell degradation under close to open-circuit conditions: Part I: In situ diagnosis[J]. Journal of Power Sources, 2010, 195(4): 1171-1176.
[42] Aoki T, Matsunaga A, Ogami Y, et al. The influence of polymer electrolyte fuel cell cathode degradation on the electrode polarization[J]. Journal of Power Sources, 2010, 195(8): 2182-2188.
[43] Liu H, Chen J, Hissel D, et al. Prognostics methods and degradation indexes of proton exchange membrane fuel cells: A review[J]. Renewable and Sustainable Energy Reviews, 2020, 123: 109721.
[44] Bressel M, Hilairet M, Hissel D, et al. Extended Kalman filter for prognostic of proton exchange membrane fuel cell[J]. Applied Energy, 2016, 164: 220-227.
[45] Zhang D, Cadet C, Bérenguer C, et al. Some improvements of particle filtering based prognosis for PEM fuel cells[J]. IFAC-PapersOnLine, 2016, 49(28): 162-167.

[46] Zhang D, Baraldi P, Cadet C, et al. An ensemble of models for integrating dependent sources of information for the prognosis of the remaining useful life of proton exchange membrane fuel cells[J]. Mechanical Systems and Signal Processing, 2019, 124: 479-501.
[47] Javed K, Gouriveau R, Zerhouni N, et al. Prognostics of proton exchange membrane fuel cells stack using an ensemble of constraints based connectionist networks[J]. Journal of Power Sources, 2016, 324: 745-757.
[48] Morando S, Jemei S, Hissel D, et al. ANOVA method applied to proton exchange membrane fuel cell ageing forecasting using an echo state network[J]. Mathematics and Computers in Simulation, 2017, 131: 283-294.
[49] Silva R E, Gouriveau R, Jemei S, et al. Proton exchange membrane fuel cell degradation prediction based on adaptive neuro-fuzzy inference systems[J]. International Journal of Hydrogen Energy, 2014, 39(21): 11128-11144.
[50] Fang S, Wang Y, Gou B, et al. Toward future green maritime transportation: An overview of seaport microgrids and all-electric ships[J]. IEEE Transactions on Vehicular Technology, 2019, 69(1): 207-219.
[51] Inal O B, Charpentier J F, Deniz C. Hybrid power and propulsion systems for ships: Current status and future challenges[J]. Renewable and Sustainable Energy Reviews, 2022, 156: 111965.
[52] Ali M Z, Awad N H, Suganthan P N, et al. An improved class of real-coded Genetic Algorithms for numerical optimization[J]. Neurocomputing, 2018, 275: 155-166.
[53] Zeng Y. Parameter optimization of plug-in hybrid electric vehicle based on quantum genetic algorithm[J]. Cluster Computing, 2019, 22: 14835-14843.
[54] Rahman I, Vasant P M, Singh B S M, et al. On the performance of accelerated particle swarm optimization for charging plug-in hybrid electric vehicles[J]. Alexandria Engineering Journal, 2016, 55(1): 419-426.
[55] Zhou Q, Zhang W, Cash S, et al. Intelligent sizing of a series hybrid electric power-train system based on Chaos-enhanced accelerated particle swarm optimization[J]. Applied Energy, 2017, 189: 588-601.
[56] Murgovski N, Johannesson L, Sjöberg J, et al. Component sizing of a plug-in hybrid electric powertrain via convex optimization[J]. Mechatronics, 2012, 22(1): 106-120.
[57] Wu P, Bucknall R. Hybrid fuel cell and battery propulsion system modelling and multi-objective optimization for a coastal ferry[J]. International journal of hydrogen energy, 2020, 45(4): 3193-3208.
[58] Vieira G T T, Pereira D F, Taheri S I, et al. Optimized configuration of diesel engine-fuel cell-battery hybrid power systems in a platform supply vessel to reduce co2 emissions[J]. Energies, 2022, 15(6): 2184.
[59] Zhu J, Chen L, Wang B, et al. Optimal design of a hybrid electric propulsive system for an anchor handling tug supply vessel[J]. Applied energy, 2018, 226: 423-436.
[60] Jianyun Z, Li C, Lijuan X, et al. Bi-objective optimal design of plug-in hybrid electric propulsion system for ships[J]. Energy, 2019, 177: 247-261.

[61] Lan H, Wen S, Hong Y Y, et al. Optimal sizing of hybrid PV/diesel/battery in ship power system[J]. Applied energy, 2015, 158: 26-34.
[62] Wang W, Chen L, Liang X. Optimal sizing of sail-assisted PV/shore power hybrid propulsion systems[C]ISOPE International Ocean and Polar Engineering Conference. ISOPE, 2020: ISOPE-I-20-4282.
[63] Xu Q, Luo X, Jiang X, et al. Research on double fuzzy control strategy for parallel hybrid electric vehicle based on GA and DP optimization[J]. IET Electrical Systems in Transportation, 2018, 8(2): 144-151.
[64] Anselma P G, Huo Y, Roeleveld J, et al. Slope-weighted energy-based rapid control analysis for hybrid electric vehicles[J]. IEEE Transactions on Vehicular Technology, 2019, 68(5): 4458-4466.
[65] Brahma A, Guezennec Y, Rizzoni G. Optimal energy management in series hybrid electric vehicles[C]Proceedings of the 2000 American Control Conference. ACC (IEEE Cat. No. 00CH36334). IEEE, 2000, 1(6): 60-64.
[66] Lin C C, Peng H, Grizzle J W, et al. Power management strategy for a parallel hybrid electric truck[J]. IEEE transactions on control systems technology, 2003, 11(6): 839-849.
[67] Tang X, Jia T, Hu X, et al. Naturalistic data-driven predictive energy management for plug-in hybrid electric vehicles[J]. IEEE Transactions on Transportation Electrification, 2020, 7(2): 497-508.
[68] Han J, Kum D, Park Y. Synthesis of predictive equivalent consumption minimization strategy for hybrid electric vehicles based on closed-form solution of optimal equivalence factor[J]. IEEE Transactions on Vehicular Technology, 2017, 66(7): 5604-5616.
[69] Li L, You S, Yang C, et al. Driving-behavior-aware stochastic model predictive control for plug-in hybrid electric buses[J]. Applied Energy, 2016, 162: 868-879.
[70] Chen Z, Mi C C, Xia B, et al. Energy management of power-split plug-in hybrid electric vehicles based on simulated annealing and Pontryagin's minimum principle[J]. Journal of Power Sources, 2014, 272: 160-168.
[71] Wu Y, Zhang Y, Li G, et al. A predictive energy management strategy for multi-mode plug-in hybrid electric vehicles based on multi neural networks[J]. Energy, 2020, 208: 118366.
[72] Dextreit C, Kolmanovsky I V. Game theory controller for hybrid electric vehicles[J]. IEEE Transactions on Control Systems Technology, 2013, 22(2): 652-663.
[73] Sun Y, Xu Q, Yuan Y, et al. Optimal energy management of fuel cell hybrid electric ships considering fuel cell aging cost[C]2020 IEEE/IAS Industrial and Commercial Power System Asia (I&CPS Asia). IEEE, 2020: 240-245.
[74] Mitropoulou D, Kalikatzarakis M, van Der Klauw T, et al. Multi-objective optimisation and Energy Management: adapt your ship to every mission[C]Conference Proceedings of iSCSS. 2020.
[75] Zhang Z, Guan C, Liu Z. Real-time optimization energy management strategy for fuel cell hybrid ships considering power sources degradation[J]. IEEE Access, 2020, 8: 87046-87059.

[76] Bassam A M, Phillips A B, Turnock S R, et al. Development of a multi-scheme energy management strategy for a hybrid fuel cell driven passenger ship[J]. International Journal of Hydrogen Energy, 2017, 42(1): 623-635.
[77] Hein K, Xu Y, Wilson G, et al. Coordinated optimal voyage planning and energy management of all-electric ship with hybrid energy storage system[J]. IEEE Transactions on Power Systems, 2020, 36(3): 2355-2365.
[78] Shang C, Srinivasan D, Reindl T. Economic and environmental generation and voyage scheduling of all-electric ships[J]. IEEE transactions on power systems, 2015, 31(5): 4087-4096.
[79] Wu P, Partridge J, Anderlini E, et al. Near-optimal energy management for plug-in hybrid fuel cell and battery propulsion using deep reinforcement learning[J]. International Journal of Hydrogen Energy, 2021, 46(80): 40022-40040.
[80] Wu P, Partridge J, Bucknall R. Cost-effective reinforcement learning energy management for plug-in hybrid fuel cell and battery ships[J]. Applied Energy, 2020, 275: 115258.
[81] Kanellos F D. Optimal power management with GHG emissions limitation in all-electric ship power systems comprising energy storage systems[J]. IEEE Transactions on power systems, 2013, 29(1): 330-339.
[82] Azad S, Alexander-Ramos M J. Robust combined design and control optimization of hybrid-electric vehicles using MDSDO[J]. IEEE Transactions on Vehicular Technology, 2021, 70(5): 4139-4152.
[83] Zeng T, Ren X, Zhang Y, et al. An integrated optimal design for guaranteed cost control of motor driving system with uncertainty[J]. IEEE/ASME Transactions on Mechatronics, 2019, 24(6): 2606-2615.
[84] Dall'Armi C, Pivetta D, Taccani R. Uncertainty analysis of the optimal health-conscious operation of a hybrid PEMFC coastal ferry[J]. international journal of hydrogen energy, 2022, 47(21): 11428-11440.
[85] Pivetta D, Dall'Armi C, Taccani R. Multi-objective optimization of hybrid PEMFC/Li-ion battery propulsion systems for small and medium size ferries[J]. International Journal of Hydrogen Energy, 2021, 46(72): 35949-35960.
[86] Zhu J, Chen L, Wang X, et al. Bi-level optimal sizing and energy management of hybrid electric propulsion systems[J]. Applied Energy, 2020, 260: 114134.
[87] Wang L, Collins E G, Li H. Optimal design and real-time control for energy management in electric vehicles[J]. IEEE Transactions on Vehicular Technology, 2011, 60(4): 1419-1429.
[88] Gong X, Wang J, Hu Y, et al. A Benchmark Study for Real-Time Optimal Control of Connected HEVs: Design, Integration and Evaluation[J]. IEEE Transactions on Transportation Electrification, 2023.
[89] Kim D, Eo J S, Kim K K K. Service-oriented real-time energy-optimal regenerative braking strategy for connected and autonomous electrified vehicles[J]. IEEE Transactions on Intelligent Transportation Systems, 2021, 23(8): 11098-11115.

[90] Biswas A, Anselma P G, Emadi A. Real-time optimal energy management of electrified powertrains with reinforcement learning[C]2019 IEEE Transportation Electrification Conference and Expo (ITEC). IEEE, 2019: 1-6.
[91] Stockar S, Marano V, Canova M, et al. Energy-optimal control of plug-in hybrid electric vehicles for real-world driving cycles[J]. IEEE Transactions on Vehicular Technology, 2011, 60(7): 2949-2962.
[92] Deshpande S R, Gupta S, Gupta A, et al. Real-time ecodriving control in electrified connected and autonomous vehicles using approximate dynamic programing[J]. Journal of Dynamic Systems, Measurement, and Control, 2022, 144(1): 011111.
[93] Deufel F, Gießler M, Gauterin F. Optimal Control of Electrified Powertrains in Offline and Online Application Concerning Dimensioning of Li-Ion Batteries[J]. Vehicles, 2022, 4(2): 464-481.
[94] Yang C, Du S, Li L, et al. Adaptive real-time optimal energy management strategy based on equivalent factors optimization for plug-in hybrid electric vehicle[J]. Applied Energy, 2017, 203: 883-896.
[95] Zhou Y, Ravey A, Péra M C. Real-time cost-minimization power-allocating strategy via model predictive control for fuel cell hybrid electric vehicles[J]. Energy Conversion and Management, 2021, 229: 113721.
[96] Ebbesen S, Salazar M, Elbert P, et al. Time-optimal control strategies for a hybrid electric race car[J]. IEEE Transactions on control systems technology, 2017, 26(1): 233-247.
[97] Hou J, Song Z, Park H, et al. Implementation and evaluation of real-time model predictive control for load fluctuations mitigation in all-electric ship propulsion systems[J]. Applied energy, 2018, 230: 62-77.
[98] Park H, Sun J, Pekarek S, et al. Real-time model predictive control for shipboard power management using the IPA-SQP approach[J]. IEEE Transactions on Control Systems Technology, 2015, 23(6): 2129-2143.
[99] Banaei M R, Alizadeh R. Simulation-based modelling and power management of all-electric ships based on renewable energy generation using model predictive control strategy[J]. IEEE Intelligent transportation systems magazine, 2016, 8(2): 90-103.
[100] Chen W, Tai K, Lau M W S, et al. Optimal power and energy management control for hybrid fuel cell-fed shipboard DC microgrid[J]. IEEE Transactions on Intelligent Transportation Systems, 2023.
[101] Chen L, Tong Y, Dong Z. Li-ion battery performance degradation modelling for the optimal design and energy management of electrified propulsion systems[J]. Energies, 2020, 13(7): 1629.
[102] Xingxing Wang, Yujie Zhang, Hongjun Ni*, Shuaishuai Lv, Fubao Zhang, Yu Zhu,*, Yinnan Yuan and Yelin Deng*, Influence of Different Ambient Temperatures on the Discharge Performance of Square Ternary Li-ion Batteries[J]. Energies, 2022, 15, 5348.
[103] Shuai Ma, Modi Jiang, Peng Tao, Chengyi Song, Jianbo Wu, Jun Wang∗, Tao Deng∗, Wen Shang∗, Temperature effect and thermal impact in Li-ion batteries:

A review[C], Progress in Natural Science: Materials International 28 (2018) 653–666, (Shanghai Jiao Tong Univ, A123).
[104] Zia M F, Elbouchikhi E, Benbouzid M. Optimal operational planning of scalable DC microgrid with demand response, islanding, and battery degradation cost considerations[J]. Applied energy, 2019, 237: 695-707.
[105] Q. Li, S. Jiao, L. Luo, M.S. Ding, J. Zheng, S.S. Cartmell, C.M. Wang, K. Xu, J.G. Zhang, W. Xu, Wide-Temperature Electrolytes for Li-ion Batteries[C]. ACS Appl. Mater. Interfaces 9 (2017) 18826–18835. (Pacific Northwest National Laboratory, US)
[106] Ugle R, Li Y. Trip specific worthiness of replacement of individual cells for battery pack in electric vehicles[C]Dynamic Systems and Control Conference. 2011, 54754: 705-711.
[107] Kalogiannis T, Hosen M S, Sokkeh M A, et al. Comparative study on parameter identification methods for dual-polarization Li-ion equivalent circuit model[J]. Energies, 2019, 12(21): 4031.
[108] Forgez C, Do D V, Friedrich G, et al. Thermal modelling of a cylindrical LiFePO4/graphite Li-ion battery[J]. Journal of power sources, 2010, 195(9): 2961-2968.
[109] Song Z, Li J, Han X, et al. Multi-objective optimization of a semi-active battery/supercapacitor energy storage system for electric vehicles[J]. Applied Energy, 2014, 135: 212-224.
[110] Wu J, Yuan X Z, Martin J J, et al. A review of PEM fuel cell durability: Degradation mechanisms and mitigation strategies[J]. Journal of Power Sources, 2008, 184(1): 104-119.
[111] El-Kharouf A, Chandan A, Hattenberger M, et al. Proton exchange membrane fuel cell degradation and testing[J]. Journal of the Energy Institute, 2012, 85(4): 188-200.
[112] Amphlett J C, Baumert R M, Mann R F, et al. Performance modelling of the Ballard Mark IV solid polymer electrolyte fuel cell: I. Mechanistic model development[J]. Journal of the Electrochemical Society, 1995, 142(1): 1.
[113] Mann R F, Amphlett J C, Hooper M A I, et al. Development and application of a generalised steady-state electrochemical model for a PEM fuel cell[J]. Journal of power sources, 2000, 86(1-2): 173-180.
[114] Fowler M W, Mann R F, Amphlett J C, et al. Incorporation of voltage degradation into a generalised steady state electrochemical model for a PEM fuel cell[J]. Journal of power sources, 2002, 106(1-2): 274-283.
[115] Z. Dong, Fuel Cell System Modelling Notes, last updated October 18, 2004.
[116] Zhang X, Yang D, Luo M, et al. Load profile based empirical model for the lifetime prediction of an automotive PEM fuel cell[J]. International Journal of Hydrogen Energy, 2017, 42(16): 11868-11878.
[117] Pei P, Chen D, Wu Z, et al. Nonlinear methods for evaluating and online predicting the lifetime of fuel cells[J]. Applied Energy, 2019, 254: 113730.

[118] Wang W, Chen Y, Yang C, et al. An efficient optimal sizing strategy for a hybrid electric air-ground vehicle using adaptive spiral optimization algorithm[J]. Journal of Power Sources, 2022, 517: 230704.
[119] Feng Y, Dong Z. Optimal energy management with balanced fuel economy and battery life for large hybrid electric mining truck[J]. Journal of Power Sources, 2020, 454: 227948.
[120] Chen H, Pei P, Song M. Lifetime prediction and the economic lifetime of proton exchange membrane fuel cells[J]. Applied Energy, 2015, 142: 154-163.
[121] Fletcher T, Thring R, Watkinson M. An Energy Management Strategy to concurrently optimise fuel consumption & PEM fuel cell lifetime in a hybrid vehicle[J]. international journal of hydrogen energy, 2016, 41(46): 21503-21515.
[122] Wang Y, Moura S J, Advani S G, et al. Power management system for a fuel cell/battery hybrid vehicle incorporating fuel cell and battery degradation[J]. International Journal of Hydrogen Energy, 2019, 44(16): 8479-8492.
[123] Hu X, Murgovski N, Johannesson L M, et al. Optimal dimensioning and power management of a fuel cell/battery hybrid bus via convex programming[J]. IEEE/ASME transactions on mechatronics, 2014, 20(1): 457-468.
[124] Feng Y, Dong Z. Integrated design and control optimization of fuel cell hybrid mining truck with minimized lifecycle cost[J]. Applied Energy, 2020, 270: 115164.
[125] Scott D S. Inside fuelcells[J]. International journal of hydrogen energy, 2004, 29(12): 1203-1211.
[126] Olmer N, Comer B, Roy B, et al. Greenhouse gas emissions from global shipping, 2013–2015 Detailed Methodology. International Council on Clean Transportation: Washington, DC, USA, 2017: 1-38.
[127] Khalili S, Rantanen E, Bogdanov D, et al. Global transportation demand development with impacts on the energy demand and greenhouse gas emissions in a climate-constrained world[J]. Energies, 2019, 12(20): 3870.
[128] Chen J, Fei Y, Wan Z. The relationship between the development of global maritime fleets and GHG emission from shipping[J]. Journal of Environmental Management, 2019, 242: 31-39.
[129] Feng Y, Zhu H, Dong Z. Simultaneous and Global Optimizations of LNG Fueled Hybrid Electric Ship for Substantial Fuel Cost, CO2 and Methane Emission Reduction[J]. IEEE Transactions on Transportation Electrification, 2022.
[130] Dedes E K, Hudson D A, Turnock S R. Assessing the potential of hybrid energy technology to reduce exhaust emissions from global shipping[J]. Energy policy, 2012, 40: 204-218.
[131] Wang Y, Cao Q, Liu L, et al. A review of low and zero carbon fuel technologies: Achieving ship carbon reduction targets[J]. Sustainable Energy Technologies and Assessments, 2022, 54: 102762.
[132] He T, Chong Z R, Zheng J, et al. LNG cold energy utilization: Prospects and challenges[J]. Energy, 2019, 170: 557-568.

[133] Burel F, Taccani R, Zuliani N. Improving sustainability of maritime transport through utilization of Liquefied Natural Gas (LNG) for propulsion[J]. Energy, 2013, 57: 412-420.
[134] Iannaccone T, Landucci G, Tugnoli A, et al. Sustainability of cruise ship fuel systems: Comparison among LNG and diesel technologies[J]. Journal of Cleaner Production, 2020, 260: 121069.
[135] Balcombe P, Brierley J, Lewis C, et al. How to decarbonise international shipping: Options for fuels, technologies and policies[J]. Energy conversion and management, 2019, 182: 72-88.
[136] Feng Y, Dong Z. Optimal control of natural gas compression engine hybrid electric mining trucks for balanced fuel efficiency and overall emission improvement[J]. Energy, 2019, 189: 116276.
[137] Damian S E, Wong L A, Shareef H, et al. Review on the challenges of hybrid propulsion system in marine transport system[J]. Journal of Energy Storage, 2022, 56: 105983.
[138] Uddin K, Perera S, Widanage W D, et al. Characterizing Li-ion battery degradation through the identification and tracking of electrochemical battery model parameters[J]. Batteries, 2016, 2(2): 13.
[139] Lyu C, Song Y, Zheng J, et al. In situ monitoring of Li-ion battery degradation using an electrochemical model[J]. Applied Energy, 2019, 250: 685-696.
[140] Zhang Y, Tang Q, Zhang Y, et al. Identifying degradation patterns of Li-ion batteries from impedance spectroscopy using machine learning[J]. Nature communications, 2020, 11(1): 1706.
[141] Hu W, Peng Y, Wei Y, et al. Application of electrochemical impedance spectroscopy to degradation and aging research of Li-ion batteries[J]. The Journal of Physical Chemistry C, 2023, 127(9): 4465-4495.
[142] Thelen A, Lui Y H, Shen S, et al. Integrating physics-based modelling and machine learning for degradation diagnostics of Li-ion batteries[J]. Energy Storage Materials, 2022, 50: 668-695.
[143] Li A G, West A C, Preindl M. Towards unified machine learning characterization of Li-ion battery degradation across multiple levels: A critical review[J]. Applied Energy, 2022, 316: 119030.
[144] Sciarretta A, Guzzella L. Control of hybrid electric vehicles[J]. IEEE control systems magazine, 2007, 27(2): 60-70.
[145] Shen J, Khaligh A. Design and real-time controller implementation for a battery-ultracapacitor hybrid energy storage system[J]. IEEE Transactions on Industrial Informatics, 2016, 12(5): 1910-1918.
[146] Li J, Wu B, Mao G. Research on the performance and emission characteristics of the LNG-diesel marine engine[J]. Journal of Natural Gas Science and Engineering, 2015, 27: 945-954.
[147] Kachhwaha A, Rashed G I, Garg A R, et al. Design and performance analysis of hybrid battery and ultracapacitor energy storage system for electrical vehicle active power management[J]. Sustainability, 2022, 14(2): 776.

[148] Fiori C, Ahn K, Rakha H A. Power-based electric vehicle energy consumption model: Model development and validation[J]. Applied Energy, 2016, 168: 257-268.
[149] Xiong R, Duan Y, Cao J, et al. Battery and ultracapacitor in-the-loop approach to validate a real-time power management method for an all-climate electric vehicle[J]. Applied energy, 2018, 217: 153-165.
[150] Li J, Gee A M, Zhang M, et al. Analysis of battery lifetime extension in a SMES-battery hybrid energy storage system using a novel battery lifetime model[J]. Energy, 2015, 86: 175-185.
[151] Dixon J W, Ortuzar M E. Ultracapacitors+ DC-DC converters in regenerative braking system[J]. IEEE Aerospace and Electronic Systems Magazine, 2002, 17(8): 16-21.
[152] Carter R, Cruden A. Strategies for control of a battery/supercapacitor system in an electric vehicle[C]2008 International Symposium on Power Electronics, Electrical Drives, Automation and Motion. IEEE, 2008: 727-732.
[153] Ferreira A A, Pomilio J A, Spiazzi G, et al. Energy management fuzzy logic supervisory for electric vehicle power supplies system[J]. IEEE transactions on power electronics, 2008, 23(1): 107-115.
[154] Rosario L, Luk P C K. Applying management methodology to electric vehicles with multiple energy storage systems[C]2007 international conference on machine learning and cybernetics. IEEE, 2007, 7: 4223-4230.
[155] Garcia F S, Ferreira A A, Pomilio J A. Control strategy for battery-ultracapacitor hybrid energy storage system[C]2009 Twenty-Fourth Annual IEEE Applied Power Electronics Conference and Exposition. IEEE, 2009: 826-832.
[156] Niemoeller B A, Krein P T. Battery-ultracapacitor active parallel interface with indirect control of battery current[C]2010 Power and Energy Conference At Illinois (PECI). IEEE, 2010: 12-19.
[157] Ansarey M, Panahi M S, Ziarati H, et al. Optimal energy management in a dual-storage fuel-cell hybrid vehicle using multi-dimensional dynamic programming[J]. Journal of Power Sources, 2014, 250: 359-371.
[158] Santucci A, Sorniotti A, Lekakou C. Power split strategies for hybrid energy storage systems for vehicular applications[J]. Journal of Power Sources, 2014, 258: 395-407.
[159] Song Z, Hofmann H, Li J, et al. Optimization for a hybrid energy storage system in electric vehicles using dynamic programing approach[J]. Applied Energy, 2015, 139: 151-162.
[160] Zhang S, Xiong R, Cao J. Battery durability and longevity based power management for plug-in hybrid electric vehicle with hybrid energy storage system[J]. Applied energy, 2016, 179: 316-328.
[161] Zhang, Wenbin, Jianqiu Li, Liangfei Xu, and Minggao Ouyang. Optimization for a fuel cell/battery/capacity tram with equivalent consumption minimization strategy [J]. Energy conversion and management, 2017, 134: 59-69.

[162] Zheng, Chunhua, Suk Won Cha, Yeong-il Park, Won Sik Lim, and Guoqing Xu. PMP-based power management strategy of fuel cell hybrid vehicles considering multi-objective optimization[J]. International Journal of Precision Engineering and Manufacturing, 2013, 14(5): 845-853.
[163] Ettihir, K., L. Boulon, and K. Agbossou. Optimization-based energy management strategy for a fuel cell/battery hybrid power system[J]. Applied Energy, 2016, 163: 142-153.
[164] Xie Y, Wang C, Hu X, et al. An MPC-based control strategy for electric vehicle battery cooling considering energy saving and battery lifespan[J]. IEEE Transactions on Vehicular Technology, 2020, 69(12): 14657-14673.
[165] Amini M R, Kolmanovsky I, Sun J. Hierarchical MPC for robust eco-cooling of connected and automated vehicles and its application to electric vehicle battery thermal management[J]. IEEE Transactions on Control Systems Technology, 2020, 29(1): 316-328.
[166] Pozzi A, Torchio M, Braatz R D, et al. Optimal charging of an electric vehicle battery pack: A real-time sensitivity-based model predictive control approach[J]. Journal of Power Sources, 2020, 461: 228133.
[167] Laldin O, Moshirvaziri M, Trescases O. Predictive algorithm for optimizing power flow in hybrid ultracapacitor/battery storage systems for light electric vehicles[J]. IEEE Transactions on power electronics, 2012, 28(8): 3882-3895.
[168] Wieczorek M, Lewandowski M. A mathematical representation of an energy management strategy for hybrid energy storage system in electric vehicle and real time optimization using a genetic algorithm[J]. Applied energy, 2017, 192: 222-233.
[169] Zhang Q, Wang L, Li G, et al. A real-time energy management control strategy for battery and supercapacitor hybrid energy storage systems of pure electric vehicles[J]. Journal of Energy Storage, 2020, 31: 101721.
[170] Tan Y K, Mao J C, Tseng K J. Modelling of battery temperature effect on electrical characteristics of Li-ion battery in hybrid electric vehicle[C]2011 IEEE Ninth International Conference on Power Electronics and Drive Systems. IEEE, 2011: 637-642.
[171] Chen K, Li X. Accurate determination of battery discharge characteristics–A comparison between two battery temperature control methods[J]. Journal of Power Sources, 2014, 247: 961-966.
[172] Hussein A A. Experimental modelling and analysis of Li-ion battery temperature dependence[C]2015 IEEE Applied Power Electronics Conference and Exposition (APEC). IEEE, 2015: 1084-1088.
[173] Barcellona S, Piegari L, Villa A. Passive hybrid energy storage system for electric vehicles at very low temperatures[J]. Journal of Energy Storage, 2019, 25: 100833.
[174] B. Manouchehrinia1, S. Molloy, Z. Dong, A. Gulliver, and C. Gough, Emission and lifecycle cost analysis of hybrid and pure electric propulsion systems for fishing boats[J]. Journal of Ocean Technology, 2018, 13(2).